

**Investigation of the Mitochondrial Translocase
of the Outer Membrane (TOM)
of *Drosophila melanogaster***

Agalya Periasamy

*Submitted in total fulfilment of the requirements of the
degree of Doctor of Philosophy*

May 2018

The Walter and Eliza Hall Institute

Department of Medical Biology

The University of Melbourne

Abstract

The macromolecular protein translocation machinery of the outer mitochondrial membrane, TOM, mediates the import of nuclear-encoded mitochondria-bound precursor proteins. Moreover, a demonstrated role in importing pathogenic polypeptides signifies its medical relevance as a potential therapeutic target. Structural investigations of TOM have to date been limited to lower eukaryotic fungi from which the components can be purified in reasonable quantities. The underlying objective of this thesis is to seek and interrogate the structure of a metazoan TOM complex in order to unravel features of greater relevance to the human TOM complex. To this end, the fruit fly *Drosophila melanogaster* was evaluated as an *in vivo* system for transgenic expression of the translocase components for production of purified TOM amenable to structural analysis by cryo-EM. The capacity for targeted, tuneable expression in specific tissues and developmental stages and a provision for phenotypic readouts in *Drosophila* flies holds particular advantages over cell culture systems for investigation of structure-function and wider interactions of TOM in the context of human biology and disease.

Chapter 1 offers an introduction to the mitochondrial import system with particular focus on the organisation of TOM, functional and structural attributes of subunits of the translocase and reported involvement in human diseases.

Chapter 2 describes the homologous expression of epitope-tagged Tom40 and Tom22 in *Drosophila* followed by an account of the characterization and successful isolation of the *Drosophila* TOM assembly suitable for single particle EM analysis. Tryptic-digest mass spectrometric analysis of purified TOM, has identified the potential *Drosophila* orthologues of Tom5 and Tom6 and, point to novel associations of TOM with other mitochondrial proteins namely, VDAC and ANT.

Chapter 3 presents preliminary cryo-EM data of purified *Drosophila* TOM. 2D class averaging has revealed the presence of three-pore particles, albeit, certain detergent related issues remain to be addressed. Further sample optimization strategies for prospective cryo-EM studies are discussed.

Chapter 4 details an investigation of a defective eye phenotype that manifests in the *Drosophila* eye as a consequence of elevated Tom40 expression. Analysis of active caspase levels has demonstrated a cell death basis for the observed phenotype.

Lastly, in Chapter 5, results and findings of the thesis are discussed in the context of reported biochemical and structural data, with emphasis on the organisation and stoichiometry of TOM. A hypothetical model that likely explains the interaction of VDAC with TOM is presented followed by some concluding remarks on the significance and future directions of the project.

Declaration

This is to certify that:

- i. the thesis comprises only my original work towards the PhD except where indicated in the Preface
- ii. due acknowledgement has been made in the text to all other material used
- iii. the thesis is less than 100,000 words in length, exclusive of tables, maps, bibliographies and appendices.

Agalya Periasamy

Preface

This thesis consists of work carried out in collaboration with the laboratories of Dr. Leonie Quinn (Department of Anatomy and Neuroscience, The University of Melbourne; currently at The John Curtin School of Medical Research, The Australian National University, Canberra) and Professor Werner Kühlbrandt (Max Planck Institute of Biophysics, Frankfurt, Germany).

The contributions of collaborators and other members of The Walter and Eliza Hall Institute of Medical Research, are outlined below.

- i. Dissection of *Drosophila* larval imaginal discs and confocal imaging of immunostained eye discs for expression and localisation analysis (Chapter 2, Section 2.4.2, Fig. 7 and Fig. 8) and cell death activity (Chapter 4, Section 4.3.2, Fig. 2.A) was performed either by Arjun Singh Chalal or Naomi Mitchell. Additionally, Arjun Singh Chalal helped me with the quantification of caspase staining (Chapter 4, Section 4.3.2, Fig. 2.B). Generation of a stable fly line expressing Tom40 and the Tom40 RNAi experiment (Chapter 4, Fig. 2.F) was done by Arjun Singh Chalal. Leonie Quinn helped with interpretation of the data for all of these experiments and prepared Figure 8.
- ii. Initial negative stain EM screening experiments with digitonin samples and the first set of 2D classifications (Chapter 2, Section 2.4.6, Fig. 16.A and 16.B) were performed with the help of Wilson Wong, The Walter and Eliza Hall Institute, at the BIO21 microscopy facility.
- iii. All cryo-EM experiments (Chapter 3) and one of the negative stain EM experiment pertaining to the LMNG sample (Chapter 2, Section 2.4.6, Fig. 17) were performed and analysed, solely, by Thomas Bausewein, Kühlbrandt Laboratory, Max Planck Institute of Biophysics.

All other experimentation comprises of my original work

Acknowledgements

First and foremost, I would like to extend my gratitude to Dr. Jacqui Gulbis, my supervisor, for her invaluable support and guidance through my entire time at WEHI. Working with you has been both pleasurable and rewarding, I surely have learned a lot and have become more resilient and independent in the process. Your enthusiasm and unwavering confidence were a major driving force behind the initiation and development of the *Drosophila* project as the major part of my study. I am also very thankful for your continual understanding and encouragement during challenging times, both professionally and personally, during this journey. This thesis would not have been possible without your guidance and useful suggestions.

To my co-supervisors, Dr. David Miller and Prof. Peter Colman, thank you for your guidance, insights and discussions regarding my research projects. Particularly, I would like to thank Peter for his ongoing support and encouragement for continuance of this project.

My sincere thanks to Dr. Leonie Quinn and members of her group, whose welcoming nature made our new collaboration delightful. Leonie, with her optimism and keen interest, was instrumental in the advancement of the project. I thank you for your helpful ideas and discussions regarding several experiments. Naomi Mitchell, Arjun Singh Chalal (AJ) and Olga Zaytseva were very helpful in teaching me “how to fly”. I thank you all for your constant patience and finding the time to answer all my questions. Particularly, I greatly appreciate AJ’s expert technical assistance and advice with the confocal experiments during this past year.

My thanks to Katrina Black, my fellow PhD student, for helpful discussions and moral support and for her friendship. I would also like to thank the entire structural biology division at WEHI for being such a lovely place to work.

I deeply appreciate the help offered by Dr. Wilson Wong from WEHI for carrying out the initial negative stain EM experiments, which were a major stepping stone for this project.

We are very fortunate to have entered into a collaboration with Prof. Werner Kühlbrandt for investigation of TOM by cryo-EM for structure determination. I would like to thank him for his valuable insights and suggestions for the progression of this project. Particularly, I would like to thank Thomas Bausewein in Kühlbrandt’s group for performing the cryo-EM trials for us. I very much look forward to continuing this exciting collaboration.

A huge thank you to Pauline Crewther who has been a great mentor to me right from the start when I began at WEHI as a research assistant. You have always been ready to lend a sympathetic ear to hear out all my troubles and your uplifting words have kept me going in those times. Thank you for finding the time for coffee sessions with me and also for proof-reading my thesis.

I would like to thank my PhD committee members, Dr. Diana Stojanovski, Assoc. Prof. Matthew Call and Assoc. Prof. Mike Lawrence for their support and time throughout my candidature.

Last but not the least, I owe my thanks to my family back home in India and all my friends in Melbourne who have become extended family members, for their love and support during this journey. Especially, I would like to acknowledge the support of my husband, Yagnesh, who has been my pillar of strength. It was definitely not an easy task to sustain a long-distance relationship, but we did it! Thank you for your unconditional love over the years and your selfless help during the past few months.

Table of Contents

Chapter 1:

Introduction to the mitochondrial import system	1
1.1 Mitochondria and their origin	1
1.1.1 Evolution of mitochondria.....	2
1.1.2 Structure of mitochondria.....	2
1.2 Protein import into mitochondria: An overview.....	3
1.2.1 The mitochondrial translocation machinery	4
1.2.2 Diverse types of precursor signal sequences	5
1.2.3 Overview of major pathways	6
1.3 TOM complex – components and stoichiometry.....	6
1.3.1 Tom40, the pore-forming subunit	8
1.3.2 Tom22, the central organiser and receptor subunit.....	9
1.3.3 Small Toms, the assembly subunits	9
1.3.4 Tom20 and Tom70, the peripheral receptor subunits	9
1.4 Structural analysis of the TOM complex	11
1.5 Import of polytopic inner membrane proteins.....	13
1.6 Underlying problems in obtaining a complete picture of translocase function.....	15
1.7 Translocases in human health and diseases	16
1.7.1 TOM components implicated in diseases	17
1.8 Variability between translocases of yeast and higher eukaryotes.....	17
1.9 Thesis outline	19

Chapter 2:

Transgenic expression of TOM components in *Drosophila* and biochemical evaluation of purified TOM complex 21

2.1	Introduction	21
2.1.1	Production of eukaryotic membrane protein complexes for structural biology...	22
2.1.2	<i>Drosophila</i> as an expression system for mitochondrial translocases	23
2.1.2.1	<i>Drosophila</i> TOM subunits have high homology to human orthologues.....	24
2.1.2.2	An established UAS-GAL4 based <i>in vivo</i> protein expression system	25
2.1.3	Overview of <i>Drosophila</i> biology and genetics	29
2.1.3.1	Life cycle and physiology	29
2.1.3.2	<i>Drosophila</i> chromosomes	29
2.1.3.3	Balancers and markers.....	30
2.2	Schematic overview of experimental strategy	32
2.3	Experimental considerations	33
2.3.1	Tag selection for protein expression	33
2.3.2	Deliberations and issues during purification trials.....	34
2.3.2.1	Fly strain for pull-down: Tom40 or Tom22.....	34
2.3.2.2	Starting material: mitochondria versus total membranes	34
2.3.2.3	Immuno-affinity purification: HA- or FLAG-based antibody resin and stringent washes.....	35
2.4	Results	36
2.4.1	Expression of FLAG.HA tagged-Tom40 and Tom22 in <i>Drosophila</i> flies.....	36
2.4.2	Eye-specific expression of TOM subunits and subcellular localization analysis by immunofluorescence confocal imaging	37
2.4.3	Integration of tagged TOM subunits into higher order complexes as assessed by BN-PAGE	37
2.4.4	Extraction and stability testing of Tom40 complexes using BN-PAGE	40
2.4.4.1	Detergent screening	40
2.4.4.2	Effect of salt and urea.....	40
2.4.5	Purification of <i>Drosophila</i> TOM complex <i>via</i> tagged Tom40 and mass spectrometry analysis	42

2.4.5.1	Observed differential extractions with digitonin and LMNG	45
2.4.5.2	Possible <i>Drosophila</i> orthologues of human Tom5 and Tom6 identified by sequence alignment	47
2.4.5.3	Co-elution of VDAC and ANT with Tom40	47
2.4.6	Negative stain EM analysis showed three-pore complexes	48
2.5	Discussion	51
2.5.1	A novel strategy for isolation of metazoan TOM from native membranes	51
2.5.2	Effect of detergents on TOM complex extraction and stability	51
2.5.3	Implications of VDAC and ANT association with TOM	52

Chapter 3:

	Preliminary structural investigation of <i>Drosophila</i> TOM by single particle cryo-EM	54
3.1	Introduction	54
3.1.1	High-resolution structure determination by single-particle cryo-EM	55
3.1.1.1	Membrane protein structures	56
3.2	Results	58
3.2.1	Preparation of samples for cryo-EM analysis	58
3.2.2	Visualization of three-pore particles in preliminary cryo-EM trials	58
3.3	Discussion	61

Chapter 4:

	Investigation of an eye phenotype caused by Tom40 expression and its implications	63
4.1	Introduction	63
4.2	Experimental considerations	64
4.3	Results	64

4.3.1	<i>GMR</i> -GAL4 driven Tom40 expression causes glossy eye phenotypes in a dose-dependent manner	64
4.3.2	Increased cell death activity correlates with increase in Tom40 expression.....	66
4.4	Discussion	68
General discussion		71

Chapter 5:

5.1	Introduction	71
5.1.1	Architecture and stoichiometry of TOM complexes	72
5.1.2	Tom40 does not exclusively associate with translocase subunits	73
5.1.3	Context for a three-pore TOM complex	74
5.1.4	A model for VDAC interaction with TOM	75
5.2	Concluding remarks and future directions	77

Chapter 6:

Materials and Methods		78
6.1	Materials and Reagents	78
6.2	General fly handling procedures	79
6.2.1	Fly food.....	79
6.2.2	Fly rearing and maintenance	79
6.2.3	Setting up of genotype crosses/genetic mating schemes	80
6.3	Experimental procedures	80
6.3.1	Establishment of <i>Drosophila</i> fly strains.....	80
6.3.1.1	Cloning and generation of new transgenic fly strains	80
6.3.1.2	Other fly strains	80
6.3.2	Immunostaining and confocal microscopy	81
6.3.2.1	Tissue dissection and fixation	81
6.3.2.2	Antibody staining.....	81

6.3.2.3	Mounting of larval eye discs	82
6.3.2.4	Microscopy imaging	82
6.3.2.5	Image analysis	82
6.3.3	Imaging of adult <i>Drosophila</i> eyes.....	82
6.3.4	Protein expression, purification and detection	84
6.3.4.1	Protein expression trials	84
6.3.4.2	Isolation of mitochondria	84
6.3.4.3	Large-scale harvesting of fly heads	84
6.3.4.4	Isolation of membranes and detergent solubilisation	85
6.3.4.5	Purification of TOM complex by immuno-affinity methods	85
6.3.5	Protein detection methods	86
6.3.5.1	SDS-Polyacrylamide Gel Electrophoresis (SDS-PAGE).....	86
6.3.5.2	Blue Native PAGE (BN-PAGE).....	86
6.3.5.3	Western blotting and immunodetection	87
6.3.5.4	In-gel tryptic digestion and mass spectrometry	87
6.3.6	Electron microscopy (EM) and image processing	89
6.3.6.1	Negative stain EM imaging.....	89
6.3.6.2	Particle selection and 2D classification of particles	89
6.3.7	Cryo-EM methods.....	89
6.3.7.1	Preparation of graphene oxide covered holey carbon grids	89
6.3.7.2	Cryo-EM specimen preparation	89
6.3.7.3	Data acquisition	89
6.3.7.4	Microscopy information	90
6.3.7.5	Image processing	90

Appendix	91
-----------------------	-----------

References	93
-------------------------	-----------

List of Figures

Chapter 1:

1	A schematic illustration of major translocases and import pathways in mitochondria	5
2	Membrane organisation of TOM	7
3	Cryo-EM structure of the <i>Neurospora</i> core TOM complex from Bausewein <i>et al.</i> (2017)	12
4	Schematic illustration of steps involved in translocation of carrier proteins	14

Chapter 2:

1	Sequence alignments of Tom40	26
2	Sequence alignments of Tom22	27
3	UAS-GAL4 protein expression system in <i>Drosophila</i>	28
4	Life cycle of <i>Drosophila</i>	30
5	Schematic of Tom40 and Tom22 constructs utilised for expression trials	32
6	Tom40 and Tom22 expression analysis by western blotting	36
7	<i>In situ</i> expression analysis of Tom40 and Tom22	38
8	Sub-cellular localisation of epitope-tagged Tom40	39
9	Assessment of tagged Tom40 and Tom22 integration into higher-order complexes	39
10	Detergent screening for extraction of entire putative TOM complex	41
11	Effect of varying concentrations of urea and NaCl salt on the stability of TOM complexes	42
12	Preparation of fly head membranes	43
13	Purification of TOM complex and identification of protein bands	44
14	Analysis of molecular mass of purified TOM complex by BN-PAGE	45
15	Protein sequence alignments of unannotated <i>Drosophila</i> proteins against human Tom5 and Tom6	47
16	Negative stain EM of a digitonin-purified TOM sample shows 3-pore complexes	49
17	Negative stain EM of a LMNG-purified TOM sample	50

Chapter 3:

1	Bar graph of number of EM maps released annually from 2002-2017	55
2	Representative micrographs showing distribution of particles	59
3	2D class averages of three-pore particles in ice	60
4	A selection of 2D class averages of particles distributed on a graphene oxide layer	60

Chapter 4:

1	Tom40 associated <i>Drosophila</i> adult eye phenotypes	65
2	Expression of Tom40 mediates apoptosis in the developing <i>Drosophila</i> eye	67

Chapter 5:

1	A hypothetical model to explain VDAC association with Tom40/TOM	76
---	---	----

List of Tables

Chapter 1:

- | | | |
|---|---|----|
| 1 | Differences in TOM subunits of fungi and humans | 19 |
|---|---|----|

Chapter 2:

- | | | |
|---|---|----|
| 1 | Percentage of similarity/identity of TOM components between different species | 24 |
| 2 | List of commonly used balancer chromosomes | 31 |
| 3 | Tryptic digest MS identification of proteins co-eluting with Tom40 | 46 |

Chapter 5:

- | | | |
|---|---|----|
| 1 | Comparison of dimensions, molecular mass and stoichiometry of TOM complexes | 73 |
|---|---|----|

Chapter 6:

- | | | |
|---|---|----|
| 1 | List of ingredients in <i>Drosophila</i> culture medium | 79 |
| 2 | List of fly strains used in the study | 81 |
| 3 | List of immunohistochemistry reagents | 83 |
| 4 | List of antibodies | 83 |
| 5 | Miscellaneous buffers and solutions | 88 |

List of Abbreviations

Å	Angström (10^{-10} metres)
β-OG	n-Octyl-β-D-Glucopyranoside
AAC/ANT	ADP/ATP Carrier or Adenine nucleotide translocase
APS	Ammonium persulfate
ATP	Adenosine triphosphate
BN	Blue native
CCD	Charge-coupled device
CFP	Cyan fluorescent protein
CO ₂	Carbon dioxide
CV	Column volume
Cymal-5	5-Cyclohexyl-1-Pentyl-β-D-Maltoside
DAPI	4',6-diamidino-2-phenylindole
DDM	n-Dodecyl-β-D-Maltopyranoside
DED	Direct electron detector
DIBMA	Diisobutylene/maleic acid
DNA	Deoxyribonucleic acid
EDTA	Ethylenediaminetetraacetic acid
EM	Electron microscopy
EMDB	Electron Microscopy Data Bank
ER	Endoplasmic reticulum
FRET	Förster Resonance Energy Transfer
GDN	Glyco-diosgenin
GFP	Green fluorescent protein
GIP	General import pore

<i>GMR</i>	Glass multiple reporter
GPCR	G-protein coupled receptor
HCl	Hydrochloric acid
HRP	Horseradish peroxidase
Hsp	Heat shock protein
IM	Inner membrane
IMP	Integral membrane protein
IMS	Intermembrane space
kDa	kilo Dalton
LC-ESI	Liquid chromatography - Electrospray ionization
LDAO	N, N-Dimethyldodecylamine N-oxide
LILBID	Laser Induced Liquid Bead Ion Desorption
LMNG	Lauryl Maltose Neopentyl Glycol
MCF	Mitochondrial carrier protein family
MIA	Mitochondrial intermembrane space assembly
MOMP	Mitochondrial outer membrane permeabilization
MPC	Membrane protein complex
MS	Mass spectrometry
NaCl	Sodium chloride
NMR	Nuclear magnetic resonance
OM	Outer membrane
OXPHOS	Oxidative phosphorylation
PAGE	Polyacrylamide gel electrophoresis
PAM	Presequence translocase-associated motor
PBS	Phosphate-buffered saline
RNA	Ribonucleic acid

RNAi	RNA interference
RT	Room temperature
SAM	Sorting and assembly machinery
SDS	Sodium dodecyl sulfate
siRNA	Small interfering RNA
SMA	Styrene-maleic acid
SMALP	Styrene-maleic acid lipid particle
TDM	Tridecyl- β -D- Maltopyranoside
TEMED	Tetramethylethylenediamine
tRNA	transfer RNA
TIM	Translocase of inner mitochondrial membrane
TOM	Translocase of outer mitochondrial membrane
TPR	Tetratricopeptide repeat
Tris	Tris (hydroxymethyl) aminomethane
TX-100	Triton X-100
UAS	Upstream activating sequence
VDAC	Voltage dependent anionic channel
XFEL	X-ray free electron laser
YFP	Yellow fluorescent protein
2D	Two-dimensional
3D	Three-dimensional

Chapter 1

Introduction to the mitochondrial import system

1.1 Mitochondria and their origin

Intracellular compartmentalisation is a defining feature of all eukaryotic cells. A network of membranes divides the cytoplasm into organelles, each with a unique biochemical environment that is optimal for its specialised role in cellular function and metabolism. Each eukaryotic cell has a nucleus where genomic DNA replication and RNA synthesis occur, an endoplasmic reticulum (ER) that is the site of protein translation, protein assembly and lipid synthesis, Golgi apparatus for post-translational processing and transport of nascent membrane proteins and mitochondria that produce energy in a form the cell can utilise. Although serving as hubs for specialised functions, the organelles within a cell do not behave as isolated entities and extensive communication and co-operation between organelles is an important factor in eliciting appropriate cellular responses (Lebiedzinska et al., 2009).

Mitochondria, often termed the ‘energy powerhouses’ of eukaryotic cells, are both indispensable and ubiquitous, the only known exception being *Monocercomonoides* sp., a flagellate gut microbe, which lacks mitochondria (Karnkowska et al., 2016). They are production sites for most of the cellular ATP via the process of oxidative phosphorylation (OXPHOS). In addition to this important role, mitochondria are involved in fundamental cellular processes such as metabolism of amino acids and lipids, calcium signalling, and the biosynthesis of haem and iron-sulfur clusters critical for cellular homeostasis (Rizzuto et al., 2012, Bhole and Letai, 2016, Wang, 2016). Some mitochondrial activities require the collaboration of other organelles; for example, contact sites between the ER and mitochondria act as regulatory centres of calcium signalling and sites of lipid synthesis, trafficking and exchange (Vance, 1990, Csordas et al., 1999, de Brito and Scorrano, 2010). Their key role in apoptosis has earned mitochondria the title “death centre of the cell” (Tait and Green, 2010). In humans, mitochondria are implicated in tumorigenicity, the innate immune response, and neurodegenerative disorders, amongst others (Cali et al., 2012, Weinberg et al., 2015). This chapter aims to give an overview of the origins and cellular integration of mitochondria, with a focus on how they import the proteins required for the many functions they carry out in cells.

1.1.1 Evolution of mitochondria

While the origins of mitochondria remain speculative, a widely accepted theory is that they evolved from an endosymbiotic event approximately two billion years ago, the engulfment of a gram-negative α -proteobacterium by a primitive eukaryotic host cell (Yang et al., 1985, Lang et al., 1999). Several features of present day mitochondria seem to reflect bacterial ancestry. These include a double-membrane boundary, rich in cardiolipin, and an oxidizing intermembrane environment, analogous to the bacterial periplasm, separating the outer and inner membranes. Also akin to bacteria, an aqueous matrix bounded by the inner membrane houses a circular genome. During the evolutionary transition from endosymbiont to integrated organelle, the mitochondrial proteome has undergone extensive retailoring and has reduced significantly in size. Most proto-mitochondrial genes have been lost or laterally transferred to the host nucleus and assimilated into the genome. Additional genes required for mitochondrial function have been acquired, invented or ‘stitched’ together during evolution (Dolezal et al., 2006, Lithgow and Schneider, 2010, Gray, 2015), enabling the vestigial symbiote to progressively integrate its functions with the host cell. Indeed, phylogenetic analysis indicates that only about 10 to 20 percent of present day mitochondrial proteomes have α -proteobacterial origins (Gray et al., 2001). The remainder have diverse origins, curiously including proteins of prokaryotic origins with no clear homologues in either bacterial or archaeal groups (Karlberg et al., 2000, Marcotte et al., 2000, Szklarczyk and Huynen, 2010).

1.1.2 Structure of mitochondria

Mitochondria are both dynamic and mobile, taking forms ranging from long filamentous structures to rod-shaped or ovoid forms and assuming function-specific shapes and intracellular positions. Morphological changes are associated with the mitochondrial fission and fusion events occurring in response to cellular requirements such as mitosis (Scott and Youle, 2010).

Mitochondria are compartmentalised into distinct microenvironments with differing protein requirements. These correspond to an outer membrane (OM), an inner membrane (IM), an intermembrane space (IMS) and an aqueous matrix.

The outer mitochondrial membrane is unique in containing several pore-forming β -barrel proteins involved in transport of ions, metabolites, and proteins in and out of mitochondria. The inner membrane is protein-rich and structured, with deep invaginations that protrude into the internal matrix affording a vast increase in surface area over the enveloping outer

membrane. These crypt-like membrane structures are known as cristae, and most of the respiratory super-complexes and ATP synthases are found here (Davies *et al.*, 2011). The viscous aqueous environment of the matrix houses more than half of all mitochondrial proteins and the mitochondrial genome. It is the site of DNA replication, transcription, synthesis of proteins encoded by the mitochondrial genome and numerous enzymatic reactions including aerobic respiration by the tricarboxylic acid (TCA) cycle, from which energy production is initiated.

1.2 Protein import into mitochondria: An overview

An estimate of the total number of mitochondrial proteins in humans comes from data curated from large-scale mass spectrometry and green fluorescent protein (GFP)-based localization studies (Calvo *et al.*, 2016, Smith and Robinson, 2016). Considering differential expression in various tissues, the range lies between 1,100 and 1,900 proteins. In humans, the mitochondrial genome encodes two rRNAs, 22 tRNAs and 13 polypeptides, all of which are essential components of oxidative phosphorylation. The residual, approximately 99 % of total mitochondrial proteins, require trafficking into mitochondria after synthesis on cytosolic ribosomes.

Over the last three decades, two ascomycete fungal models, *Saccharomyces cerevisiae* and *Neurospora crassa*, have been employed in detailed investigations into mitochondrial protein import, a field pioneered by Walter Neupert, Gottfried Schatz and Nikolaus Pfanner. Import is thought to occur mainly in a post-translational manner (Reid and Schatz, 1982, Wienhues *et al.*, 1991, Neupert, 1997, Pfanner and Geissler, 2001), although there is also some evidence for co-translational import and localised translation of precursors near the mitochondrial surface (Fujiki and Verner, 1993, Garcia *et al.*, 2007, Lesnik *et al.*, 2015, Gold *et al.*, 2017). In all cases, proteins to be imported are referred to as precursors or ‘preproteins’ meaning that they have yet to fully fold and adopt a tertiary or quaternary structure. After synthesis on cytoplasmic ribosomes, specific classes of preproteins are engaged by molecular chaperones in the cytosol, including Hsp90 and Hsp70/Hsp40, to prevent aggregation or irreparable misfolding (Murakami *et al.*, 1988, Young *et al.*, 2003b, Bhangoo *et al.*, 2007). They are thus maintained in an import-competent state and targeted to the mitochondrial surface by means of molecular interactions between chaperones and mitochondrial surface receptors. The downstream import process is mediated by dynamic macromolecular protein assemblies in the mitochondria, known as translocases. These modular machines recognise mitochondria-bound precursors and

accept them into a general import pore from where they are directed into appropriate pathways for assembly in their final destination (detailed in section 1.2.3). Recent studies suggest that the import process is regulated by specific phosphorylation events. In *Saccharomyces*, cytosolic kinases, casein kinase 2 (CK2), protein kinase A (PKA) and cyclin-dependent kinase (Cdk1) have been shown to phosphorylate both incoming precursors and assembled translocases, resulting in stimulation or inhibition of import (Rao *et al.*, 2011, Schmidt *et al.*, 2011, Harbauer *et al.*, 2014).

1.2.1 The mitochondrial translocation machinery

Integration of primitive mitochondria as central players in the working environment of eukaryotic cells has necessitated co-evolution of machinery that facilitates import of proteins required for host cells to benefit from the association. It has thus been speculated that the mitochondrial protein translocation machinery has its origins as early as the mitochondria (Fukasawa *et al.*, 2017). Extensive genetic and biochemical studies in *Saccharomyces* and *Neurospora*, combined with the development of precursor import assays, successfully led to the identification of the principal protein components of translocase complexes and elucidation of major protein assembly routes, as reviewed in Chacinska *et al.* (2009), Wiedemann and Pfanner (2017). These studies paint a complex picture, as each unique precursor type has specific requirements with respect to reaching its final destination, which may include controlling the propensity to aggregate *en route*, formation of intramolecular disulfides, or co-assembly with other proteins. The need for a variety of translocase components to meet these specific needs has resulted in the genesis of multiple co-operating ‘pathways’. The translocation machinery has been classified into four major membrane embedded modular assemblies, two in the outer membrane and two in the inner membrane (Fig. 1), as listed below:

- Translocase of the Outer membrane (TOM)
- Sorting and Assembly Machinery (SAM)
- Translocase of the Inner Membrane 23 (TIM23)
- Translocase of Inner Membrane 22 (TIM22)

Each assembly is a multi-protein complex with a central translocase unit accompanied by accessory subunits involved in recognition of precursors or stabilisation and organisation of the translocase scaffold. Additionally, the IMS region contains hexameric TIM9.10 and TIM8.13 chaperone complexes that facilitate carriage of membrane-bound precursors (Curran *et al.*, 2002, Hoppins and Nargang, 2004, Webb *et al.*, 2006) and a Mitochondrial

Intermembrane Space Assembly (MIA) complex, involved in the oxidative folding and assembly of cysteine-rich IMS-bound precursors (Chacinska *et al.*, 2004, Stojanovski *et al.*, 2008).

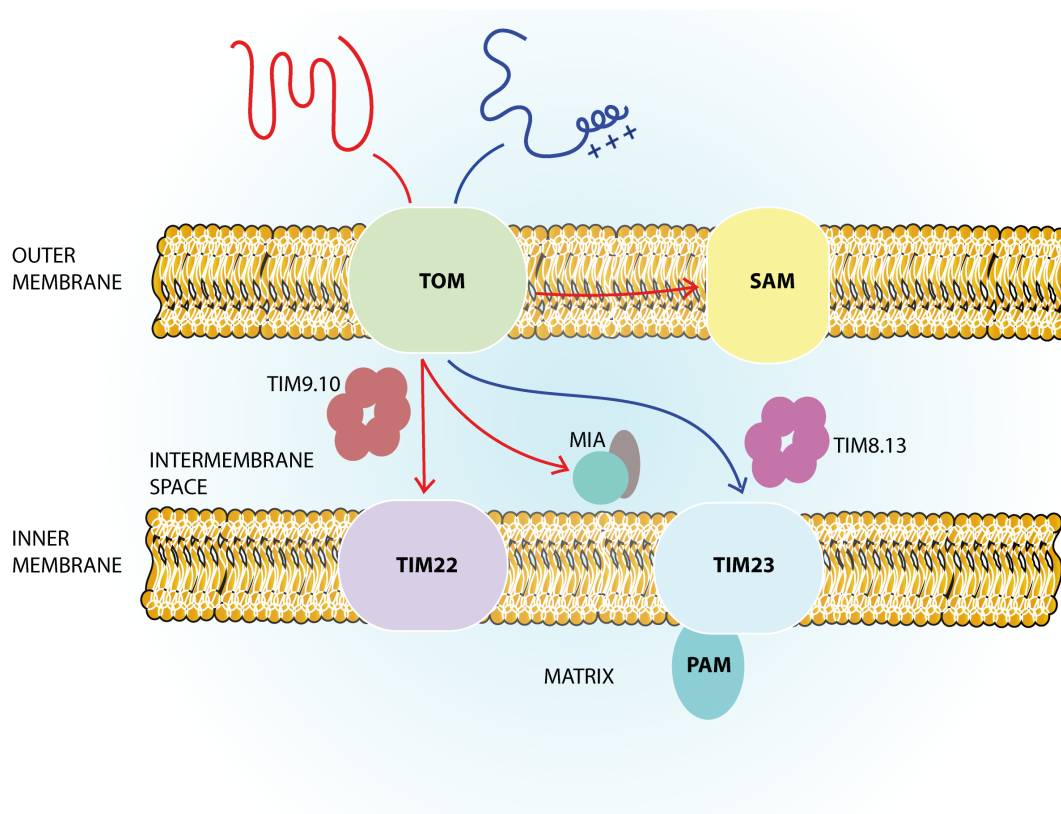


Figure 1: A schematic illustration of major translocases and import pathways in mitochondria. The translocase complex of the outer membrane (TOM) is the main entry portal into mitochondria. After channelling into mitochondria via TOM, the precursor proteins follow different pathways, depending on the nature of the precursor and the destination compartment. Subsequent transfer of the precursor to SAM, TIM22, TIM23, MIA, TIM9.10 or TIM8.13 is governed by targeting signal(s) in the precursor. A presequence-carrying precursor is coloured in blue, while a precursor with internal targeting signals is shown in red.

1.2.2 Diverse types of precursor signal sequences

The fidelity of import into mitochondria is ensured by the presence of targeting sequences or ‘signals’ present within the mitochondrial precursors. These versatile signals are utilised at many stages of the import process, including initial recognition, translocation, transfer and final

assembly, determining which of the pathways a precursor will navigate. The signals have been classified into two groups (Fig. 1). The first and best characterised class contains N-terminal amphipathic helices rich in arginine and lysine, which occur in matrix-targeted proteins as either cleavable ‘presequences’ or non-cleavable signals (Roise and Schatz, 1988, von Heijne *et al.*, 1989). In contrast, all precursors of outer membrane proteins and selected precursors of intermembrane space and inner membrane proteins contain internal targeting sequences that are non-cleavable (Diekert *et al.*, 1999, Chacinska *et al.*, 2009). Notably, multi-spanning inner membrane precursors contain multiple internal targeting signals (Brix *et al.*, 1999, Wiedemann *et al.*, 2001), although the consensus binding motifs have not yet been defined.

1.2.3 Overview of major pathways

To date, four different major import pathways have been described (Fig. 1). The TOM complex is common to every pathway and serves as a portal for nearly all incoming precursors. Receptor-like proteins with soluble domains, which are part of the TOM complex, serve as the first point of contact for precursors, before translocation into the organelle. Beyond TOM, the pathways diverge, and precursors are sorted to one of the following assemblies: i) TIM23, a general pore in the inner membrane for soluble precursors with presequences, targeting them to the matrix compartment; a ATP-driven presequence translocase-associated import motor (PAM) complex in the matrix drives the process, ii) TIM22, also found in the inner membrane, is implicated in the assembly of multispinning (or polytopic) precursors with internal targeting sequences into the inner membrane in a membrane potential-dependent manner (Sirrenberg *et al.*, 1996), iii) SAM in the outer mitochondrial membrane is involved in the folding and assembly of β -barrels (Wiedemann *et al.*, 2003), and iv) MIA carries out redox-active preprotein import to the intermembrane space (Stojanovski *et al.*, 2008)

Association of translocase complexes into supramolecular assemblies has been reported in recent years. Using immuno-precipitation and cross-linking approaches, super-complexes between TOM-SAM (Qiu *et al.*, 2013), TOM-TIM23 (Waagemann *et al.*, 2015) and TOM-TIM22 (Kang *et al.*, 2016) have been reported, indicating some functional co-operation between the import and assembly machineries.

1.3 TOM complex – components and stoichiometry

The common insertion site for incoming precursors, termed the general import pore (GIP), and an associated receptor complex of the outer mitochondrial membrane (Pfaller *et al.*, 1988,

Kiebler et al., 1990) came to be referred to collectively as the TOM complex (Pfanner et al., 1996). Following this, further investigations into the assembly, organisation and function of the complex were carried out using *Saccharomyces* and *Neurospora* as the subjects (Dekker et al., 1998, Kunkele et al., 1998a, Kunkele et al., 1998b, Rapaport et al., 1998a, Meisinger et al., 2001). Mammalian counterparts were subsequently identified and characterized (Saeki et al., 2000, Suzuki et al., 2000, Johnston et al., 2002, Kato and Mihara, 2008).

TOM is composed of seven protein subunits, Tom40 being the central pore-forming subunit. Tom40 is a β -barrel and forms a stable association with Tom22. When the small TOM components, Tom5, Tom6 and Tom7, are also present, a 'core' complex (GIP) of 148 kDa is formed. The precise stoichiometry of the core complex of *Neurospora*, Tom40:Tom22:Tom5:Tom6:Tom7, was recently determined by native mass spectrometry to be 1:1:1:1:1 (Bausewein *et al.*, 2017). Tom20 and Tom70 associate with the core complex to form a 'holo-complex' (Fig. 2), of as yet indeterminate stoichiometry, with an apparent molecular mass of approximately 500 kDa, based on blue-native PAGE (BN-PAGE) analysis.

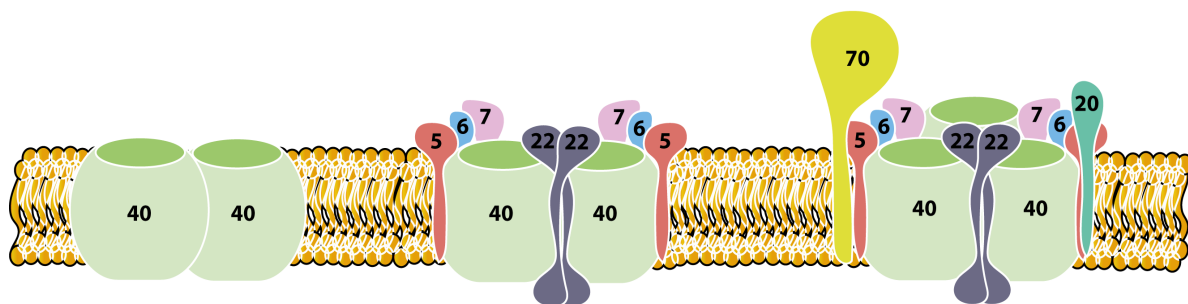


Figure 2: Membrane organisation of TOM. A schematic representation of membrane organization of TOM complex. Tom40 assembled in a dimeric state (left) associates with Tom22, Tom5, Tom6 and Tom7 to form a 'core' complex (middle). Two other subunits namely, Tom20 and Tom70 interact more loosely with the core complex into an ensemble that is referred to as a 'holo' complex (right). The stoichiometry and interactions between components are uncertain.

The core components, Tom40 and Tom22, are essential for survival (Baker *et al.*, 1990, Lithgow *et al.*, 1994). In general, the other subunits are not; however specific deletions of

certain subunits, in combination, can lead to lethality (Sherman *et al.*, 2005). The components of the TOM complex are broadly conserved from yeast to humans; although comparison of the yeast and human components show some significant differences (Table 1).

1.3.1 Tom40, the pore-forming subunit

Tom40 was first identified in yeast, as an outer membrane protein component of the import machinery specifically cross-linked to a precursor in transit (Vestweber *et al.*, 1989). Tom40 accepts precursors from the surface receptor proteins on the *cis* side of the membrane and passes them to downstream components present on the *trans* side (Rapaport *et al.*, 1998b). Electrophysiological analysis of refolded and reconstituted *Saccharomyces* Tom40 (expressed in *Escherichia coli*), showed that it formed a cation selective channel, capable of interacting with presequence peptides, with a pore width of approximately 22 Å (Hill *et al.*, 1998). A recent study based on interpreting chemical crosslinking data in the context of a topological model, showed that the interior of the pore contains distinct hydrophilic and hydrophobic patches that respectively interact with sequence stretches of presequence-containing and hydrophobic precursors. It was proposed that this denoted separate transport paths for different precursor types (Shiota *et al.*, 2015).

Sequence analysis of Tom40 predicts an N-terminal α -helical region (Zeth, 2010, Gessmann *et al.*, 2011, Kuszak *et al.*, 2015), which has been shown to engage with Tim10 (Shiota *et al.*, 2015), a subunit of the intermembrane space TIM9.10 chaperone complex. This suggests that TIM9.10 may be involved in the recruitment of precursors for downstream transfer to SAM and/or TIM22. It has also been proposed that, in the membrane, Tom40 exists in a dynamic equilibrium between a dimeric assembly intermediate and the mature three-pore TOM complex (Rapaport *et al.*, 1998a, Model *et al.*, 2001, Shiota *et al.*, 2015), as depicted in Fig. 2.

The evolutionary origins of Tom40 are not very clear. While no direct bacterial homologues for Tom40 have been identified so far, phylogenetic analysis suggests that Tom40 is distantly related to the voltage-dependent anion channel (VDAC) of the mitochondrial outer membrane (Bayrhuber *et al.*, 2008, Bay *et al.*, 2012). In the absence of crystal structures of Tom40, homology models have been based on the three-dimensional structure of VDAC (Gessmann *et al.*, 2011, Lackey *et al.*, 2014). Molecular 3D structures of refolded VDAC protein determined by X-ray crystallography and Nuclear Magnetic Resonance (NMR) Spectroscopy, determined simultaneously by three independent groups, show an atypical β -barrel with 19 uneven β -strands (Bayrhuber *et al.*, 2008, Hiller *et al.*, 2008, Ujwal *et al.*, 2008). There has been some

contention as to whether this represents the native conformation of VDAC (Hiller *et al.*, 2010, Colombini, 2012), since a 13 β -strand structural model had been proposed on the basis of biochemical and functional data (Thomas *et al.*, 1993).

1.3.2 Tom22, the central organiser and receptor subunit

Tom22 is central to the organisation of the TOM complex. Genetic deletion studies on yeast strains revealed Tom22 as a key determinant of the higher order organisation of TOM. Deletion of Tom22 results in the absence of the higher order TOM with only a small complex (~100 kDa on BN-PAGE) containing Tom40 (Model *et al.*, 2002). Tom22 also functions as a receptor for incoming precursors, in cooperation with Tom20 and Tom70 (van Wilpe *et al.*, 2000).

Tom22 has a single pass transmembrane helix that anchors its soluble domains, which are exposed in both cytosol and IMS. The cytosolic domain is conserved across fungal and animal species and its preponderance of acidic residues formed the basis of early hypotheses regarding binding of precursors with complementary charged surfaces (Kiebler *et al.*, 1993, Bolliger *et al.*, 1995, Macasev *et al.*, 2004). A later study, however, showed that negatively charged residues in the cytosolic domain of Tom22 were not critical for binding and import (Nargang *et al.*, 1998). Sequence conservation in the IMS domain is poor in comparison; a negatively-charged domain in fungi is replaced by a neutral glutamine-rich domain in mammals (Yano *et al.*, 2000).

1.3.3 Small Toms, the assembly subunits

The small Tom proteins, namely Tom5, Tom6 and Tom7, have single-pass transmembrane helices and are thought to function in assembly and structural integrity of the TOM complex. A review of their reported roles suggests functional differences between the small Toms in fungi and humans. In the former, experiments using strains devoid of single small Toms indicate that the TOM complex is stabilized by Tom6 and destabilized by Tom7 (Alconada *et al.*, 1995, Sherman *et al.*, 2005). In humans, by comparison, Tom7 appears critical for stability of the TOM complex; siRNA knockdown of hTom7 strongly disrupts the complex, whereas knocking down of Tom5 and Tom6 has only slight effects (Kato and Mihara, 2008).

1.3.4 Tom20 and Tom70, the peripheral receptor subunits

Although not a constituent of the core TOM complex, Tom20 appears to be an important structural component of three-pore TOM complexes, first observed in negative stain electron

micrographs (Kunkele *et al.*, 1998a). Negative stain EM on purified yeast TOM correlates the presence of Tom20 with a third pore. Genetic deletion of Tom20 in yeast gives rise exclusively to two-pore complexes that exhibit slightly higher mobility on BN-PAGE in comparison to the wild-type strain (Model *et al.*, 2002). Tom70 was absent in the purified two/three-pore complexes, thus demonstrating that the presence of Tom70 is not critical for the integrity of either of these complexes.

Tom20 and Tom70 are best known as membrane-anchored surface receptors with hydrophilic domains exposed to the cytosol. These translocase receptors serve as initial contact sites that must recognise and accept incoming precursors before they can be translocated. Tom70 contains a docking site for molecular chaperones, Hsp90 and Hsp70 (Young *et al.*, 2003b), which maintain hydrophobic precursors in an import-competent, non-aggregated state for transfer to Tom70. An early view in the field was that Tom70 and Tom20 operated independently in two separate pathways, with Tom70 binding hydrophobic precursors and Tom20 binding presequence-containing soluble precursors (Brix *et al.*, 1997, Brix *et al.*, 1999). However, this view has changed and there are indications that human Tom70 and Tom20 might form a hetero-dimeric receptor where they act in tandem or sequentially (Fan *et al.*, 2011). Also, it was recently shown, using a cross-linking approach, that Tom70, once thought to be solely dedicated to binding hydrophobic precursors, engages a soluble presequence peptide of Mdl1, an ABC transporter protein, in a dedicated groove (Melin *et al.*, 2015).

Tom70 and Tom20 both have tetratricopeptide repeat (TPR)-based folds, in common with the cytosolic chaperones and co-chaperones that deliver precursors to them. This is suggestive of an evolutionary relationship with TPR co-chaperones like Hop (Hsp70-Hsp90 Organizing Protein) (Young *et al.*, 2003a). TPR domains have from three to 16 tandem 34-amino acid motifs that fold into super-helical scaffolds with prominent surface grooves that mediate a wide range of protein-protein interactions (D'andrea and Regan, 2003).

Two structures of truncated *Saccharomyces* Tom70/Tom71 (a homologue of Tom70 that is absent in humans) showed a total of 11 TPR repeats organised into two domains (Wu and Sha, 2006, Li *et al.*, 2009), as previously predicted by Chan *et al.* (2006). These structures were enlightening, but insufficient to illuminate the molecular basis of precursor interaction with Tom70 or Tom71.

Tom20, by contrast, has only a single TPR motif. When the cytoplasmic domain of rat Tom20 was analysed by NMR, the chemical shift data was modified significantly when a presequence

peptide derived from aldehyde dehydrogenase (ALDH) was also present. The data implicated a LSRLI amino acid sequence motif on the presequence as the region interacting with Tom20, primarily *via* three hydrophobic residues, with the motif adopting the anticipated amphiphilic α -helical conformation. The TPR region of Tom20 constituted a part of the recognition motif (Abe *et al.*, 2000). Crystallographic snapshots were later obtained of a shorter Tom20 construct, representing the ‘core’ region, with a nine residue presequence fragment tethered through formation of an intermolecular disulphide. Two structures differing in the relative orientation of the peptide prompted the interpretation of a dynamic equilibrium between multiple bound states (Saitoh *et al.*, 2007), although this remains to be verified.

1.4 Structural analysis of the TOM complex

Early low-resolution single particle EM reconstructions of TOM complexes purified from *Saccharomyces* and *Neurospora* has provided a first glimpse of the overall shape and appearance. Two- and three-pore complexes revealed single pore dimensions of approximately 20 Å, sufficient to accommodate an unfolded or partially folded precursor protein (Kunkele *et al.*, 1998a, Ahting *et al.*, 1999). A cryo-EM model of *Saccharomyces* TOM containing Tom20, referred to as the ‘Tom20-core complex’ later reported at a resolution of 18 Å (Model *et al.*, 2008) showed the three-pore arrangement was triangular in cross-section. Gold-labelling studies with His-tagged Tom22 indicated that up to three molecules of Tom22 were present at the periphery of the complex. No labelling was observed at the centre of the complex. Based on this observation, the cytosolic domain of Tom20 was assigned to the centrally located protrusion by default. The stoichiometry and architectural detail of the complex could not be determined at the resolution of the study.

Very recently, a cryo-EM structure of a 148 kDa *Neurospora* TOM core complex was published (Bausewein *et al.*, 2017). With a significant gain in resolution to 6.8 Å, the model shows the two-pore complex (Fig. 3A) has overall dimensions of 130 Å by 100 Å, and that each pore is a stoichiometric complex of five subunits - Tom40, Tom22, Tom5, Tom6 and Tom7 - with a two-fold axis of symmetry generating the second pore. A homology model of Tom40 (Gessmann *et al.*, 2011), based on the monomeric structure of VDAC (Ujwal *et al.*, 2008) is an excellent fit to the density envelope of a single pore (Fig. 3B and 3C), although the finer molecular details are unclear at the moderate resolution. Density corresponding to Tom22 was identified in a cleft formed at the periphery between the two Tom40 β -barrel pores, consistent with a role in stabilisation of the complex. Other subunits, Tom5, Tom6 and Tom7

were assigned to cohesive density external to the β -barrel, with the help of reported cross-linking, biochemical and mutational analysis data, and secondary structure predictions. Apart from a 20 Å protrusion of the Tom22 IMS domain, the structural model indicates the core complex would be almost completely embedded in a lipid bilayer, with minimal extra-membraneous features (Fig. 3).

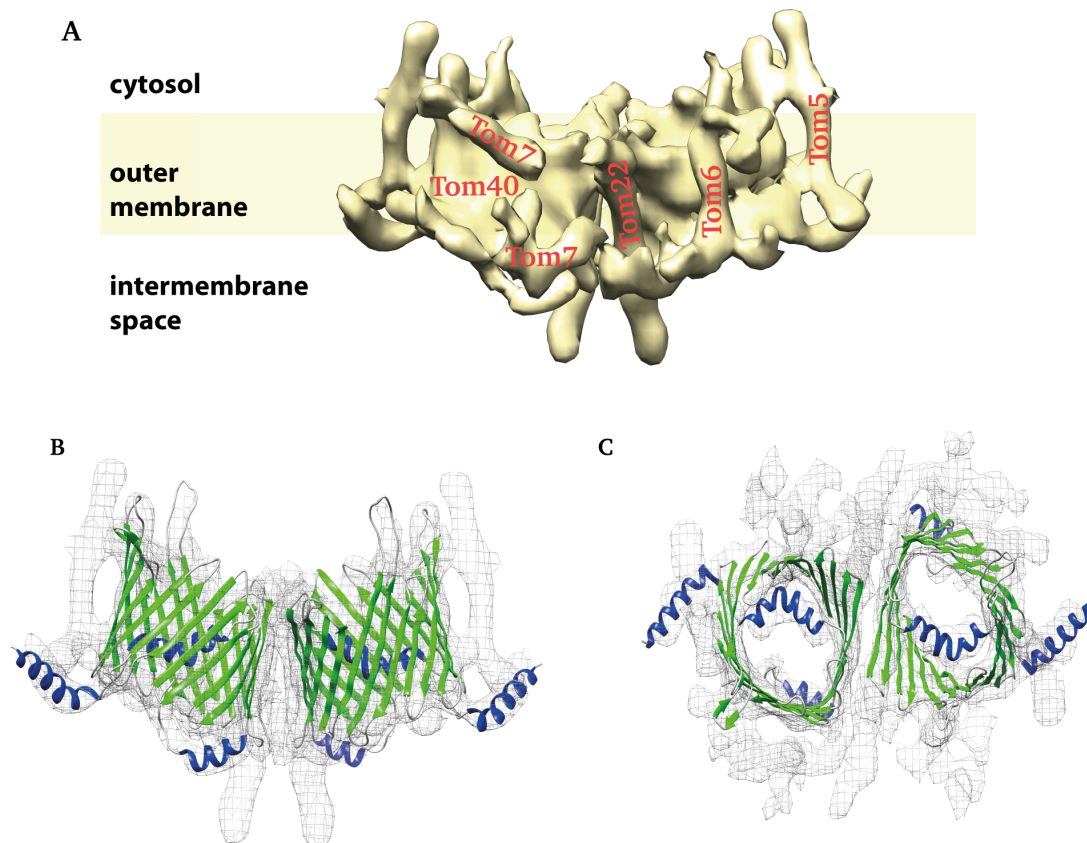


Figure 3: Cryo-EM structure of the *Neurospora* core TOM complex from Bausewein et al. (2017). **A)** A surface model of the overall structure of core TOM contoured at a high-density threshold sigma level of 0.0684 and viewed from within the plane of the membrane. The identities of the individual TOM subunits, as reported, are indicated in red. The heteromeric complex is two-fold symmetrical and almost entirely membrane-embedded. Only the Tom22 subunit extends significantly out of the plane of the membrane. **B)** A comparable view and **C)** A view from the IMS of the cryo-EM map and a refined model of the Tom40 β -barrel depicted as a ribbon diagram (PDB:5O8O). Tom40 was initially placed using a homology model derived from a VDAC1 structure (PDB: 3EMN). Each pore is formed by a single Tom40 molecule, with the top view showing an N-terminal α -helix (coloured in blue) located inside the pore.

An overlay of the *Saccharomyces* and the *Neurospora* TOM complexes presented in Bausewein *et al.* (2017) showed that the two and three-pore structures do not superimpose well, indicating differences in quaternary architecture. On this basis, the authors suggested that the three-pore complex, which also contains Tom20, may adopt an alternative subunit arrangement.

In summary, despite significant progress in structural characterization of the TOM complexes, there are many open questions with respect to the details of membrane organisation of the TOM machinery and the mechanistic basis of precursor translocation.

1.5 Import of polytopic inner membrane proteins

The structural basis of translocation of the polytopic precursors that utilize the TIM22 pathway is a long-standing interest of our group. As described earlier, these hydrophobic precursors do not possess the classical N-terminal presequence signal and instead contain internal ‘cryptic’ targeting motifs. The main clients of this pathway are the members of the mitochondrial carrier protein (MCF) family that transport metabolites, including nucleotides, amino acids, and inorganic ions across the inner membrane and play a supporting role in mitochondrial bioenergetics.

The MCF carriers are characterized by six transmembrane helices corresponding to three internal two-helix repeats, or modules, connected by hydrophilic loops (Palmieri, 2004). The ATP/ADP carrier protein (AAC), also known as the adenine nucleotide translocase (ANT), is representative of the carrier protein family and has served as an experimental model precursor in a number of studies (Pfaller *et al.*, 1988, Sollner *et al.*, 1990, Ryan *et al.*, 1999).

General features of the pathway by which these proteins are imported have been elucidated, although not to the same level of detail as the TIM23 pathway for soluble precursors. Translocation of ANT has been characterised by experiments in *Saccharomyces* where precursors are arrested at specific points during import (Ryan *et al.*, 1999). This has provided a convenient frame of reference for dissecting the process of import. Conceptually, the process has been divided into stages (I – V) (Fig. 4). After synthesis on ribosomes, the precursor protein is guided to the surface of mitochondria by cytosolic chaperones (Stage I) and targeted to the surface receptor Tom70 (Stage II). The precursor is then translocated through the TOM complex to the intermembrane space with the three partially folded modules sequentially translocating (Wiedemann *et al.*, 2001). There, it interacts with the hexameric Tim9-Tim10 complex (TIM9.10) (Truscott *et al.*, 2002) (Stage IIIa). In the aqueous environment of the IMS,

TIM9.10 acts as a chaperone for the precursor, shielding the hydrophobic regions (in an as yet undefined manner) until the precursor is transferred to TIM22 (Translocase of the Inner membrane) complex (Stage IIIb). Insertion of the precursor into the inner membrane *via* TIM22 is contingent on an intact membrane potential (Stage IV) followed by functional assembly in the inner membrane (Stage V).

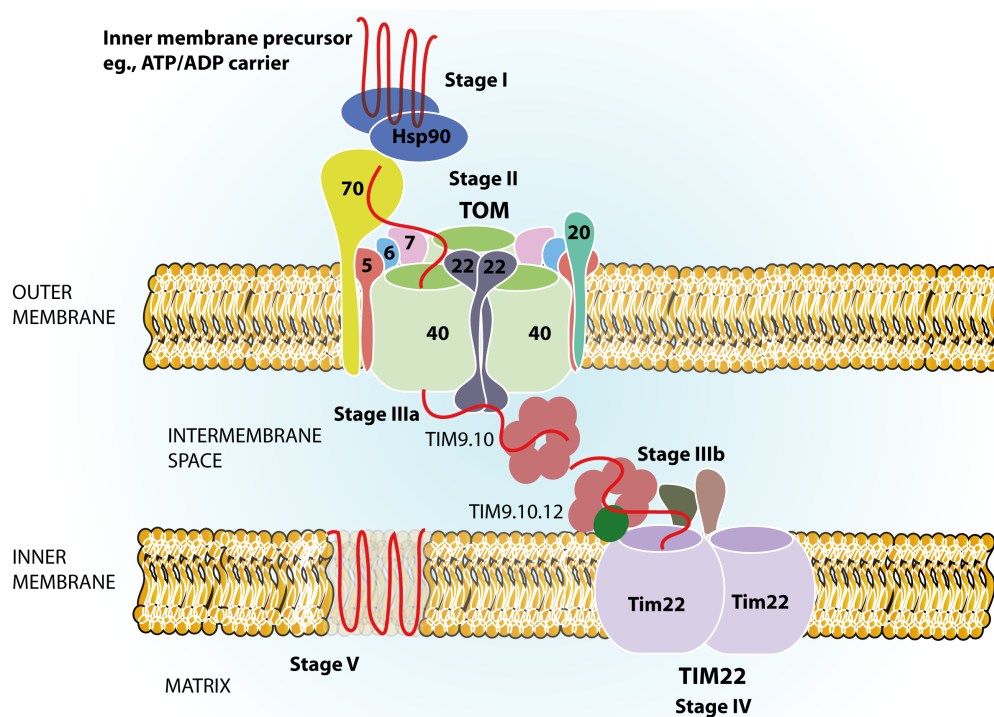


Figure 4: Schematic illustration of steps involved in translocation of carrier proteins. The hydrophobic precursor is targeted to the mitochondrial surface by cytosolic chaperones (Hsp90 and Hsc70; Stage I), engages with Tom70 (Stage II), and is translocated through the TOM complex partially folded. In the aqueous IMS, the TIM9.10 complex acts as a chaperone and binds to the precursor (Stage IIIa) until the precursor is transferred to the TIM22 translocase (Stage IIIb). Translocation occurs in a membrane potential dependent manner (Stage IV), followed by integration and assembly in the inner membrane (Stage V).

Despite extensive cellular characterisation of the pathway and identification of several transient precursor-translocase complexes along the way, none of the complexes have been captured by biochemical means using purified proteins. Structures of the complexes would help to address the issue of how precursors engage with the translocase components, the nature of the binding

interfaces and the mode of binding and transfer. Some of the challenges inherent in such studies are discussed in the following section.

1.6 Underlying problems in obtaining a complete picture of translocase function

Despite an enormous amount of information gained from identification and characterization of individual translocase components and some elements of translocation pathways, a complete picture of how mitochondrial translocases operate is still elusive. Dissecting out the molecular mechanisms of targeting and translocation has been largely difficult due to the following reasons:

- *Dynamics and complexity of translocation* – Interactions between translocase components and precursors, especially involving hydrophobic precursors, reported in whole cells or isolated mitochondria are difficult to reproduce *in vitro* with purified proteins; a general lack of reports in the literature is indicative. Our own attempts to capture a stable complex between human ANT, a hydrophobic precursor protein with hTIM9.10 or hTom70 were only partially successful. This may be due to the absence of unknown/unidentified co-factors, co-chaperones or regulatory mechanisms. It may be possible to capture precursor-translocase transient complexes with the reconstitution of a near complete system providing multiple translocase/chaperone components acting concertedly to mediate the process, but this approach is prohibitive with respect to time, cost, and likelihood of success.
- *Purified and validated translocases complexes are required for high-resolution structural studies* – In general, high-resolution structural studies using X-ray crystallography, NMR spectroscopy and more recently, cryo-EM contribute significantly to the elucidation of fundamental molecular mechanisms. High-resolution structures of mitochondrial translocases have not yet been achieved, with the recent cryo-EM structure of core TOM coming closest. Structure determination has been limited by the ability to obtain sufficient amounts of purified homogeneous material. The main challenges lie in the low abundance of translocases in native membranes, precluding direct purification from native sources. Problems in heterologous overexpression in *E. coli* include toxicity, misfolding, and the requirement for several subunits per complex. So far, the most successful approach reported has been the isolation of endogenous membrane translocase complexes from engineered strains of *Saccharomyces* and *Neurospora* with epitope tagged

sub-units, TOM via tagged Tom22 (Ahting et al., 1999, Model et al., 2008) and TIM22 via Tim18 (Rehling et al., 2003). High-resolution structures of soluble domains of individual translocase components have been determined, including those of *Saccharomyces* Tom70/71 (Wu and Sha, 2006, Li et al., 2009), rat Tom20 (Abe et al., 2000, Saitoh et al., 2007), TIM9.10 (Webb et al., 2006, Baker et al., 2009) and *Saccharomyces* Tim21 (Albrecht et al., 2006). Available crystal structures of the cytoplasmic receptor domains of Tom70/71 and the IMS TIM9.10 chaperone complex offer some insight into the precursor binding interfaces, but crystallising co-complexes or validating models experimentally has thus far proved intractable. While presequence peptide binding to the soluble receptor domain of Tom20 has been demonstrated, the important question of how the mature regions of precursors engage with the receptor and facilitate transfer remains unanswered.

1.7 Translocases in human health and diseases

Many of the translocase components are essential for survival, and loss-of-function mutations typically lead to neonatal lethality. For this reason, mutations in translocase components directly causing disease are rarely reported. Nevertheless, the indirect roles of some components in various pathological disorders have been documented. Up- or down-regulation of translocases and their involvement in import of pathogenic proteins and peptides play major roles in mitochondrial dysfunction.

Deafness dystopia and infantile autosomal recessive myopathy (ARM) are two rare genetically inherited syndromes that are caused by direct mutations in translocase components. Deafness dystopia, leading to hearing loss, mental retardation and blindness, is caused by X-chromosome-linked recessive mutations in the CX3C motif of TIMM8 gene, a component of TIM8.13 complex in the IMS. The mutations impair folding and assembly of TIM8.13 (Koehler et al., 1999, Tranebjaerg et al., 2000). Patients diagnosed with ARM contain a homozygous single-point mutation in sulfhydryl oxidase Erv1/ALR, a component of the MIA pathway (Di Fonzo et al., 2009, Daithankar et al., 2010). This syndrome is characterized by congenital cataracts, muscle hypotonia, hearing loss and developmental delay.

Translocase components have been implicated in various other disorders including cancer and neurodegenerative diseases. Overexpression of several human translocase components namely, Mia40, Tim17 and Tim50 have been reported as having a direct bearing on several cancer types (Wadhwa et al., 2006, Xu et al., 2010, Sankala et al., 2011).

1.7.1 TOM components implicated in diseases

Several human pathologies have been linked to components of the TOM complex. The core subunit, Tom40 has been linked to neurodegenerative disorders such as Alzheimer's, Parkinson's and Huntington's diseases. Polymorphisms in Tom40, along with apolipoproteinE (apoE), are classified as a primary genetic risk factor for Late-onset, sporadic Alzheimer's disease (LOAD) (Mise *et al.*, 2017, Zeitlow *et al.*, 2017). The import of the pathogenic amyloid- β peptide (Hansson Petersen *et al.*, 2008) or accumulation of α -synuclein through binding to Tom40 (Bender *et al.*, 2013) or Tom20 (Di Maio *et al.*, 2016), lead to mitochondrial dysfunction. Moreover, there is accumulating evidence that up- or down-regulation of Tom40 expression levels affects mitochondrial function and underlies neurodegenerative disease states. Tom40 mRNA expression was found to be significantly lower in the blood samples of Alzheimer's Disease (AD) patients in comparison to age-matched control patients (Goh *et al.*, 2015, Mise *et al.*, 2017). Similarly, Tom40 protein levels were found reduced in neuronal tissues of a murine model of Parkinson's disease (PD) against wild-type controls (Bender *et al.*, 2013). Also, Tom40 has been demonstrated to translocate influenza A viral protein leading to impairment of innate immunity (Yoshizumi *et al.*, 2014). Tom70 mediates the import of PINK1 (PTEN induced kinase 1), a mitochondrial kinase that recruits Parkin, both being involved in Parkinson's disease (Kato *et al.*, 2013). A truncation mutant of Tom22, identified in zebrafish, is causal in hepatocyte apoptosis (Curado *et al.*, 2010).

Some of the above-mentioned associations of TOM components with disease related polypeptides, as characterised by genetic, cellular and biochemical studies have led to suggestions they could serve as therapeutic targets (Gottschalk *et al.*, 2014, Yoshizumi *et al.*, 2014). While this may be possible, targeting any of these events for potential therapeutic or prevention strategies requires a detailed understanding of the molecular mechanism of translocation and factors influencing translocase activity.

1.8 Variability between translocases of yeast and higher eukaryotes

For over 30 years, ascomycetes *Saccharomyces* and *Neurospora* have served as excellent model organisms to study mitochondrial translocation, contributing significantly to a fundamental understanding of the processes. Similar studies undertaken in mammalian cell lines in recent years have highlighted commonalities and unique features, as well as differences. While the fundamental processes of translocation are essentially conserved from yeast to humans, considerable evolutionary distance between eukaryotic kingdoms shows up

in translocases as variability in topology, structure and function, as found by a number of studies, reviewed in Sokol *et al.* (2014). Moreover, some subunits present in humans (and other higher eukaryotes) lack homologues in yeast and *vice versa*. Key phylogenetic differences in TOM components are summarised in Table 1. Notable examples are also found in the IMS translocases and the TIM22 complex. In humans, TIM9.10 is exclusively found associated with the inner membrane, whereas in yeast it is present in the aqueous IMS region (Muhlenbein *et al.*, 2004). Mia40 is a soluble protein in humans, lacking the N-terminal transmembrane anchor characterising yeast Mia40 (Hofmann *et al.*, 2005, Chacinska *et al.*, 2008). There is significant difference in the subunit composition of TIM22 translocase between yeast and humans. Tim18 and Tim54 identified in yeast (Kerscher *et al.*, 1997, Kerscher *et al.*, 2000) have no homologues in humans. Two recently identified human TIM22 subunits, Tim29 (Callegari *et al.*, 2016, Kang *et al.*, 2016) and acylglycerol kinase (AGK) (Kang *et al.*, 2017, Vukotic *et al.*, 2017), appear not to have counterparts in yeasts.

Other features unique to higher eukaryotic organisms, including mammals, plants, worms and insects is the presence of multiple isoforms of several translocase components, such as Tom40, Tom20 and Tim17, and differences in tissue-specific expression patterns (Hwa *et al.*, 2004, Likić *et al.*, 2005, Kinoshita *et al.*, 2007). Although the functional relevance of having multiple isoforms is yet to be identified, it underscores the complexity of the mitochondrial import system in metazoans. In humans, three distinct TIM23 complexes, based on variations in subunit composition, have been identified (Sinha *et al.*, 2014), with one of these complexes specifically containing a Tim17a isoform that has been implicated in the import of oncoproteins lacking a presequence. *Saccharomyces* and *Neurospora* on the other hand, contain only a single TIM23 translocase.

Table 1: Differences in TOM subunits of fungi and humans

TOM sub-unit	Reported variations		References
	Fungi	Human	
Tom40	<p>Absence of multiple isoforms</p> <p>Shorter N-terminus region, not proline-rich</p> <p>An α-helix is predicted at the C-terminus</p>	<p>Two isoforms present</p> <p>The ubiquitous isoform has an extended N-terminal region, rich in proline residues</p> <p>Shorter C-terminus with no α-helix predicted</p>	<p>(Kinoshita <i>et al.</i>, 2007)</p> <p>(Mager <i>et al.</i>, 2011)</p>
Tom22	<p>A highly positively charged IMS domain</p>	<p>No highly positively charged IMS domain, instead has a glutamine-rich motif</p>	<p>(Yano <i>et al.</i>, 2000)</p>
Tom20	<p>Absence of multiple isoforms</p>	<p>Two isoforms present</p>	<p>(Likić <i>et al.</i>, 2005)</p>
Tom70	<p>Low sequence identity (20 %) to human Tom70</p>	<p>Human Tom70 does not substitute for yeast Tom70</p>	<p>(Young <i>et al.</i>, 2003b)</p>
Small Toms	<p>Tom6 stabilizes TOM assembly & Tom7 destabilizes TOM</p>	<p>Tom7 stabilizes TOM assembly, with Tom6 displaying little effect</p>	<p>(Alconada <i>et al.</i>, 1995)</p> <p>(Sherman <i>et al.</i>, 2005)</p> <p>(Kato and Mihara, 2008)</p>

1.9 Thesis outline

A major challenge to high-resolution structural analysis of TOM from higher eukaryotic animals has been the requirement of adequate amounts of functional purified complex, for which, appropriate means have not been established yet. Consequently, structure and organisation of metazoan TOM (of human, or of other higher eukaryotic organisms) has not been investigated so far.

In this thesis, as a new approach, *Drosophila melanogaster* is investigated as a host system for *in vivo* homologous expression of TOM core components, in an effort to isolate TOM for cryo-EM analysis and perform further structure-function correlation studies by exploiting the versatility of fly genetics.

The experimental aims of the thesis are as follows:

- i. assessment of *Drosophila* flies as a host system for functional expression of epitope-tagged Tom40 and Tom22
- ii. preparative-scale purification of *Drosophila* TOM from native fly membranes
- iii. preliminary structural analysis of purified translocase complex by cryo-EM

Chapter 2

Transgenic expression of TOM components in *Drosophila* and biochemical evaluation of purified TOM complex

2.1 Introduction

This chapter offers an introduction to *Drosophila* as an *in vivo* expression system and discusses its significant advantages for the study of mitochondrial translocases. It provides an account of optimisation of expression conditions for the core TOM components, Tom40 and Tom22, and their characterization. It also describes development of an efficient purification method for isolation of mitochondria-localised *Drosophila* TOM generated *in vivo*, and biochemical evaluation of the purified complexes to determine their suitability for cryo-EM analysis.

2.1.1 Production of eukaryotic membrane protein complexes for structural biology

Integral membrane proteins (IMPs) generally exist as homo- or hetero-oligomeric complexes rather than as isolated subunits. To obtain a clear understanding of how they function in a biological context, the determination of stoichiometry, subunit organization and the molecular structure of intact membrane protein complexes (MPCs) are prerequisites. A major bottleneck for such studies is the requirement of substantial amounts of purified material, with the difficulty increasing for recombinant hetero-oligomeric and/or eukaryotic MPCs. Select MPCs, like respiratory and photosynthetic complexes, by virtue of their natural abundance and biochemical stability, have been directly purified from native membranes and utilised for high-resolution structure determination by X-ray crystallography (Zouni *et al.*, 2001), X-ray free electron laser (XFEL) serial femtosecond crystallography (Suga *et al.*, 2015) and by cryo-EM in recent years (Vinothkumar *et al.*, 2014, Allegretti *et al.*, 2015). However, the majority of MPCs are sparse in native membranes and recombinant material has been the preferred option, in part for ease of expressing truncation or point mutants of the protein of interest. A variety of approaches have been taken to obtain sufficient quantities of purified MPC for structural analysis.

Specifically, for most hetero-oligomeric MPCs, two strategies are applicable as follows:

- Replacing an endogenous subunit with an affinity-tagged version, followed by affinity-based purification of an entire MPC, or
- Individual expression/co-expression of subunits in a heterologous host system of choice, followed by *in vitro* assembly

Although heterologous expression systems for production of membrane proteins have improved significantly over the years, overexpression and purification of eukaryotic hetero-oligomeric MPCs remains challenging. *E. coli* is the most widely employed host system for protein expression. While useful for the expression of many prokaryotic IMPs, it has not been as successful in the production of functional eukaryotic IMPs. Cytotoxicity, poor expression and/or misfolding of proteins are common owing to differences in membrane lipids and lack of appropriate folding and assembly machinery (Sahdev *et al.*, 2008). In addition, our observation is that many eukaryotic proteins typically undergo appreciable degradation or clipping in *E. coli*, possibly during growth, that is not significantly ameliorated by the presence of protease inhibitors during processing. As a result of one or more of the above-mentioned

issues, few structures of eukaryotic IMPs expressed in *E. coli* have been obtained (He *et al.*, 2014).

Various Tom40 constructs based on the sequences of a diversity of species, from yeast to human, have been attempted for expression in *E. coli*; but the protein is invariably found in inclusion bodies (Suzuki *et al.*, 2000, Mager *et al.*, 2011, Kuszak *et al.*, 2015). Inclusion bodies are insoluble aggregates of misfolded or partially folded protein molecules and may also contain other *E. coli* proteins such as chaperones. Non-integration into *E. coli* cell membranes could be due to the absence of export and membrane targeting signals in Tom40, or of host specific assembly factors. Refolded *Saccharomyces* Tom40 has been shown to differ in its electrophysiological and spectral properties from *Neurospora* Tom40 purified from native membranes (Hill *et al.*, 1998, Ahting *et al.*, 2001), which may indicate that refolded Tom40 does not form a native higher order structure, although this difference may also be due to species variation.

Eukaryotic expression systems such as yeast, baculovirus-infected insect cell culture and mammalian cell cultures are increasingly popular as a means of eukaryotic IMP expression. Proper post-translational modifications and the presence of right lipids, binding partners and assembly machineries are some of the benefits. Another is the ability to express point or truncation mutants for testing hypotheses. Baculovirus-infected insect cell cultures, in particular, have been highly successful for expression and purification of human G-protein coupled receptors (GPCRs) for structure determination (Rasmussen *et al.*, 2007, Haga *et al.*, 2012). Some disadvantages of insect and mammalian cell culture systems are the high cost and batch-to-batch variability in yields (Sunley and Butler, 2010, He *et al.*, 2014) and in some cases, build-up of immature proteins that are non-functional (Petaja-Repo *et al.*, 2000, Massotte, 2003).

With any eukaryotic expression systems, production of soluble, purified, recombinant Tom40, either by itself or co-expressed with associated TOM components, in amounts required for structural biology studies, has not been reported in the literature. Isolation of the entire native TOM complex from any higher eukaryotic source has not been reported.

2.1.2 *Drosophila* as an expression system for mitochondrial translocases

Drosophila melanogaster, commonly known as the vinegar- or fruit-fly, is a leading model organism for investigating metazoan biology, being widely employed in genetic and developmental biology studies for more than a century. Its tractability as an experimental

organism, combined with genetic homology to humans, ease of genetic manipulation and a short lifecycle, has placed it as a useful experimental model for investigating gene function and initial hypothesis testing. Notably, almost 75 % of disease-associated human genes have orthologues in *Drosophila* (Reiter et al., 2001) allowing for human cancers, neurodegenerative and cardiovascular diseases to be modelled in *Drosophila* (Pandey and Nichols, 2011, Prussing et al., 2013).

Drosophila offers several advantages for investigating a higher eukaryotic TOM complex, as presented in the following sub-sections. Most importantly, *Drosophila* offers the unprecedented potential of performing tandem structure-function studies *in vivo* in a multi-cellular organism and, including provision of phenotypic readouts.

2.1.2.1 *Drosophila* TOM subunits have high homology to human orthologues

At the start of this venture, an important point of consideration was the homology between *Drosophila* and human TOM components. Global pair-wise sequence alignments of human Tom40 and Tom22 performed against *Drosophila* and *Saccharomyces* orthologues demonstrated a high degree of conservation between *Drosophila* and humans (Fig. 1 and 2). Percentage identity/similarity calculations demonstrate that human TOM core components have higher homology to *Drosophila* orthologues than the *Saccharomyces* and *Neurospora* orthologues (Table 1.).

Table 1: Percentage of similarity/identity of TOM components between different species

Species	% Identity/Similarity to human orthologs		
	Tom40	Tom22	Tom7
<i>Drosophila</i>	51.8/65.5	38.3/54.5	49.1/63.6
<i>Saccharomyces</i>	23.5/40.1	18.2/32.4	25.0/45.3
<i>Neurospora</i>	22.6/39.3	20.6/37.5	33.3/63.2

It is to be noted that there are two paralogues of Tom40 identified in *Drosophila* namely, Tom40-1 and Tom40-2. Both these protein forms have high sequence identity, in all but the N-terminal region (see Appendix B). Tom40-2 (also known as Tomboy40) is expressed

predominantly in the male germ line (Hwa et al., 2004). Tom40-1 is ubiquitously expressed and was thus selected for sequence alignments and homology calculations. Two isoforms of Tom40 have also been reported in mammalian systems; in the rat genome, in addition to the ubiquitous isoform, a shorter isoform, ‘Tom40B’ is expressed in all tissues except the testis. The Tom40B gene was found to be present in human, monkey, mouse and dog DNA databases as well (Kinoshita *et al.*, 2007). The potential physiological relevance of the tissue specific expression of Tom40 paralogues in higher eukaryotes is currently unclear.

There is only one orthologue of Tom22 in *Drosophila*, known as Maggie. Loss-of-function mutations in *Drosophila* Tom22 arrest development in the larval stage (Vaskova *et al.*, 2000). Two shorter alternate splice variants of *Drosophila* Tom22 have been annotated in the Uniprot protein database (primary accession numbers, Q9I7T5 and M9PEJ). RNA sequencing data presented in FlyBase, a *Drosophila* data repository, indicate that the Q9I7T5 variant is expressed mostly in pupal stages and adult males (Graveley *et al.*, 2010).

2.1.2.2 An established UAS-GAL4 based *in vivo* protein expression system

In *Drosophila*, a targeted protein expression system based on the bipartite UAS-GAL4 transcriptional switch in yeast, was developed by Brand and Perrimon (1993). This highly versatile and powerful tool, described as a ‘fly geneticist’s Swiss Army knife’ (Duffy, 2002) has been primarily employed to investigate gene function during animal development (Rodríguez *et al.*, 2011, Rodal *et al.*, 2015). This system allows for controlled or tuneable expression of any cloned homologous or heterologous gene not only in desired tissues, but also during specific developmental stages and/or in a temperature-sensitive manner. GAL4 strains with a variety of promoter elements have been generated and made available in the *Drosophila* research community for this purpose (e.g., The Bloomington Stock Center, Indiana).

In this system, the UAS-transgene and promoter-driven GAL4 (a yeast transcriptional activator binding upstream activating sequences (UAS) sites), are brought together by crossing paternal fly strains (Fig. 3). GAL4 expression is dictated by the promoter elements derived from the particular endogenous gene, enabling cell and developmental time point specific expression. Thus, when the ‘UAS-responder’ and ‘GAL4-driver’ strains are mated, GAL4 binds to the Upstream Activating Sequence (UAS) and induces expression of the downstream gene of interest in specific tissues of the progeny that are defined by the GAL4 promoter element. This can be selected to drive expression in a particular tissue or at a specific stage of larval or fly development. For example, a Tubulin promoter drives expression in all tissues in a ubiquitous

A.

```

TOM40_Hs  MGNVLAASSPPAIPPPPAPAI-VGPPPPSPPGFTPLGLGAGSTSRSETPGAATASASGAEAGCGCPNPGTFECHRKCKELFPIQMEVLTV
TOM40_Dm  MGNVLAASS-----AAGSGSNGLDQEA-----SNSST-----ESLSAAGLDSL-----SKA-----E-----V-----L-----K-----DIQA-----TF-----A-----IML
*****      *.*.....* :*.....*      **.....**      *.*.*:*.....*      **.*.*      *.....**.*:*.....*:*.....*:*.....*

TOM40_Hs  RGLSNRFDNVALTIGENHGVTVGTVQLPTEAFPVLMNSLSAQVILGLPGSSMLITQSFNWDGEGRNFPAAVLGLDVL
TOM40_Dm  RGLSNRFDNVALTIGENHGVTVGTVQLPTEAFPVLMNSLSAQVILGLPGSSMLITQSFNWDGEGRNFPAAVLGLDVL
*****:*.*:*.....*:*.....*:*.....*:*.....*:*.....*:*.....*:*.....*:*.....*:*.....*:*.....*:*.....*:*.....*

TOM40_Hs  VGSILVAHYLQSITPCLALGGLVTH---RRPCEEGTVMSLAGKYTLNWLATVTLGQAMHATYHKASDQLQVGFVFASTRMQDTSVVSFGVQLDLPKANLLF
TOM40_Dm  TNSGVVVGQYLSVFPALALSRLAYQFGPNVGRQIAIMSVVRYTAGSSVWSGTLGCSLHVCYQKASDQLQIGAVTFLRMCESVATLAVCIDLPKANLVE
..*:*.....*:*.....*:*.....*.....*.....*.....*.....*.....*.....*.....*.....*.....*.....*.....*.....*.....*

TOM40_Hs  KSVDSNWIVGATLEKKLPPLPLFLALGAFLNHRKPKFQCFGLITG
TOM40_Dm  RCGDSNWQIFGVLEKRIAPLFLALSGRMNVNFRKCGGLMIG
:*.....*.....*.....*.....*.....*.....*.....*.....*.....*.....*.....*.....*.....*.....*.....*.....*.....*

```

B.

```

TOM40_Hs  MGNVLAASSPPA-GPPPPAPAI-VGPPPPSPPGFTLPPLGLGAGSTSRSETPGAATASASGAAAGACGCNPNPGTFECHRKCKELFPI--MEV
TOM40_Sc  ----MSAPTELEASQIPTIPALSPITAKQSKGNFTSSNFI-SFVVDYKQLHSHRQ-----SL-----LVNPGTVENLNKEVSRDVFLSYFFFTGL
:*.....*.....*.....*.....*.....*.....*.....*.....*.....*.....*.....*.....*.....*.....*.....*.....*.....*

TOM40_Hs  KLTVNRGLSNH--FCVNHTVALSTIGESNHGVTVGTVKQLSPTTEAFPVLMNDNSGLNAQVIHQLGPLRSKMAITQQSKFVNWDGEGYRGSDFTAAT
TOM40_Sc  RADLNKAFSMNPAFGTSHTFSIGSQALPKAASALFANDNLFAQ-----GNIDNDLVSGRLNYGWDKKNISKVNLISDGOPTMCLQDYQASDFSVNKK
*.....*.....*.....*.....*.....*.....*.....*.....*.....*.....*.....*.....*.....*.....*.....*.....*.....*

TOM40_Hs  LGNEFDVLVG---SILVAHYLQSITPCLALGGLVTHR---RRPCEEGTVMSLAGKYT--LNNWLATVTLGQAMHATYHKASDQLQVGFVFASTR-----
TOM40_Sc  TLNFSFSEKGEFTVAVASFLQSVTPQLALCLTLYSFTDGSAPCDAG--VYLTRYVSKKQDIFSGQANALIASLWRVAQNVEAIFTTLQAGVPIITD
..*.....*.....*.....*.....*.....*.....*.....*.....*.....*.....*.....*.....*.....*.....*.....*.....*.....*

TOM40_Hs  -----D-----SVSFYQLDLPKANLLFKSVDSNWIIVGATLEKKLPPLPLFLALGAFLNHRKPKFQCFGLITG-----I-----
TOM40_Sc  PLMGTPIGIPVEGTTIAKYEYRQS--VYR-----TL-----GKACF-----R-----V-----L-----S-----V-----F-----E-----I-----D-----F-----D-----T-----K-----I-----C-----Q-----F-----E-----A-----N-----Q-----E-----L-----L-----M-----L-----Q-----G-----L-----D-----A-----D-----G-----N-----P-----L-----Q-----A-----L-----P-----Q-----L
*.*      *.....*.....*.....*.....*.....*.....*.....*.....*.....*.....*.....*.....*.....*.....*.....*.....*.....*

```

Figure 1. Sequence alignments of Tom40. Pair-wise sequence alignment of *Homo sapiens* (Hs) Tom40 sequence against **A)** *Drosophila melanogaster* (Dm) and **B)** *Saccharomyces cerevisiae* (Sc) homologues. Alignments were performed using EMBOSS Needle program (EMBL-EBI). Primary accession numbers of Hs, Dm and Sc Tom40 sequences used are O96008, Q9U4L6 and P23644 respectively.

manner, whereas a Glass Multiple Reporter (*GMR*) promoter directs expression specifically in the developing eye, in the photoreceptor and surrounding cells posterior to the morphogenetic furrow (Freeman, 1996).

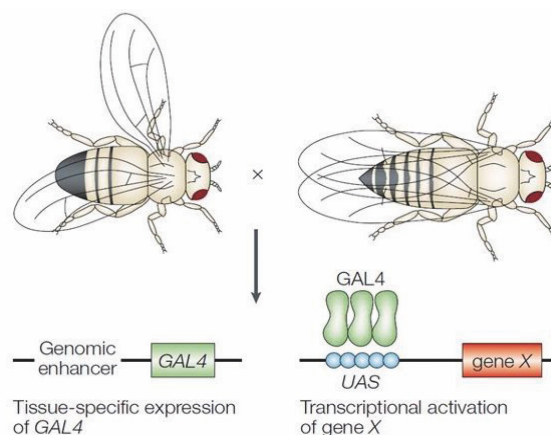


Figure 3. UAS-GAL4 protein expression system in *Drosophila*. Image adapted from St Johnston (2002). In one parental fly strain, promoter regions for a particular gene drive expression of the yeast transcription factor GAL4 in defined tissues. In the other fly strain, GAL4 response elements (UAS) are upstream of the desired transgenic element. When the two strains are mated, the progeny express the transgene in specific tissues, directed by a GAL4 promoter element.

Experimental trials for genetic and cell biology studies require only small-scale cultures in the order of a few hundred flies. On the other hand, utilization of this system for obtaining the milligram amounts of purified protein required for structural biology studies demands a significant scale-up. Although this kind of approach is uncommon, it has been applied previously. Histidine-tagged version of skeletal muscle myosin II isoforms were expressed in flies and purified in mg quantities sufficient for production of crystals (Caldwell *et al.*, 2012). More significantly, expression of membrane proteins has been achieved; by targeting protein expression to the rhabdomere membranes of fly eyes, the Sinning laboratory (Panneels *et al.*, 2011) demonstrated expression of GFP fusions of human G-protein coupled receptors (GPCRs), transporters and channels to a level comparable to the native fly rhodopsin and were able to purify these to homogeneity in quantities sufficient for crystallography, albeit crystals were not reported subsequently. An earlier study by the same group found that the yield of

Drosophila metabotropic glutamate receptor, a member of the GPCR family from fly heads was at least 3-fold higher than from baculoviral culture (Eroglu *et al.*, 2002).

2.1.3 Overview of *Drosophila* biology and genetics

This section provides a brief introduction to fly biology and will describe elements of fly genetics, definitions, uses and applicability, of relevance to the thesis.

2.1.3.1 Life cycle and physiology

Drosophila undergo a four-stage life cycle comprising embryo, larvae, pupae, and adult, over a period of approximately ten days (at 25 °C) (Fig. 4). Once fertilized, each embryo develops in the eggshell for approximately 24 hours before hatching as a larva. The larva eats, grows and goes through three molts over five days before pupating. Metamorphosis into an adult fly occurs over the course of five days. During metamorphosis, larval tissue no longer required for adult life cycle is removed through histolysis. The adult tissues (e.g., wing, leg, eye, brain) are remodelled from “imaginal discs” present since early embryonic development.

In the laboratory, all these stages take place in a culture vial containing a solidified food source (shown in Fig. 4), made up of basic ingredients including cornmeal, sugar and yeast.

2.1.3.2 *Drosophila* chromosomes

The *Drosophila* genome contains four sets of chromosomes. Chromosome 1 is the heterosomal sex chromosome (X/X or X/Y) and chromosomes 2, 3 and 4 are autosomes. Chromosome 4 is extremely small, containing very few genes. Thus, chromosomes 1, 2 and 3 are the focus of genetic manipulation and research. Standard nomenclature in fly genetics utilises a “+” for wild type with the four chromosomes separated by a “;” (i.e., a wild-type fly would be represented as +;+;+;+). The two alleles of sister chromosomes are separated by a bar, either “/” or “_”. The ‘+’ sign is substituted by descriptions of any genetic modifications. Usually, for ease of writing, only chromosomes that have been modified or are the focus for a particular experiment are denoted.

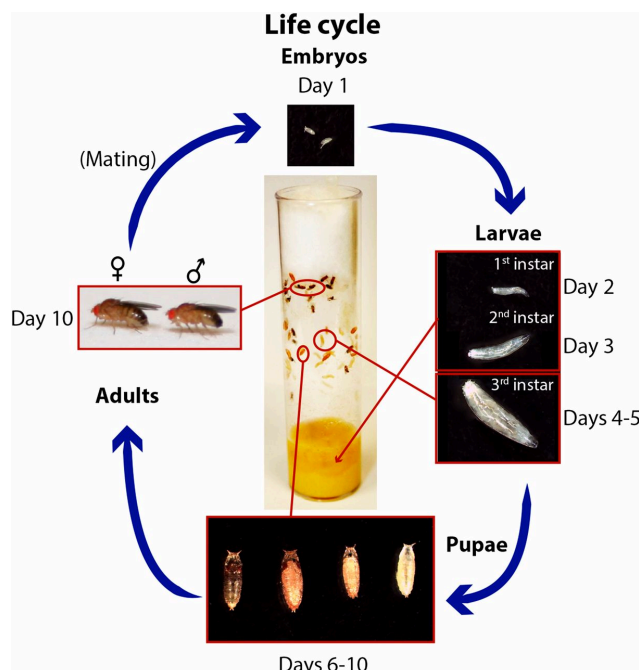


Figure 4. Life cycle of *Drosophila*. In the laboratory, *Drosophila* are reared in vials with solidified food in the bottom and closed with a cotton plug at the top. The vial in the image shows each major stage of the life cycle, which is completed in approximately ten days when flies are maintained at 25 °C. Embryos hatch from the egg laid on the food after ~1 day and spend ~4 days growing as larvae in the food. Around day 5, third instar larvae crawl out of the food and pupate on the sides of the vial. During days 5 - 10, metamorphosis occurs, and adult flies emerge from pupal cases around days 9 - 10. Image reproduced from Hales et al. (2015).

2.1.3.3 Balancers and markers

Drosophila geneticists have developed a useful genetic tool known as ‘balancers’ for maintenance of an introduced gene of interest or mutation in a fly strain, which work by preventing meiotic recombination. Balancers for each of the major chromosomes have been developed (Lindsley and Zimm, 1992). Some of the most commonly used are listed in Table 2. These are engineered chromosomes carrying multiple inversions with significant rearrangements of genes, meaning that crossing of ‘balanced’ transgenic flies ensures that the gene of interest is inherited by the offspring. In addition, as all balancer chromosomes contain recessive lethal mutations *i.e.*, they are not viable when homozygous, genes or mutations will not be selected out of an inbred population. Thus, balancing enables fly stocks to be maintained

in a heterozygous state in instances where a gene is homozygous lethal. A major advantage experimentally, is that one does not need to manually select and mate hundreds of flies each generation to maintain the introduced gene, enabling mass stock transfer.

Balancers also possess added dominant marker mutations enabling the chromosomes inherited to be followed during genetic mating schemes (Ashburner *et al.*, 2005). These mutations manifest as variations in body colour, eye colour and shape, wing shape and bristle length. For example, rather than the usual round eye the *FM7* balancer contains the bar mutation, which results in a bar-shaped eye. The *SM6a* balancer contains the *CyO* marker and has curly wings unlike straight-winged wild-type flies. *TM6B* flies have additional bristles on the shoulder due to the *Humeral* marker and are distinguished in the larval and pupal stages as being shorter and fatter than wild-type due to the *tubby* marker. Other independent markers are also available and are used in conjunction with balancers during multi-generational crossing schemes for following chromosomes and genetic selection purposes

Table 2. List of commonly used balancer chromosomes

Chromosome	Balancer(s)	Examples of associated phenotype markers
X	<i>FM7a</i> (1st multiply-inverted 7a)	reduced bar-shaped eyes
	<i>FM7c</i> (1st multiply-marked 7c)	reduced bar-shaped eyes
2	<i>CyO</i> (Curly derivative of Oster)	curly wings
	<i>SM6a</i> (2nd multiply-inverted 6a)	curly wings
3	<i>TM3</i> (3rd multiply-inverted 3)	serrated wing tips
	<i>TM6B</i> (3rd multiply-inverted 6B)	additional humeral bristles shorter and fatter larvae

2.2 Schematic overview of experimental strategy

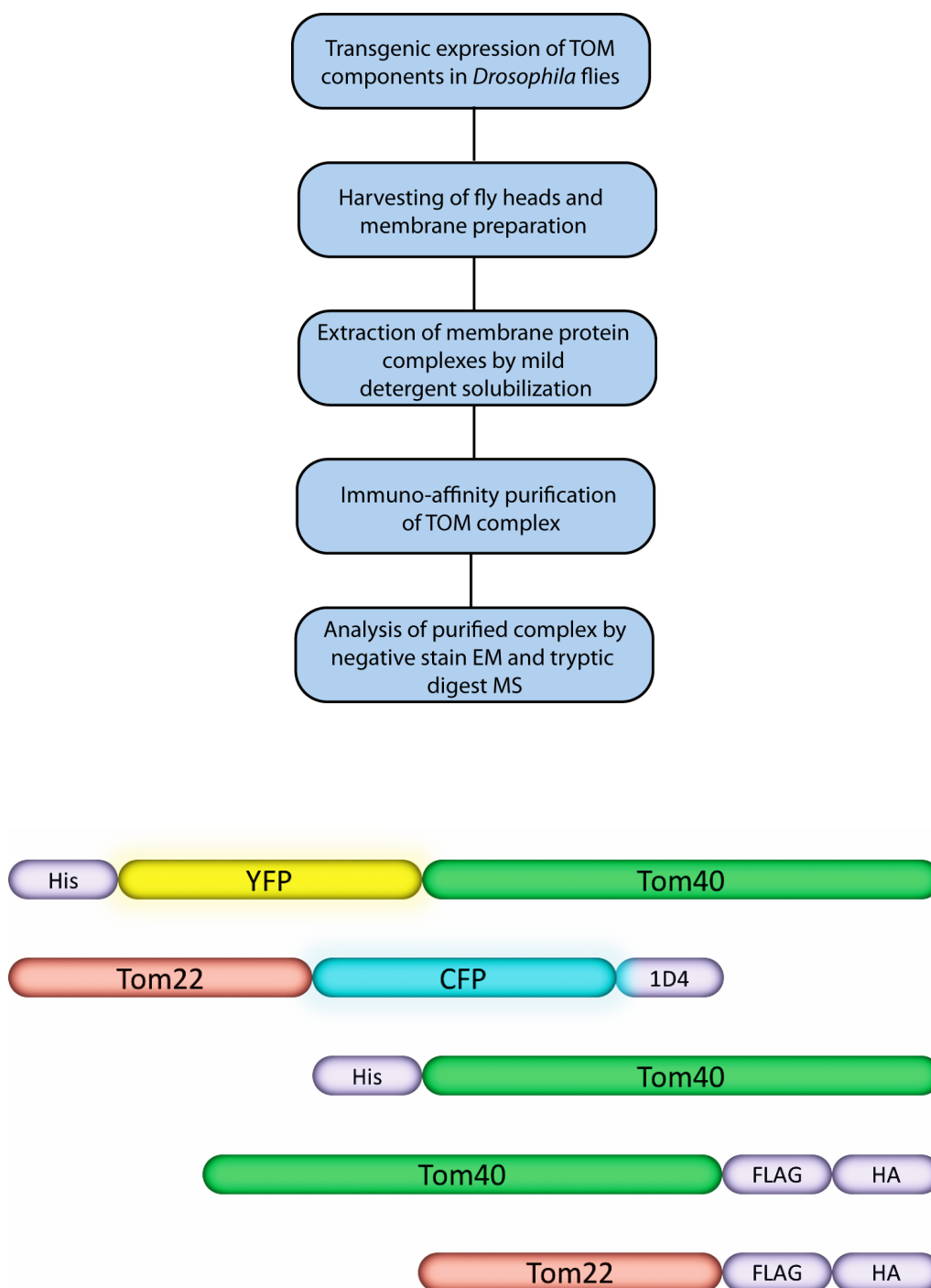


Figure 5. Schematic of Tom40 and Tom22 constructs utilised for expression trials. A set of Tom40 and Tom22 constructs were designed to accommodate a YFP or CFP fusions respectively, for potential FRET analysis, alongside affinity tags. Other constructs contained short affinity tags such as 8x-His, 1D4 or FLAG.HA placed at either the N- or C- terminus.

2.3 Experimental considerations

At the start of the *Drosophila* project, the question arose as to whether to use the transgenic system to express human or *Drosophila* TOM components. Although it is possible to express the human components in *Drosophila*, we opted to use the *Drosophila* counterparts (which display very high homology to human TOM) to avoid potential problems with endogenous components co-assembling into hetero-complexes. Silencing of the *Drosophila* counterparts and heterologous expression of human homologues was contemplated, but not taken forward owing to the greater technical challenges, particularly given the lethality associated with the loss of TOM function (Vaskova *et al.*, 2000, Peter *et al.*, 2002)

2.3.1 Tag selection for protein expression

Transgenic fly strains containing variously tagged versions of Tom40 and Tom22 (schematic of constructs in Fig. 5) were tested for expression in larval and adult fly tissues. The first fly strains tested were UAS-8xHis-YFP-Tom40 and UAS-Tom22-CFP-1D4, which contained FRET-compatible fluorescent protein fusions alongside affinity tags: an octahistidine tag for Tom40 and a rhodopsin based antibody epitope tag, 1D4 (Molday and Molday, 2014) with an amino acid sequence of TETSQVAPA for Tom22 for purification purposes. Fluorescent protein tags, appropriately positioned, offer advantages in terms of monitoring of protein expression *in vivo* and for purification (Hammon *et al.*, 2009) and have been used on Tom40 in cellular experiments (Humphries *et al.*, 2005, Kuzmenko *et al.*, 2011). A FRET compatible pair was generated for probing inter-subunit interaction and dynamics, both *in vivo* and *in vitro* (Lippincott-Schwartz, 2011, Crivat and Taraska, 2012). However, no expression was detected in these fly strains when driven with the ubiquitous *Tubulin*-GAL4 driver, as analysed by SDS-PAGE and western blotting. It is possible that the addition of bulky fluorescent tags at N or C-terminus was detrimental to protein expression, post translational processing or folding and assembly.

In this light, another fly strain, UAS-8xHis-Tom40, lacking a fluorescent tag was tested. In this case, expression was observed in larval tissues as well as adult tissues when ubiquitously expressed using the *Tubulin*-GAL4 driver or specifically expressed in the eye using the *GMR*-GAL4 driver. This data indicated that N-terminal tagging of Tom40 was not deleterious for expression, but that the nature of the tag was critical. However, this fly line was not used for further studies due to issues encountered during downstream purification. In brief, several endogenous *Drosophila* proteins bound non-specifically, to Tom40 and the Ni²⁺ resin used for

affinity purification, which were difficult to separate away by gradient affinity chromatography. Moreover, the monoclonal His-antibody employed for western blot analysis reacted non-specifically with endogenous proteins, complicating further analysis.

Following this, Tom40 and Tom22 fly strains with alternate antibody epitope tags, namely UAS-Tom40-FLAG.HA and UAS-Tom22-FLAG.HA were trialled. These were obtained from Bangalore Fly Resource Centre, India, generated as part of a *Drosophila* Protein interaction Map (DPiM) project (Guruharsha *et al.*, 2012). Successful expression was achieved with both fly strains; antibody-based affinity purification methods were developed for subsequent isolation of *Drosophila* TOM as discussed below.

2.3.2 Deliberations and issues during purification trials

The purification of TOM complexes was established by empirical means. Using the two strains UAS-Tom40-FLAG.HA and UAS-Tom22-FLAG.HA, specific issues pertaining to various stages of the process were investigated as follows:

- Choice of fly strain for pull-down
- Crude purification step: mitochondria or total cellular membranes
- Choice of immuno-affinity resin
- Tolerance to additional wash steps, *in lieu of* size exclusion chromatography

2.3.2.1 Fly strain for pull-down: Tom40 or Tom22

Tagged Tom22 is invariably used as the bait to isolate TOM complexes from *Saccharomyces* and *Neurospora* membranes (Ahting *et al.*, 1999, Model *et al.*, 2008). In this study, initial attempts to pull-down TOM were trialled with both tagged core components Tom40 and Tom22 for comparison. Both Tom40 and Tom22 were able to pull out a supramolecular TOM complex (~480 kDa) from a membrane preparation, albeit in varying proportions. The pull-down *via* tagged Tom40 gave higher protein yields overall, and hence was chosen to obtain material for large-scale purifications.

2.3.2.2 Starting material: mitochondria versus total membranes

A differential centrifugation method (refer section 2.6.4.2) for isolation of crude intact mitochondria (from fly heads) proved inefficient. It was found that only approximately half of the total amount of epitope tagged Tom40 and Tom22, as well as a mitochondrial marker

protein, VDAC, came down with this fraction. The remainder was detected in microsomal fractions prepared by high speed ultracentrifugation post the mitochondrial fractionation step. A ‘microsomal’ membrane fraction collected at 100,000 x g is an inclusive term for plasma membranes and other organellar membranes such as ER, Golgi, endosomes etc. The presence of endogenous mitochondrial protein VDAC in this fraction suggested that some mitochondria were broken or fragmented during the isolation procedure. Since the goal was to enrich the starting material, we proceeded by pelleting total membranes from lysates, with mitochondrial fractionation omitted, ensuring the collection of both intact and fragmented mitochondria for increased yields.

2.3.2.3 Immuno-affinity purification: HA- or FLAG-based antibody resin and stringent washes

Taking advantage of the tandem FLAG.HA tag, affinity purification was tested using both HA and FLAG antibody coupled resins. The HA-based purification proved sub-optimal; a persistent contaminant (identified by mass spectrometry as innexin channel) formed pore-like structures that were difficult to differentiate from the TOM complex in negative stain EM (data not shown). Also, poor elution efficiency using HA peptide resulted in low yields of purified sample.

FLAG-based purification, by comparison, exhibited superior binding and elution efficiencies translating to higher protein yields. However, some non-specific contaminating proteins eluted with TOM, as judged by silver staining (data not shown). To address this, inclusion of a size exclusion chromatography step was explored. However, a substantial loss of protein during this step adversely impacted on the final yields. Thus, additional on-column urea and high salt washes were tested as a means of eliminating non-specific contaminants. Successive washes at concentrations not detrimental for the stability of the complex (section 2.4.4.2) were incorporated into the protocol prior to elution of the translocase under a non-denaturing excess of FLAG peptide. The approach was successful in improving the purity of the TOM sample, which showed clear single particles with only limited aggregation or contaminating particles when screened by negative stain EM (detailed in Sections 2.4.5 and 2.4.6).

2.4 Results

2.4.1 Expression of FLAG.HA tagged-Tom40 and Tom22 in *Drosophila* flies

UAS-Tom40-FLAG.HA and UAS-Tom22-FLAG.HA (henceforth referred to as Tom40 and Tom22) were tested for expression with *Tubulin*-GAL4 and *GMR*-GAL4 driver strains, corresponding to global and eye-specific expression, respectively. Tissue lysates of ten progeny (whole flies or heads) were subjected to SDS-PAGE and transferred to PVDF membranes by electrophoresis. Western blot analysis using an anti-HA antibody showed positive expression for Tom40 and Tom22 with both drivers, in comparison to wild-type (w1118 strain) controls. Expression of both Tom40 and Tom22 lines were superior when the eye-specific driver, *GMR*-GAL4 was used (Fig. 6). Protein expression was quantitatively higher, with lower degradation overall, in comparison to global expression using *Tubulin*-GAL4; likely a consequence of the relatively higher expression of *GMR* in the eye. Following these experiments, *GMR*-GAL4 based expression was selected for further characterization.

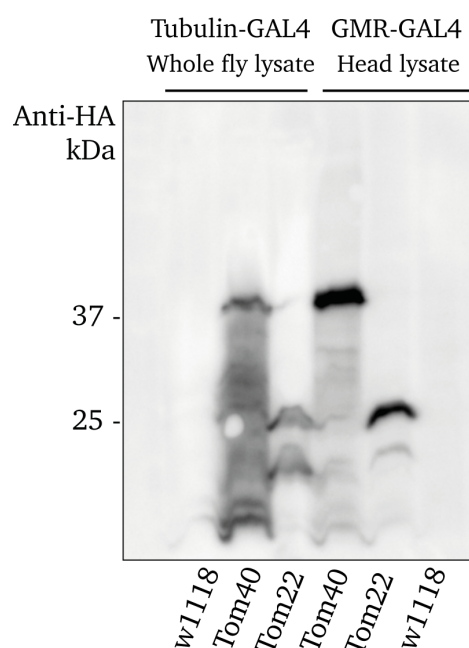


Figure 6. Tom40 and Tom22 expression analysis by western blotting. Expression of Tom40 and Tom22 was tested with *Tubulin*-GAL4 and *GMR*-GAL4. Tissue lysates of ten progeny (whole flies or heads) were subjected to SDS-PAGE and immunodetection was performed using an HA antibody. Protein expression induced by *GMR*-GAL4, targeted to the eye, yielded relatively higher expression levels and fewer degradation products.

2.4.2 Eye-specific expression of TOM subunits and subcellular localization analysis by immunofluorescence confocal imaging

Induction of protein expression by *GMR-GAL4* occurs specifically in the third in-star larval stage and continues through the adult lifespan. Thus, we analysed the expression pattern of Tom40 and Tom22 in larval imaginal eye discs by immuno-staining with HA antibody against the epitope tag. Both proteins were found to be distributed around the nuclei (Fig. 7), confined to the region posterior to the morphogenetic furrow where photoreceptor cells differentiate.

The subcellular localisation of Tom40 was further investigated by co-expression with an enhanced Yellow Fluorescent Protein (eYFP) molecule fused to a signal sequence that directs it to the mitochondrial matrix (LaJeunesse *et al.*, 2004). Immuno-staining analysis showed some overlap between Tom40 (red) and mito-eYFP (green) signals (Fig. 8), suggesting mitochondrial localisation of epitope tagged Tom40. However, while the mito-YFP signal was distributed evenly around the nuclei (blue), Tom40 appeared in a more restricted punctate pattern. The reason behind this is unclear, but one interpretation might be that TOM complexes cluster at mitochondrial cristae junctions (Gold *et al.*, 2017).

2.4.3 Integration of tagged TOM subunits into higher order complexes as assessed by BN-PAGE

To evaluate whether tagged versions of Tom40 and Tom22 assembled into higher order complexes by association with endogenous TOM subunits, isolated mitochondria were solubilised with digitonin, a mild detergent well-documented for extraction of intact TOM complexes (Model *et al.*, 2002). Digitonin-solubilised membranes subjected to BN-PAGE were analysed by western blot analysis using an HA antibody against the epitope tag. Both Tom40 and Tom22 co-migrated with higher order complexes of a nominal mass of ~480 kDa (Fig. 9). Migration of the band on BN-PAGE was consistent with that observed for *Saccharomyces* and mammalian TOM complexes (Dekker *et al.*, 1998, Saeki *et al.*, 2000). *Drosophila* Tom40 also migrated in bands at ~146 kDa and ~720 kDa, suggesting a sub-complex and super-complex, respectively. The ~146 kDa assembly is likely to correspond to an intermediary assembly of dimeric Tom40 (Model *et al.*, 2001, Shiota *et al.*, 2015). The super-complex, on the other hand, suggests associations with other translocase complexes, perhaps SAM (Qiu *et al.*, 2013), TIM23 (Waegemann *et al.*, 2015) or TIM22 (Kang *et al.*, 2016), as reported.

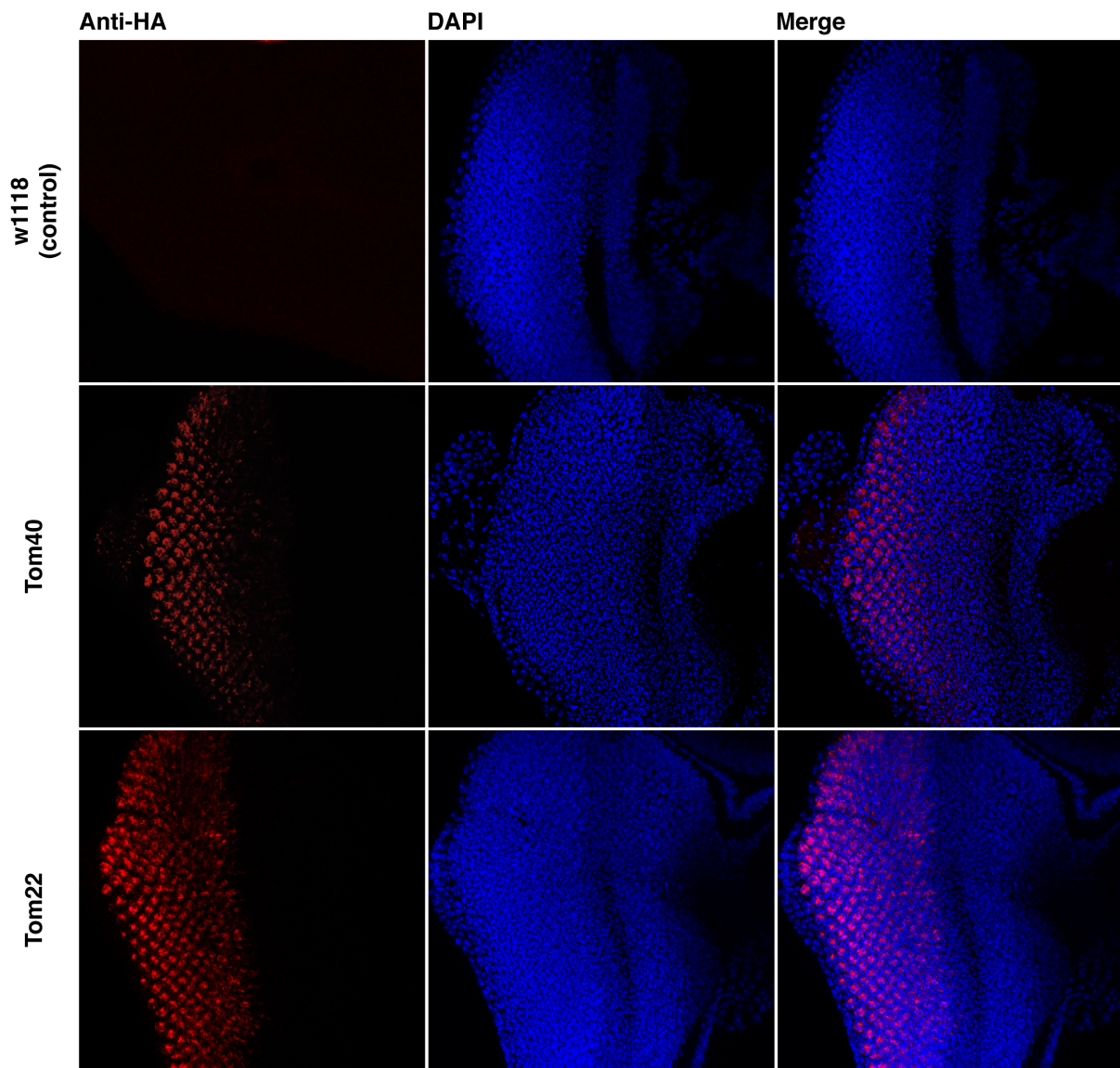


Figure 7. In situ expression analysis of Tom40 and Tom22. Immunofluorescence confocal imaging analysis of Tom40 and Tom22 expression in imaginal eye discs of third instar Drosophila larvae stained with HA antibody. GMR-GAL4 based expression of Tom40 and Tom22 (coloured in red) was found to be localized around the nuclei (coloured in blue) in the posterior region of eye discs.

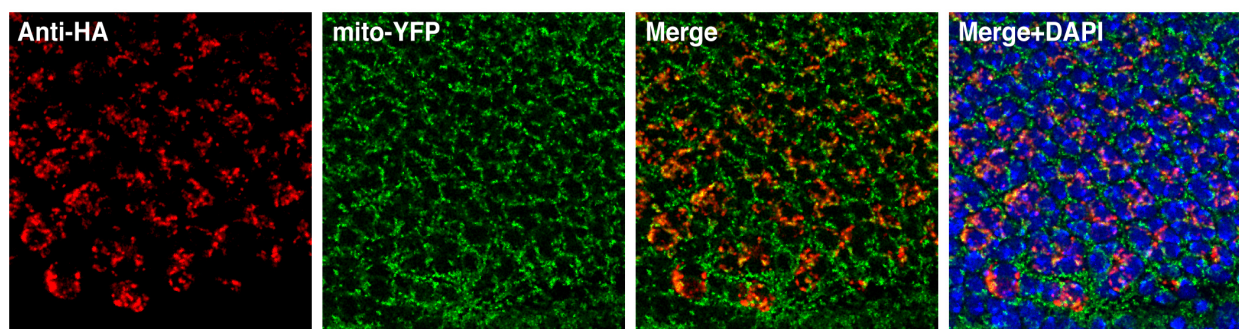


Figure 8. Sub-cellular localisation of epitope-tagged Tom40. Imaginal eye discs from third instar *Drosophila* larvae expressing mitochondria targeted eYFP (mito-eYFP) and UAS-Tom40 were immunostained with HA antibody. Confocal fluorescence microscopy showed some overlap (yellow) between the eYFP (green) and Tom40 (red).

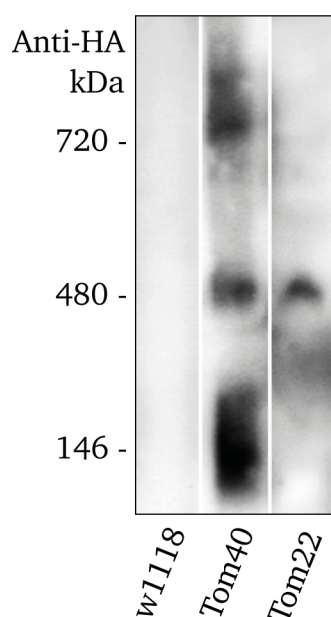


Figure 9. Assessment of tagged Tom40 and Tom22 integration into higher-order complexes. Digitonin-solubilised mitochondria were separated by BN-PAGE. Western blot analysis showed that epitope-tagged Tom40 and Tom22 assembled into a higher order complex of ~480 kDa. Additional bands were observed with Tom40, around 146 kDa and 720 kDa indicating the presence of Tom40 containing sub- and super-complexes

2.4.4 Extraction and stability testing of Tom40 complexes using BN-PAGE

BN-PAGE western blot analysis of tagged Tom40 membranes solubilised with digitonin reproducibly displayed the characteristic three-band pattern shown previously (Fig. 9). Further, extraction properties of various detergents and the conditions that the complexes would tolerate without falling apart were assessed.

2.4.4.1 Detergent screening

A selection of detergents with differing qualities were screened to identify candidates able to extract a ~480 kDa TOM complex while maintaining its structural integrity. Suspensions of Tom40 membranes in buffer were divided into several aliquots, each solubilised with a high concentration of detergent (1 % w/v) and analysed by BN-PAGE and western blotting. Figure 10 shows the results from a panel of nine detergents with subtle variations in chain length, functional groups and micellar properties. Relative to digitonin, glyco-diosgenin (GDN), a synthetic alternative, was able to extract complexes that migrated similarly to digitonin. LMNG reproducibly extracted a complex that migrated slightly faster than digitonin, indicative of a more compact molecule. Other detergents typically used for extraction and stabilisation of membrane proteins such as DDM and Triton X-100 were unsuccessful in extracting a ~480 kDa complex. Most, irrespective of chain length or headgroup chemistry, showed only a lower order band just above the 66 kDa standard, suggesting disassociation of the quaternary translocase complex.

2.4.4.2 Effect of salt and urea

The stability of Tom40-containing complexes in digitonin solubilised membranes was challenged by varying concentrations of sodium chloride (NaCl) and urea. This was done in order to determine the maximum tolerable concentrations that may serve useful for designing wash steps during later purification attempts. Urea, a chaotropic agent used as a denaturant at concentrations of 8 M, is known to disrupt hydrophobic interactions whereas NaCl, drives such interactions. BN-PAGE and western blot analysis of digitonin-solubilised samples demonstrated the differential stability of the complexes under the conditions tested (Fig. 11). Under increasing concentrations of NaCl (up to 2 M), no change in the banding pattern of the digitonin-only sample was observed, signifying hydrophilic interactions were not important in maintaining the complex. Lower concentrations of urea (up to 2 M) did not affect the stability of the complexes, as would be expected. At higher concentrations, however, gradual dissociation into lower order bands was observed. At 4 M urea, the super-complex was not

detected and a slight shift in size of the sub-complex was observed, while the ~480 kDa complex was unaffected. At the higher urea concentration of 6 M, only a single band just above the 66 kDa standard was observed, similarly sized to Tom40 bands when solubilized with harsher detergents (Fig. 10 and Fig. 11). The behaviour of the ~480 kDa Tom40 complex concurs with that of the yeast TOM complex tested under similar salt and urea conditions (Dekker et al., 1998, Meisinger et al., 2001).

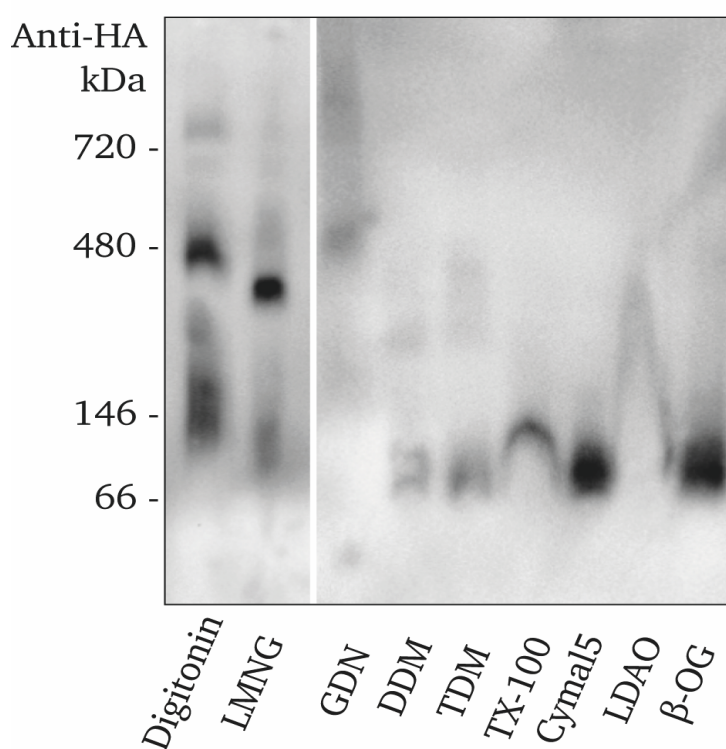


Figure 10. Detergent screening for extraction of entire putative TOM complex. Tagged Tom40 membranes were solubilised with various detergent classes, as labelled in the image. BN-PAGE-western blotting analysis showed that, in addition to digitonin, LMNG and GDN were capable of extracting higher-order Tom40 containing complexes, while usage of other classes of detergents resulted in smaller complexes less than 150 kDa.

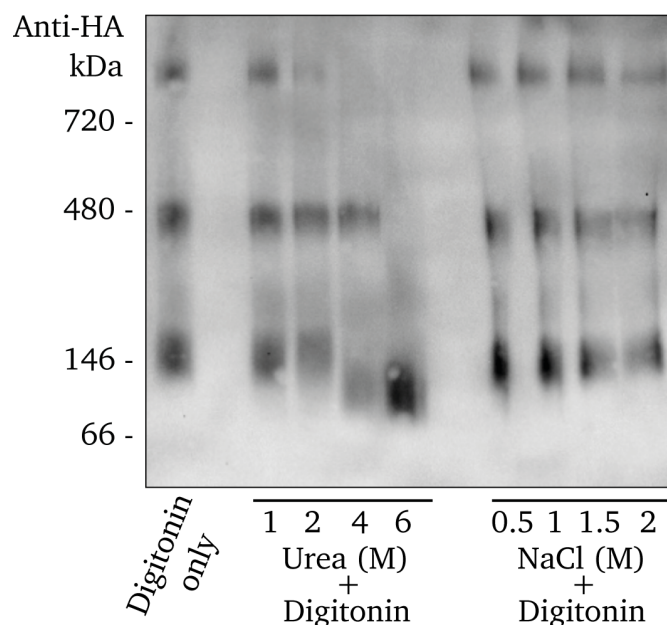


Figure 11. *Effect of varying concentrations of urea and NaCl salt on the stability of Tom40 containing complexes. Tagged Tom40 membranes were solubilised with digitonin and subsequently incubated with urea and NaCl, Samples were analysed by BN-PAGE-western blotting. Lanes 3-6: As the concentration of urea increases the higher order complexes increasingly dissociate. Lanes 8-11: Concentrations of NaCl up to 2M had no discernible effect on the integrity of the complexes.*

2.4.5 Purification of *Drosophila* TOM complex via tagged Tom40 and mass spectrometry analysis

Fly heads were isolated from the rest of the body parts and collected in a separate sieve compartment (Fig. 12.A and B) as described in Chapter 6, Section 6.3.4.4. A total volume of 50 ml of flies (approximately 10, 000 flies), yielding 2.5 ml of fly heads was used per experiment. Fly heads were homogenised and the resulting lysate (Fig. 12.C) was centrifuged at high speed (100, 000 x g) and membrane fractions were collected (Fig. 12.D). These high-speed membranes were used for extraction and purification of the TOM complex. Two detergents, digitonin and LMNG were selected on the basis of extracting a high molecular weight complex (Fig. 10). GDN was not used, on the basis of its similarity to digitonin.

Purified TOM samples at ~0.5 mg/ml, (as determined from a silver-stained SDS-PAGE and measurement of direct absorbance at 280 nm using a UV-Vis spectrophotometer – NanoDrop)

in a total volume of 50 μ l, obtained after immuno-affinity purification (described in Chapter 6, Section 6.3.4.5) were subjected to SDS-PAGE; gels were silver-stained to detect other proteins co-eluting with Tom40 and to assess overall purity. A control sample of wild-type fly membranes purified according to the same protocol was performed to identify non-specific binding contaminants. Silver-staining revealed the presence of protein bands co-eluting specifically with Tom40. A few higher molecular weight protein bands were inferred to be contaminants based on their presence in the control sample (Fig. 13).

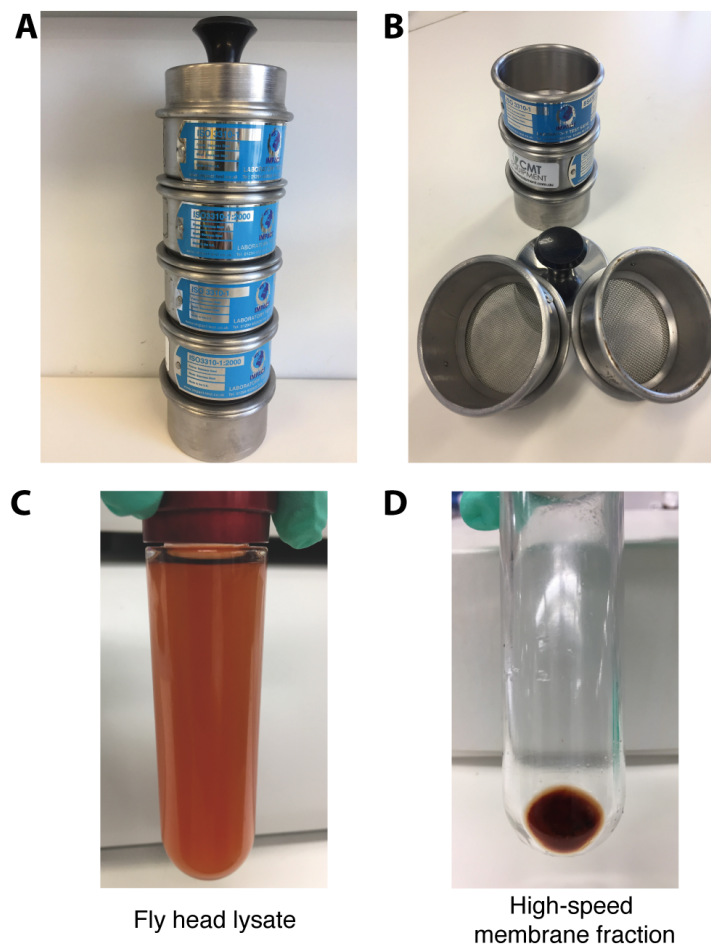


Figure 12. Preparation of fly head membranes. **A)** Image of a metal sieve stack consisting of individual sieves with decreasing pore diameters from top to bottom. **B)** shows the inside of the metal sieves. Decapitated flies are transferred to the top of the stack and fly heads are collected in the second sieve compartment (500 μ m) from top, while the fly bodies are retained in the top compartment. **C)** Isolated fly heads are homogenised to obtain a lysate. **D)** Lysates are centrifuged and a high-speed membrane fraction is obtained. The red colour of the membrane is caused by the eye pigment present in *Drosophila* eyes.

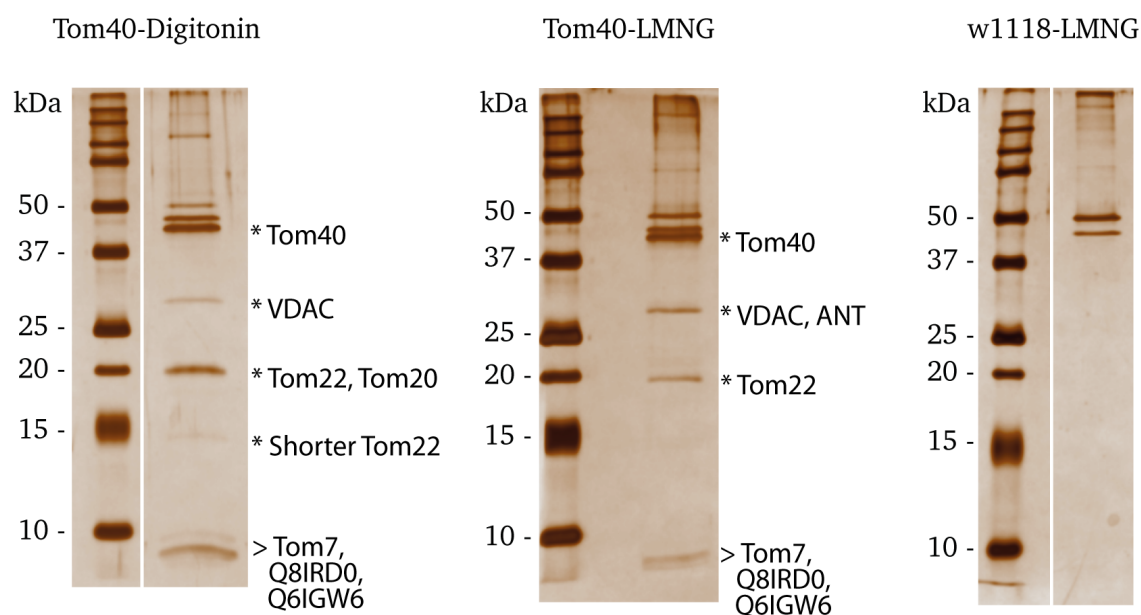


Figure 13. Purification of TOM complex and identification of protein bands. 10 μ l of each sample after FLAG based immuno-affinity purification equivalent to 800 fly heads (left: Digitonin-purified TOM, middle: LMNG-purified TOM and right: LMNG-purified w1118 control) was subjected to SDS-PAGE and visualised by silver staining. Visible protein bands were excised and analysed by tryptic digest mass spectrometry. Identified bands are labelled in the image. A separate band for Tom20 was not readily visible on a 15 % Tris-Glycine gel; Tom22 (molecular weight of 18.7 kDa) co-migrates with Tom20, which has a molecular weight of 16.1 kDa, under the electrophoresis resolving conditions.

Samples were analysed by BN-PAGE and western blotting to ensure the integrity of the complex after purification. Both digitonin and LMNG purified samples contained higher order bands in the ~480 kDa range as well as smaller complexes in the ~100-150 kDa range (Fig. 13).

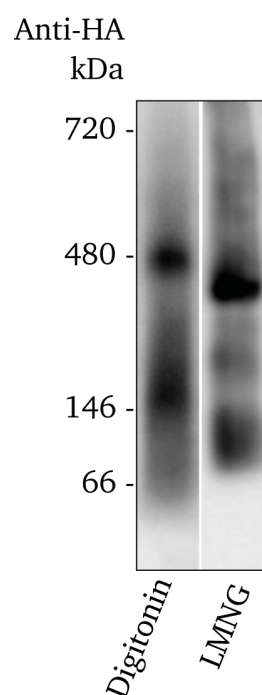


Figure 14. Analysis of molecular mass of purified TOM complex by BN-PAGE. 5 μ l of digitonin and LMNG purified samples were analysed by BN-PAGE-western blotting. Both samples contained a prominent intact complex of ~480-450 kDa. Additional smaller complexes were also seen: ~146 kDa in the digitonin sample and ~100 kDa and ~230 kDa (faint band) in the LMNG sample.

2.4.5.1 Observed differential extractions with digitonin and LMNG

Visual comparison of eluate banding pattern of digitonin and LMNG samples by silver staining showed apparent variations (Fig. 13), suggesting differential extraction properties of the detergents. The main protein bands were subject to tryptic digest MS to identify co-eluting partners of Tom40. Identified proteins are labelled with an asterisk (*) in Figure 13 and listed alongside their primary accession numbers in Table 3. While this is by no means an exhaustive list, these are the major protein bands with significant peptide matches that were not excluded as non-specific background proteins.

Some of the identified proteins were common to both digitonin and LMNG samples and included known components of the TOM complex namely Tom22 and Tom7 plus two previously unannotated *Drosophila* proteins (Uniprot primary accession numbers: Q8IRD0 and Q6IGW6) of estimated molecular weights of 5.5 kDa and 5.8 kDa, respectively.

In the experiments, Tom20 was visible only under digitonin extraction conditions. It was not detected by MS in the LMNG purified sample.

Table 3. Tryptic digest MS identification of proteins co-eluting with Tom40

Proteins pulled down via Tom40 identified by tryptic digest MS		
Uniprot primary accession no.	Detergent used	
	Digitonin	LMNG
Q9U4L6	Tom40	Tom40
Q9VZL1	Tom22	Tom22
Q7K036	Tom7	Tom7
Q6IGW6	Tom6-like	Tom6-like
Q8IRD0	Tom5-like	Tom5-like
Q94920	VDAC	VDAC
Q95RF6	Tom20	-
Q26365	-	ATP/ADP carrier (ANT)

2.4.5.2 Possible *Drosophila* orthologues of human Tom5 and Tom6 identified by sequence alignment

Tom5 and Tom6 have not hitherto been identified in *Drosophila*. Two low molecular weight proteins (5.5 kDa and 5.8 kDa) co-eluting with Tom40 were investigated for their possible orthology with Tom5 and Tom6. Pair-wise sequence alignments against human orthologues (Fig. 15) show that Q8IRD0 has significant homology to human Tom5 with 35 % sequence identity (and a similarity of 58.9 %) whereas Q6IGW6 has a 26.7 % sequence identity (and a similarity of 41.3 %) to Tom6. While this is promising, protein import assays would be required to verify that these small proteins co-eluting with Tom40 are *Drosophila* Tom5 and Tom6.

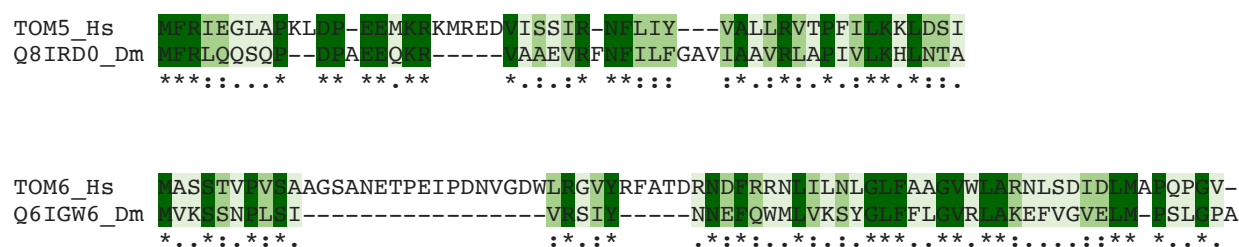


Figure 15. Protein sequence alignments of unannotated *Drosophila* proteins against human Tom5 and Tom6. Previously unannotated proteins, Q8IRD0 and Q6IGW6, that were observed in the Tom40 pull-down experiment, as identified by MS, were aligned against human Tom5 and Tom6 respectively using the EMBOSS Needle program (EMBL-EBI). In both cases, despite some gaps, there are extended sequence stretches that display significant homology.

2.4.5.3 Co-elution of VDAC and ANT with Tom40

The voltage-dependent anion channel (VDAC, or mitochondrial porin) and the Adenine Nucleotide Translocase (ANT, or AAC), with molecular weights of 30.5 kDa and 34.2 kDa respectively, represent the two most abundant proteins in mitochondria (Wang, 2001). Mass spectrometry analysis of prominent silver stained bands identified VDAC co-eluting with Tom40 extracted in either LMNG or digitonin. Another significant match corresponded to ANT, but this was found only in LMNG-extracted samples. In contrast, protein bands corresponding to VDAC and ANT are conspicuously absent (Fig. 13) in the control sample, indicating that pull down of the two proteins is occurring through direct interaction with Tom40 or indirectly *via* other associated TOM components identified in the eluate. A caveat is that the

relationship does not appear to be stoichiometric, something that will be discussed further in Chapter 5.

The significance of this observation is yet to be determined and we seek to interrogate this by native mass spectrometry for qualitative and quantitative assessment of molecular composition of complexes. To this end, we have established a collaboration with Prof. Carol Robinson (University of Oxford, UK), and provided digitonin-solubilised TOM complexes for native mass spectrometry analysis.

2.4.6 Negative stain EM analysis showed three-pore complexes

Negative stain EM was employed as a screening tool for preliminary assessment of purified samples at a single particle level to determine suitability of the samples for structure determination by cryo-EM. Assessment of the EM micrographs of digitonin-purified sample definitively showed three-pore particles (Fig 16.A, denoted by red circles) with clear resemblance in overall appearance to early EM images of *Saccharomyces* and *Neurospora* holo complexes (Kunkele *et al.*, 1998a, Model *et al.*, 2002). There were also some two-pore particles.

Reference-free 2D class averaging was performed on manually picked particles from a set of 75 micrographs. Several classes of three-pore particles with face-on views were visible (Fig. 16.B). While other particle classes of disparate morphology were seen to a lesser extent, it is not unusual to observe such classes during initial 2D classifications, either from negative stain EM or cryo-EM. On this basis, digitonin-purified TOM appeared was adjudged to be a good candidate for further analysis by cryo-EM.

The LMNG-purified TOM, on the other hand, did not behave well under negative stain EM conditions. Although analysis of purified sample by BN-PAGE showed a band at a nominal mass of ~450 kDa, the micrographs revealed low particle density accompanied by aggregation (Fig. 17.A). The 2D class-averaged particles were small relative to those observed in digitonin-purified TOM (Fig.17.B), more resembling the two-pore structure. On this basis, LMNG-purified TOM was deemed unsuitable for further analysis.

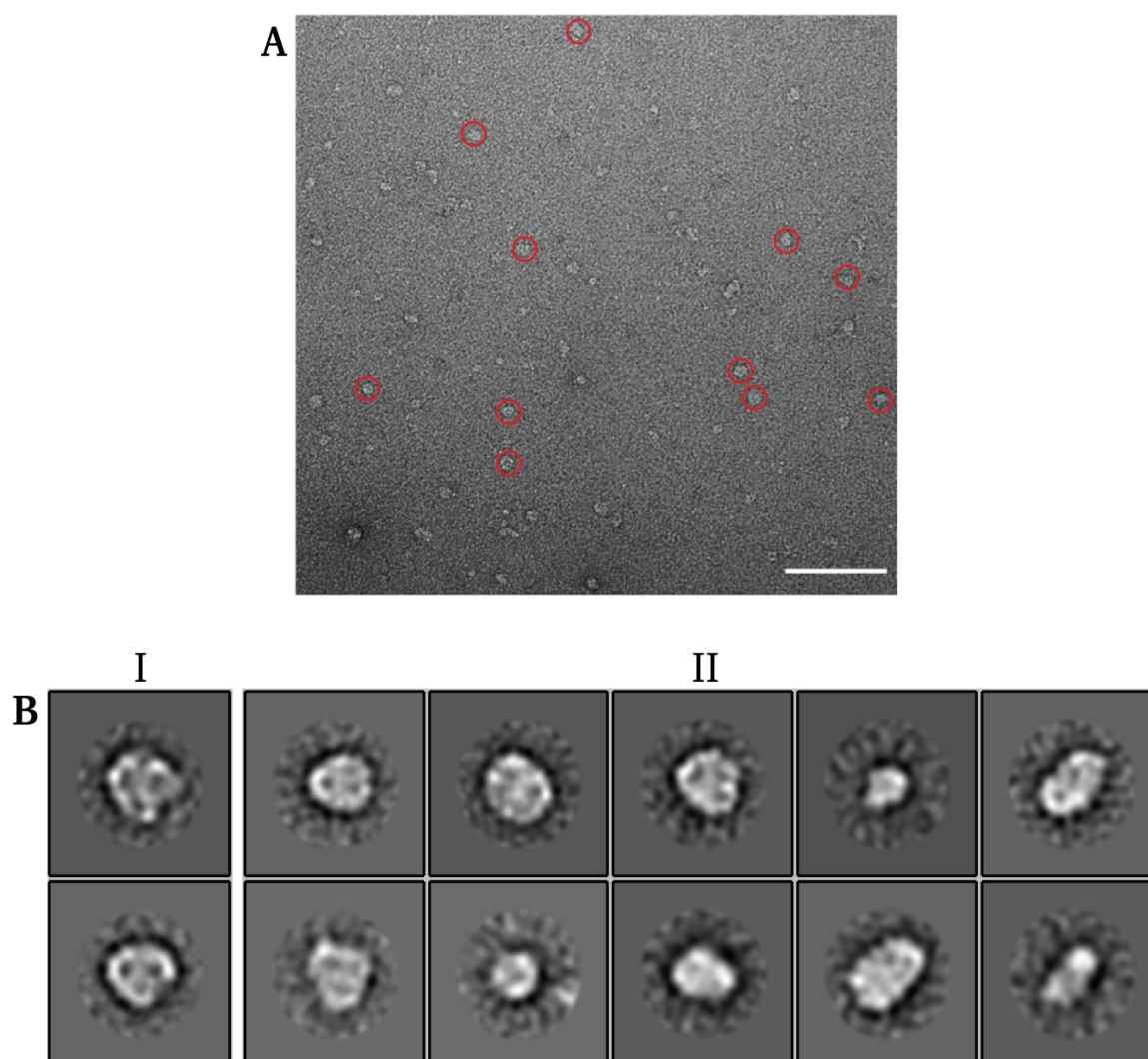


Figure 16. Negative stain EM of a digitonin-purified TOM sample shows 3-pore complexes. **A)** A representative micrograph showing single particles of TOM. Some three-pore particles are denoted with a red circle around them. The scale bar is 100 nm. **B)** 2D classes obtained by averaging using RELION. The classes shown in panel I are from an initial trial with 1,652 manually picked particles. Panel II contains classes from a larger dataset from which particles were auto-picked. Apart from classes with three-pore particles, other classes with smaller particle sizes can also be seen.

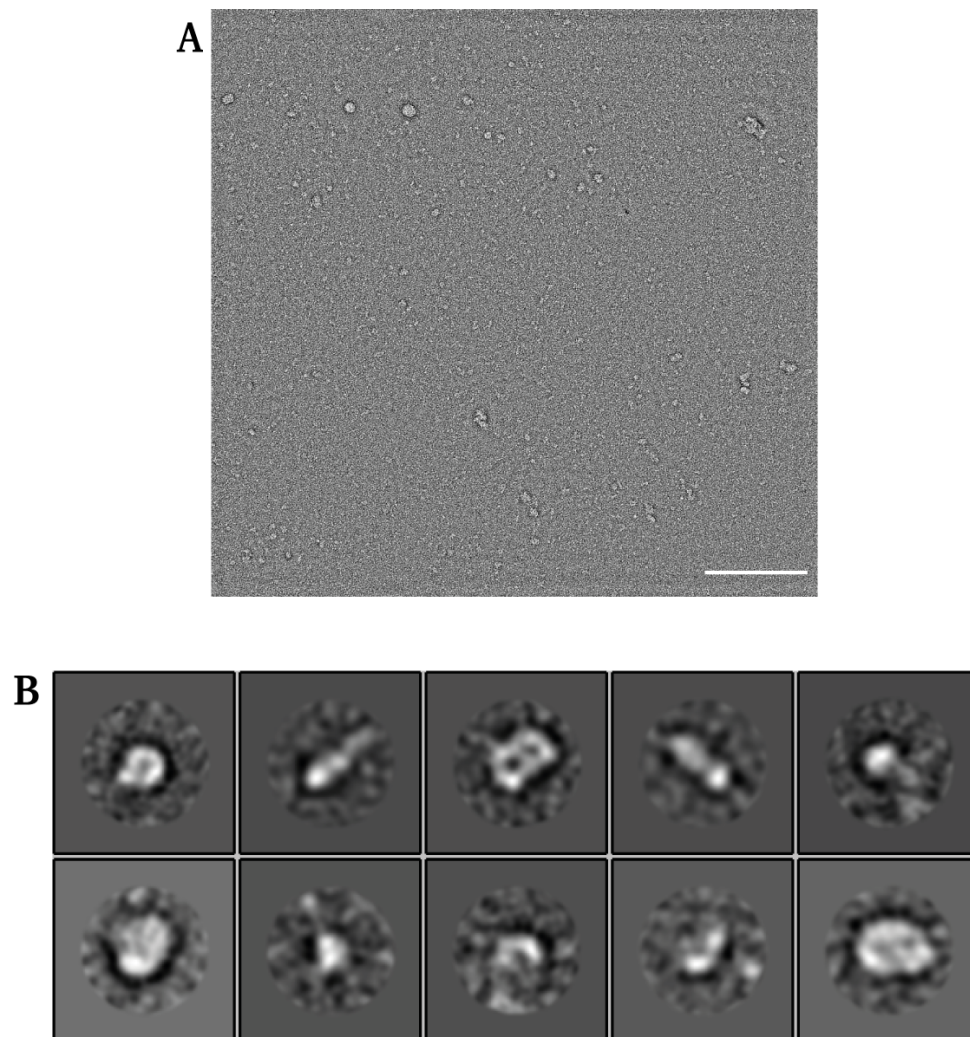


Figure 17. *Negative stain EM of a LMNG-purified TOM sample* **A)** A representative negative stain EM micrograph showing single particles of a LMNG purified TOM sample. Smaller particles alongside some larger aggregates are visible. Scale bar is 100 nm. **B)** 2D classes obtained by averaging using RELION.

2.5 Discussion

Traditionally, study of mitochondrial translocases and import processes has focussed on the *Neurospora* and *Saccharomyces* systems in which the machineries were first identified. Of late, these studies have been extended to higher eukaryotes by utilizing mammalian cell culture model systems by several laboratories, with additional translocase components and a few variations in assembly pathways being identified (Humphries *et al.*, 2005, Kang *et al.*, 2016). These efforts have not yet resulted in published structures of eukaryotic TOM complexes.

2.5.1 A novel strategy for isolation of metazoan TOM from native membranes

We undertook an innovative approach to investigate a higher eukaryotic TOM from *Drosophila*, which has components with high sequence homology to the human system. *Drosophila* flies were exploited for homologous transgenic expression of core TOM components, namely, Tom40 and Tom22. The highest protein expression achieved occurred when expression was targeted to photoreceptor cells of fly eyes which, notably, contain densely packed mitochondria (Eakin, 1972) to support high energy requirements of photoreceptor cell processes; in particular, transduction (Tinbergen and Stavenga, 1987, Laughlin *et al.*, 1998). *In vivo* localisation analysis by immunofluorescence microscopy and the assembly of FLAG.HA tagged versions of both Tom40 and Tom22 into higher order complexes suggested successful trafficking to the mitochondria. This was independently confirmed during reciprocal pull-down experiments via tagged Tom40 or Tom22 where known endogenous subunits of TOM were effectively pulled out. For large-scale purification purposes, tagged Tom40 was utilised since it provided higher final yields of purified TOM.

2.5.2 Effect of detergents on TOM complex extraction and stability

The choice of detergent was found to be crucial for extraction of the three-pore *Drosophila* TOM. While the steroidal glycoside-based detergent, digitonin, was successful, LMNG was not. Extraction with LMNG results in complex with slightly higher mobility on BN-PAGE (in comparison to digitonin; Fig. 10), and tryptic-digest mass-spectrometry analysis showed that LMNG-purified complex did not contain any Tom20 (Fig. 13). In a similar case, when the maltoside detergent, DDM is employed for extraction, only the core TOM complex is pulled out (Ahting *et al.*, 1999, Bausewein *et al.*, 2017). LMNG, used in this study, has two maltoside ring structures and thus may possess similar extraction properties to DDM, explaining the loss of Tom20. Tom20 is a key factor for the occurrence of three-pore TOM in yeast; yeast strains lacking Tom20 produce only two-pore complexes (Model *et al.*, 2002). Tom20 is known to be

loosely associated with the core TOM complex; thus far only digitonin has been used successfully to extract a yeast Tom20 bound core TOM complex, showing the presence of three-pore complexes (Model *et al.*, 2008). This is in agreement with our results, where Tom20 co-elution occurs only with digitonin. Tom70, a loosely associated TOM receptor, was not observed under any extraction conditions tested in this study. While the newly developed synthetic alternative of GDN was tested in the screening stage, time limitations precluded more extensive purification trials with this detergent.

2.5.3 Implications of VDAC and ANT association with TOM

The pull-down of VDAC with digitonin extraction and VDAC and ANT, with LMNG extraction, was unexpected. VDAC did not pull down in the absence of tagged Tom40, indicating that co-elution occurred by direct interaction with Tom40 or *via* other TOM subunits. To determine whether VDAC and ANT form a part of the higher order TOM complexes, preliminary western blot analysis on samples resolved on a BN-PAGE was carried out with the aid of antibodies (albeit against human orthologues) of respective proteins. Faint bands observed for VDAC and ANT at ~450-480 kDa by BN-PAGE western, require cross-validation by other techniques (native mass spectrometry).

While interaction of TOM with other membrane translocase and assembly complexes has been documented by several studies, an association with VDAC was only recently noted in the literature. A novel assembly of TOM-VDAC was identified in adult rat brain mitochondria (Muller *et al.*, 2016) using a novel high resolution cryo-slicing Blue Native-Mass Spectrometry technique coupled with correlation analysis. They further extended the study to yeast mitochondria and demonstrated association of Tom40 and Tom22 in a 440-kDa complex with Porin1 (VDAC ortholog in yeast) by BN-PAGE and pull-down experiments. This association has not previously been observed in yeast, but differences in experimental conditions might possibly account for the discrepancy. The identification of the inner membrane protein, ANT, under LMNG extraction conditions is a novel finding that has not been previously reported. It suggests an interaction at the outer and inner membrane contact junctions. Given that both digitonin and LMNG extraction experiments utilised fly eyes of the same genotype and expression conditions, the disparity is puzzling. It is possible that digitonin does not preserve the interaction between the TOM complex and ANT by virtue of its extraction properties.

It will be of interest to determine the molecular basis of these protein interactions with TOM and their significance. Native mass spectrometry would enable characterization and determine

if there is more than one distinct complex present in the purified samples, i.e., a standard TOM complex and another with VDAC/ANT as additional components. As VDAC and ANT are known regulators of apoptosis (Brenner *et al.*, 2010, Trindade *et al.*, 2016), this raises the interesting issue of whether these associations are exclusive to specific physiological states of the mitochondria or the cell.

Chapter 3

Preliminary structural investigation of *Drosophila* TOM by single particle cryo-EM

3.1 Introduction

Following an introduction to cryo-EM, this chapter focusses on a preliminary structural analysis of the three-pore *Drosophila* TOM complex, extracted and purified in digitonin by cryo-EM for potential structure determination.

Cryo-EM trials were performed using different grid types and other variables to assess the behaviour of the sample under cryogenic conditions. In this chapter, two-dimensional (2D) reference-free class averages obtained from initial screening are presented, followed by discussion of what has been accomplished to date, and the challenges still to be met.

3.1.1 High-resolution structure determination by single-particle cryo-EM

Single particle electron microscopy under cryogenic conditions (cryo-EM) involves imaging monolayers of randomly oriented macromolecules embedded in a thin layer of vitreous ice. The images take the form of projections viewed along an axis parallel to the electron beam, where each particle represents a specific orientation of the macromolecule in question. By classifying the particles according to their orientation and combining the resultant class-averaged views of particles, a three-dimensional (3D) structure of the macromolecule can be reconstructed computationally. Cryo-EM was first developed thirty years ago (Dubochet et al. (1988)), but for many years its use was largely restricted to analysis of symmetrical and/or large particles like viruses, ribosomes etc.; smaller macromolecules suffered from low signal to noise ratios at the dose and defocus ranges that were commonly used.

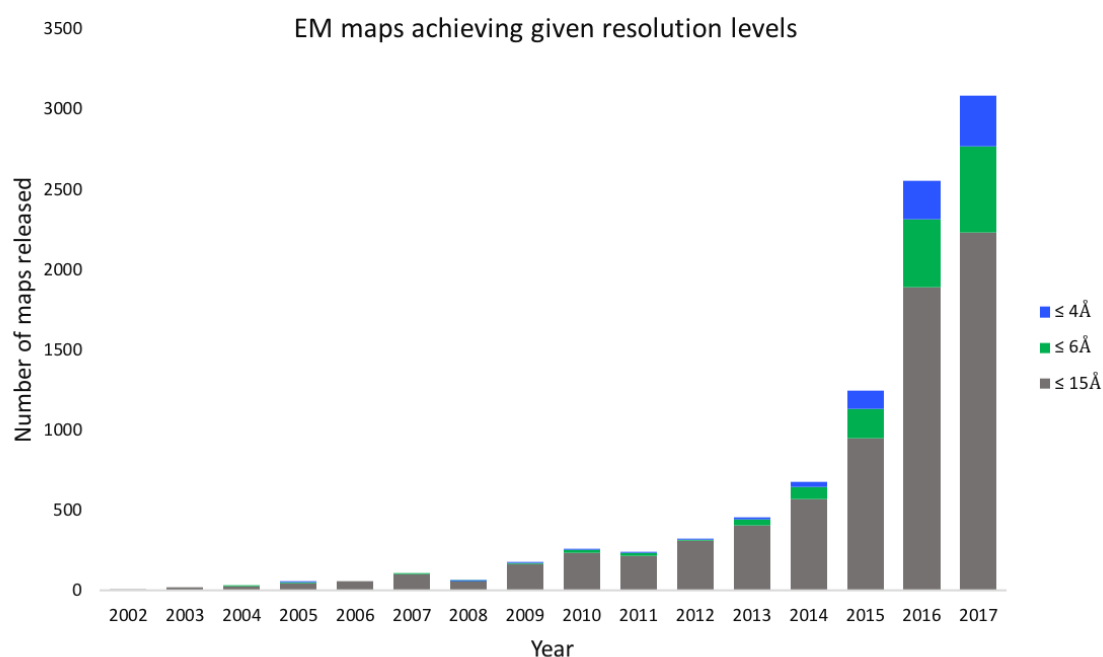


Figure 1. Bar graph of number of EM maps released annually from 2002-2017. The proportion of maps with a resolution of $\leq 6\text{\AA}$ and $\leq 4\text{\AA}$ are coloured in green and blue, respectively. An exponential increase in map numbers is seen with respect to the total annual maps as well as maps of $\leq 6\text{\AA}$ and $\leq 4\text{\AA}$ being deposited in the Electron Microscopy Data Bank (EMDB).

This changed in the early 2010s as single particle cryo-EM emerged as a mainstream method of structural analysis, with structures of relatively smaller protein assemblies being determined

without the need to enforce symmetry. Data from the Electron Microscopy Data Bank (EMDB) show an exponential increase in the total number of maps released annually, with more than 3000 deposited maps in 2017 (Fig. 1). More significantly, the proportion of high resolution maps has increased exponentially over the years. While maps at a resolution higher than 6 Å made up approximately 4 % of the total in the year 2012, this increased to 25 % of the total maps deposited per year, on average, in the period from 2014 - 2017.

This rapid progression, dubbed a ‘revolution’ (Kühlbrandt, 2014), has principally been attributed to the development of direct electron detectors (DEDs) (Milazzo *et al.*, 2011, Bamme *et al.*, 2012, Veesler *et al.*, 2013) and concomitant availability of better microscopes and superior image processing algorithms (Scheres, 2012, Punjani *et al.*, 2017). Direct electron detectors offer increased detective quantum efficiency over the photographic films and charge-coupled device (CCD) cameras previously used, thus significantly improving the resolution of recorded images. They also offer a much faster read-out, with many images recorded per second, resulting in movies which can be processed to correct for beam-induced sample movements. Other ongoing technological improvements in the imaging process include the introduction of phase plates (Nagayama and Danev, 2009) to enhance image contrast, spherical aberration (Cs) and chromatic aberration (Cc) correctors of the objective lens for higher effective resolution (Kabius *et al.*, 2009, Fischer *et al.*, 2015) and gold support grids for possible minimization of beam-induced particle movement (Russo and Passmore, 2014). Very recently, a structure of human haemoglobin molecule was determined at a resolution of 3.2 Å using volta phase plate technology (Khoshouei *et al.*, 2017). At 64 kDa, the structure demonstrates the potential applicability of cryo-EM for particles less than 100 kDa, substantiating Henderson’s theoretical prediction that structures of 100 kDa proteins can be determined at a 3 Å resolution by cryo-EM (Henderson, 1995).

3.1.1.1 Membrane protein structures

Since the widespread adoption of these new technologies, structure determination of membrane protein assemblies by single particle cryo-EM has rapidly progressed and has become the method of choice for structural candidates refractory to conventional techniques such as X-ray crystallography and Nuclear Magnetic Resonance (NMR) spectroscopy. X-ray crystallography, which to date has been the most successful method for structure determination of membrane proteins, suffers from a series of bottlenecks in the process to a structure, of which the most serious are discussed here. Crystallization screening and optimisation requires substantial quantities (of the order of mg) of homogenous protein, which can be limiting for

many eukaryotic membrane proteins. Detergent micelles typically mediate a proportion of the lattice contacts in crystals of detergent-solubilised membrane proteins, which can adversely impact on diffraction quality, limiting the attainable resolution of the data (Iwata, 2003). Cryo-EM, on the other hand, requires significantly less material (μg quantities of pure protein), and accommodates some conformational heterogeneity and any inherent flexibility, both of which feature highly in membrane proteins. Classification and reconstruction of different molecular conformations in a single image is feasible using newly developed computational algorithms (Scheres, 2016).

Selected examples of membrane protein structures representing landmarks in the field are discussed as follows. The mammalian TRPV1 ion channel was the first membrane protein structure determined at 3.4 Å (Liao *et al.*, 2013) using DEDs and new image processing algorithms to correct motion-induced image blurring. Other membrane protein structures of varying sizes quickly followed this. The first structures of human γ -secretase, a 170 kDa asymmetric four component heteromer were determined *de novo* at two resolutions of 4.5 Å and 3.4 Å (Lu *et al.*, 2014, Bai *et al.*, 2015); this complex had never yielded to crystallography due to challenges in expression and purification of the intact complex in sufficient quantities combined with inherent flexibility and heterogeneity (Rawson *et al.*, 2016). At the other end of the molecular mass spectrum, several structures of large protein complexes include the ryanodine receptors of ~ 2.2 MDa (Zalk *et al.*, 2014, Yan *et al.*, 2015), the mitochondrial respiratory Complex 1 of ~ 1 MDa comprising 45 different subunits in different conformational states (Vinothkumar *et al.*, 2014, Blaza *et al.*, 2018) and the Sec61-ribosome complex captured in both idle and translating states (Voorhees *et al.*, 2014); all have been recently reported at resolutions of 5 Å or better.

Notably, all of the large assemblies mentioned above were purified from the endogenous mammalian tissues. All of them have large structured soluble domains, which is advantageous for particle picking, resulting in higher signal to noise in class averages and thus higher resolution maps. These domains also serve as markers in building a protein model. Complexation with antigen binding fragments (Fab) is being explored as an avenue to increasing mass, classifying particles and aiding in map interpretation for proteins lacking large ectodomains or intracellular assemblies (Wu *et al.*, 2012). This is not the only route to success, however, and in a recent example Huynh *et al.* (2018) reported the structure of a eukaryotic Na^+ -coupled homodimeric transporter (NBCe1) at 3.9 Å. Despite very minimal extra-membraneous regions present, an atomic model was built using bulky amino acid side-chains

that were well-resolved in the density as markers to locate the sequence register, with promising prospects for other small integral membrane proteins.

3.2 Results

3.2.1 Preparation of samples for cryo-EM analysis

Negative stain EM analysis of a *Drosophila* TOM complex containing Tom40, Tom22, Tom5, Tom6, Tom7 and Tom20, with a nominal mass on blue native PAGE of ~480 kDa, revealed predominantly three-pore complexes, as elaborated in the previous chapter. On the basis of the negative stain data, we entered into a collaboration with Prof. Werner Kühlbrandt (Max Planck Institute of Biophysics, Frankfurt) to carry out cryo-EM analysis with the aim of structure determination.

Protein samples for cryo-EM analysis are required at a concentration approximately ten-fold higher than is needed for negative stain EM assessment, since sample preparation includes a step involving particle incorporation into the ice layer. To this end, a significant scale-up of fly cultures was engineered to produce sufficient purified complex for visualization on cryo-EM grids. Digitonin-purified TOM at ~0.25 mg/ml was utilised for the experiments.

3.2.2 Visualization of three-pore particles in preliminary cryo-EM trials

Glow-discharged holey carbon grids of varying hole diameter, untreated or treated with graphene oxide were screened for good particle distribution and incorporation into vitrified ice. Graphene oxide is hydrophilic by nature and is used as a support layer to promote particle adsorption onto the grids (Pantelic *et al.*, 2010). Of the conditions tested, the C-Flat 1/1 grid with a hole diameter of 1.0 μm x 1.0 μm had an acceptable number of particles embedded in the vitreous ice layer (Fig. 2A), albeit only when the grids had been pre-treated with graphene oxide. The graphene oxide layer was discontinuous in this instance and empty regions/holes with only an ice layer could be distinguished in the micrographs. Preliminary 2D classification of 14,000 particles selected from micrographs of the ice layer showed several classes of three-pore complexes, albeit all oriented face-on or in a slightly tilted plane (Fig. 3). No side views were noted, indicating a strong preferential orientation for these macromolecules in the ice layer.

In micrograph images from samples in a continuous layer of graphene oxide, a substantially higher number of particles was observed (Fig. 2.B). Here, 2D class averages showed a few

classes with three-pore complexes (marked with a red box; Fig. 4). The three-pore complexes were outnumbered by classes corresponding to large spherical blobs (of varying size), with some similarly sized to the three-pore particles. These classes were interpreted as digitonin micelles. These empty micelles sometimes overlapped the three-pore particles (Fig. 4), complicating further analysis.

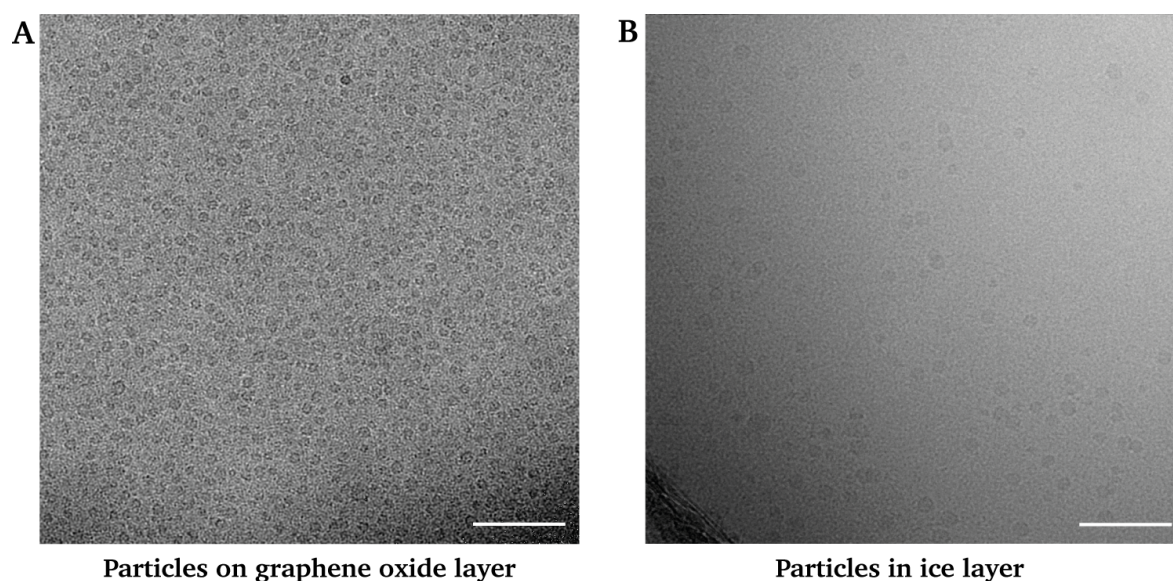


Figure 2. *Representative micrographs showing distribution of particles. A) Particles are shown on a continuous layer of graphene oxide, or B) embedded within a layer of ice. The scale bar is 100 nm. Considerably fewer particles incorporated into the empty ice layers in comparison to the layer of graphene oxide.*

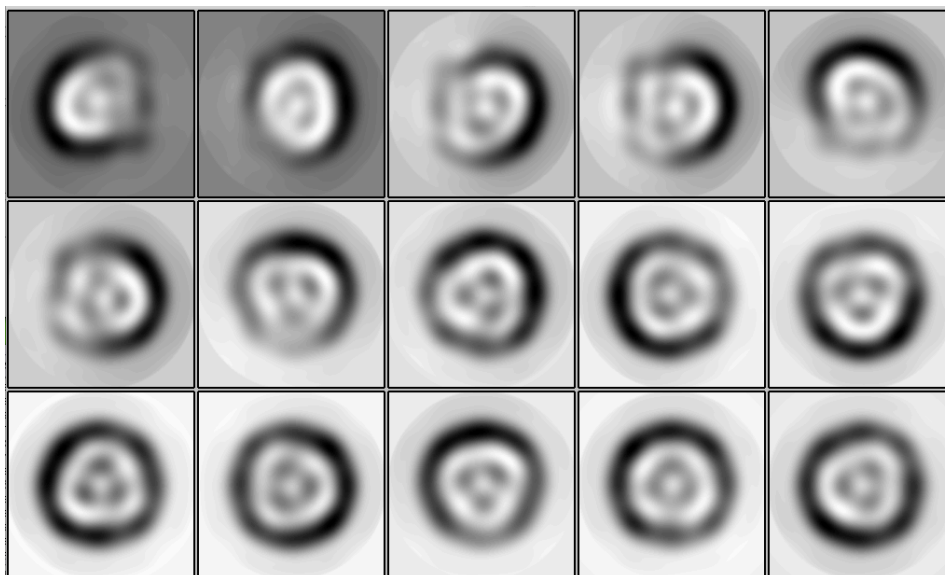


Figure 3. 2D class averages of three-pore particles in ice. 14,000 particles (out of 159,717 in total) were selected, aligned and classified in 2D with Relion2.1. Particle averages displayed preferential orientation, limited to face-on views.

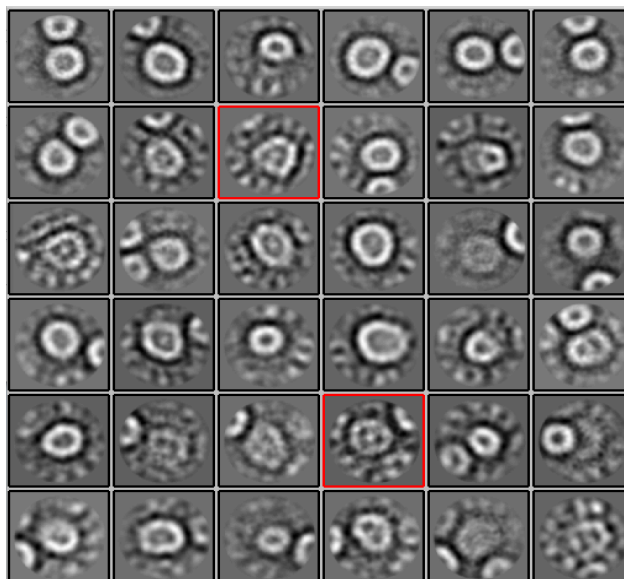


Figure 4. A selection of 2D class averages of particles distributed on a graphene oxide layer. Two classes representing three-pore particles are marked with red boxes. The large roundish rings seen in many of the other classes are likely to be digitonin micelles.

3.3 Discussion

Information regarding the structural organisation and stoichiometry of the three-pore TOM complex from any species is limited. While a ~ 7 Å structure of a two-pore TOM core complex from *Neurospora* was recently determined by cryo-EM, the only available 3D structural model of a three-pore complex is that of one from *Saccharomyces* reported prior to the development of DEDs (Model *et al.*, 2008). At an effective resolution of 18 Å, this structure is a little more than a molecular envelope revealing a triangular complex with near-three-fold symmetry but offers little insight into the arrangement of subunits or translocation mechanism. The underlying objective of this thesis was thus to better understand the architecture and molecular organisation of the TOM complex of a higher eukaryote. The relatively small quantity of purified *Drosophila* three-pore complex that we obtain precludes crystallographic structure determination and instead we have directed our efforts towards cryo-EM analysis.

Several membrane protein structures solubilised in digitonin have now been determined by cryo-EM at resolutions better than 5 Å (Voorhees *et al.*, 2014, Sun *et al.*, 2015, Twomey *et al.*, 2017). However, digitonin is not without issue. Extracted from natural sources it suffers batch-to-batch variability, which can be problematic for reproducibility at all steps. In our preliminary cryo-EM trials, three-pore complexes incorporated into ice were visible but the efficiency of was quite low and not very reproducible. The large circular particles frequently observed (Fig. 4), are likely to be excess digitonin micelles that build up in the sample during post-purification concentration. These particles dominate the micrographs, making it harder to identify and classify TOM particles. Some other issues with detergent are that its presence in cryo-EM specimens can affect particle incorporation (Rawson *et al.*, 2016), and the presence of excess detergent in our case might possibly explain its low incorporation efficiency into ice. In order to proceed further using digitonin, a reduction of the effective concentration would be required. By avoiding the final filter-concentration step during purification, issues related to particle incorporation or detergent background might be alleviated but would require an alternative means of achieving the desired final protein concentrations. Avenues we are exploring include stepping off an anion exchanger or using a density gradient (Hauer *et al.*, 2015).

Another issue is the preferential orientation of three-pore particles with face-on views during our limited trials, which may be due to the attraction of the polar faces of the TOM complex for the graphene-oxide treated grid. This behaviour was previously observed for the yeast TOM complex (Model *et al.*, 2002). Random orientation might be achieved on grids with more

hydrophobic surfaces, for example rendered by treatment with amyl amine (Miyazawa *et al.*, 1999, da Fonseca and Morris, 2015). A tilt-based approach during imaging is another option, albeit with limited scope (Tan *et al.*, 2017).

Other strategies for consideration to improve the quality of cryo-EM micrographs include, testing new detergent combinations for extraction and stabilisation, complete replacement of digitonin with other model membrane bilayer systems by reconstitution of digitonin purified TOM into amphipols (Tribet *et al.*, 1996, Flotenmeyer *et al.*, 2007), tailored nanodiscs (Ritchie *et al.*, 2009) or saposin-lipoprotein nanoparticles (Frauenfeld *et al.*, 2016). A bilayer environment is likely to improve stability of the complex and prevent conformational artefact that could potentially result from solubilisation. Of late, several cryo-EM structures of membrane proteins have been obtained by exchanging into amphipols or nanodiscs after solubilisation with mild detergents (Liao *et al.*, 2013, Mi *et al.*, 2017, Huynh *et al.*, 2018). Emerging systems like styrene-maleic acid (SMA)-lipid particles (SMALP) (Lee *et al.*, 2016), diisobutylene/maleic acid copolymer (DIBMA) (Oluwole *et al.*, 2017) which provide the capacity for direct extraction of intact protein complexes in native membranes are other options for investigation.

Chapter 4

Investigation of an eye phenotype caused by Tom40 expression and its implications

4.1 Introduction

This chapter describes the discovery of a phenotype associated with increased expression of Tom40 in *Drosophila* eyes. Following a serendipitous observation of an aberrant eye morphology in a Tom40 expressing fly strain, studies were carried out to understand its significance. The expression levels of Tom40 were modulated in a temperature and dose dependent manner and the resulting eye phenotypes were characterized, revealing a basis in cell death.

4.2 Experimental considerations

Purification of the TOM complexes, as dealt with in the preceding chapters, utilised flies that contained a single copy of tagged UAS-Tom40 and *GMR-GAL4*, brought together by genetic crossing of the two fly strains. These flies, raised at the standard experimental temperature of 25 °C exhibited normal eye morphology.

In the latter stages of the project, in order to bypass the laborious step of setting up crosses to obtain Tom40 expressing flies, a stable fly strain carrying both UAS-Tom40 and *GMR-GAL4* was established. The homozygous flies of this strain (i.e., carrying two copies of UAS-Tom40 and *GMR-GAL4*) displayed an aberrant glossy eye morphology, characterized by fused ommatidia accompanied by pigment loss when maintained at 25 °C. The observed phenotype was distinct from the phenotype of homozygous *GMR-GAL4* driver flies, which display rough eyes with no regular patterning as a result of developmental defects and apoptosis caused by ectopic GAL4 expression in the tissue (Kramer and Staveley, 2003); heterozygous *GMR-GAL4* driver flies, on the other hand, tend to have normal eye morphology. The difference in phenotype in the presence and absence of Tom40 expression suggested that the targeted expression of Tom40 in eyes might have an effect on the eye morphology that is independent of GAL4, leading us to investigate it further.

4.3 Results

4.3.1 *GMR-GAL4* driven Tom40 expression causes glossy eye phenotypes in a dose-dependent manner

GAL4 protein displays a temperature-dependent activity in *Drosophila*, showing higher activity levels at 29 °C and, consequently, higher expression of UAS-responder gene (Duffy, 2002), Tom40 in this case. Thus, experiments were carried out at the higher temperature of 29°C to study the effect of Tom40 expression by analysis at two dosages, represented by flies with single or double copies of the Tom40 gene. A control experiment with wild-type flies was also carried out to account for any effects caused by GAL4 alone.

In comparison to eye morphologies of control flies (Fig. 1.A and 1.B), progeny flies expressing Tom40 had distinctive morphologies. A single copy expression of Tom40 exhibited a glossy eye phenotype characterized by fused ommatidia and pigment loss (Fig. 1.C), whereas flies homozygous for Tom40, i.e., a double copy expression led to a more severe morphology showing a reduction in eye size accompanied by necrotic black spots (Fig. 1.D), indicating a

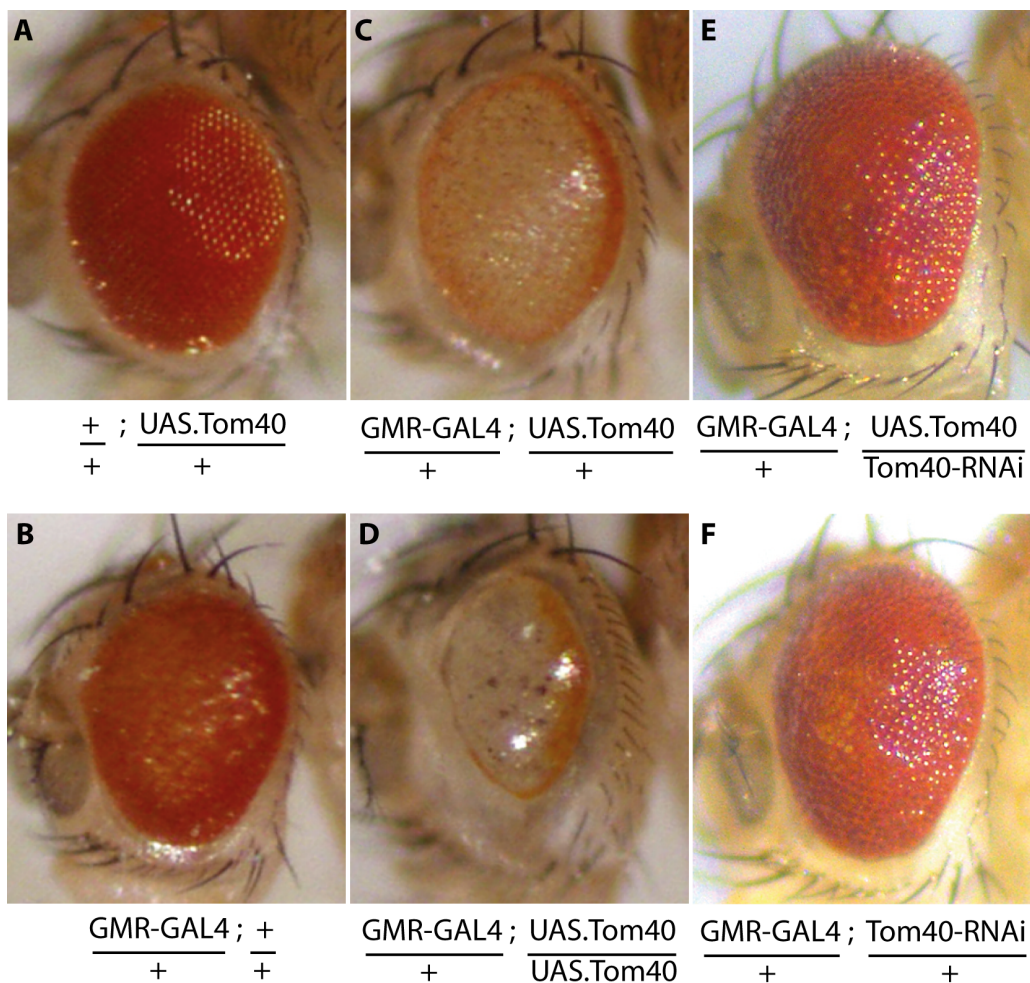


Figure 1. *Tom40* associated *Drosophila* adult eye phenotypes. Representative images of **A)** *UAS-Tom40* only (no *GMR-GAL4* driver), effectively equivalent to a normal compound eye morphology with regular arrays of individual ommatidia **B)** *GMR-GAL4* only (no *UAS-Tom40* responder) control displaying a rough eye phenotype. **C)** *GMR-GAL4* with one copy of *UAS-Tom40* (heterozygous) showing a glossy eye phenotype, characterized by pigment loss and fusion of ommatidial arrays **D)** *GMR-GAL4* with two copies of *UAS-Tom40* (homozygous) displaying a more severe phenotype with reduced eye size and necrotic spots. **E)** *GMR-GAL4* with one copy of *UAS-Tom40* plus *Tom40-RNAi*, showing near complete reversal of the *Tom40* eye phenotype **F)** *GMR-GAL4* with targeted co-expression of *Tom40 RNAi*, showing an alleviation of the rough eye phenotype.

correlation between the amount of Tom40 expressed and severity of the eye phenotype. In both of these cases, only a single copy of *GMR-GAL4* was present to drive the expression, ruling out GAL4 as the causative factor. Control progeny flies with a single copy of *GMR-GAL4* had a rough eye texture as expected (Fig. 1.B), compared to flies without *GMR-GAL4* which had normal eye morphology characterized by a regular ommatidial lattice (Fig. 1.A). As another independent control, flies expressing a single copy of Tom22 were of similar eye morphology to *GMR-GAL4* only flies (data not shown), indicating that Tom40 is solely responsible for the glossy eye phenotype. To test this further, targeted co-expression of Tom40 RNAi in the eyes was utilised to knockdown Tom40 expression. This strategy resulted in near complete rescue of the phenotype (Fig. 1.E), substantiating the direct involvement of Tom40. Unexpectedly, the Tom40-RNAi co-expression in *GMR-GAL4* flies also appeared to slightly diminish the impact of the *GMR-GAL4* rough eye phenotype (Fig. 1.F), which could mean that Tom40-RNAi directly suppresses the *GMR-GAL4* phenotype or, alternatively, may indicate non-specific effects of Tom40-RNAi expression on free GAL4 levels in the tissue, thereby influencing the associated phenotype.

4.3.2 Increased cell death activity correlates with increase in Tom40 expression

Disorganised ommatidial array and pigment loss are recognized features of programmed cell death, or apoptosis in *Drosophila* eyes (Ye and Fortini, 1999, Quinn *et al.*, 2003, Choi *et al.*, 2017). To confirm that the observed phenotypes occurs as a result of this phenomenon, third instar larval eye discs were immuno-stained with an antibody against cleaved caspase-1, which is selective for an active processed form of caspase found in cells undergoing apoptosis. Confocal imaging followed by 3D volume-based quantification of caspase levels relative to DAPI (nuclei) levels, showed that both single copy and double copy Tom40 expression at 29°C led to significant increase in cleaved caspase levels, in comparison to a *GMR-GAL4* only control (Fig. 2). This corresponded to the severity of eye phenotype severity in adult eyes.

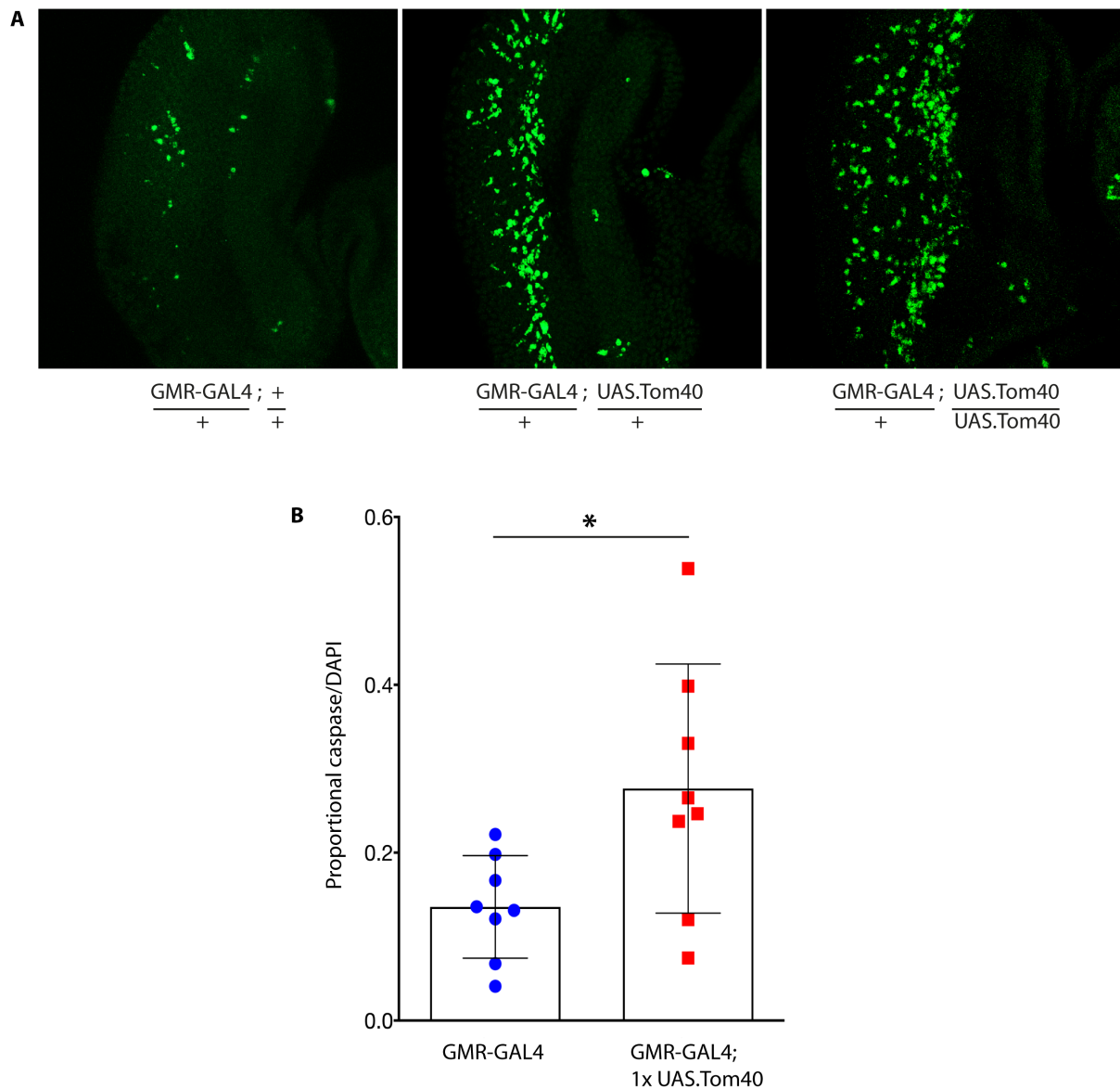


Figure 2. Expression of Tom40 mediates apoptosis in the developing *Drosophila* eye. A) Representative larval eye discs images of control GMR-GAL4 (left), 1x UAS-Tom40 (middle) and 2x UAS-Tom40 (right) immuno-stained with cleaved caspase-1, visible as bright green spots in the posterior region of the disc. An increase in levels of caspase staining is observed, in a dose-dependent manner, when UAS-Tom40 is expressed B) A bar graph shows a significant increase in proportional caspase/DAPI (nuclei) intensity corresponding to expression of 1x UAS-Tom40 compared to GMR-GAL4 only control. Statistical significance was calculated using unpaired t-test. $n = 8$ per fly genotype and * denotes $p = 0.0262$ (< 0.05).

4.4 Discussion

The intrinsic pathway of programmed cell death or apoptosis in cells is triggered by intracellular stress signals, such as oxidative stress (Roos and Kaina, 2006) and DNA damage (Orrenius *et al.*, 2007) and the role of mitochondria in this process is widely recognized (Green and Reed, 1998, Wang and Youle, 2009). A transition in mitochondrial permeability state is thought to cause mitochondrial outer membrane permeabilization (MOMP) and release of pro-apoptotic IMS proteins, including cytochrome C, eventually leading to caspase activation and cell death. The mechanisms by which MOMP and release of apoptosis initiator molecules occur remains controversial, and currently several proposed models exist. These include i) osmotic swelling and rupture of the mitochondrial membrane (Vander Heiden *et al.*, 2001, Lemasters and Holmuhamedov, 2006) (ii) opening of a membrane permeability transition pore (Petronilli *et al.*, 2001, Biasutto *et al.*, 2016), the molecular components of which remain ill-defined (iii) formation of large channels by oligomers of the pro-apoptotic proteins, Bax/Bak on the outer membrane (Antignani and Youle, 2006, Westphal *et al.*, 2014, Uren *et al.*, 2017) or (iv) hetero-oligomers of VDAC1 and Bax (Shimizu *et al.*, 1999, Banerjee and Ghosh, 2004) or VDAC1 oligomers (Shoshan-Barmatz *et al.*, 2013).

There could be several explanations for the observed cell death phenotype caused by Tom40 transgenic expression in the eyes. One scenario could be that overexpression causes integration of too much Tom40 into the outer membrane leading to increased porosity and permeability of the outer membrane, ultimately resulting in permeabilization and eventual cell death. Alternatively, the phenotype could be a consequence of mitochondrial stress and mitophagy caused by perturbation of the outer membrane by overexpression, indirectly causing apoptosis. Yet another plausible explanation is that excess Tom40-containing complexes associate with pro-apoptotic regulators, thereby promoting apoptosis.

On the last point, it has been demonstrated that exogenous overexpression of VDAC1 causes apoptosis in several cellular model systems, accompanied by proposals that overexpression induces oligomerization of VDAC1, leading to the release of IMS apoptotic factors and apoptosis (Godbole *et al.*, 2003, Zaid *et al.*, 2005, Ghosh *et al.*, 2007, Weisthal *et al.*, 2014). Conversely, several apoptotic stimuli have been shown to induce up-regulation of VDAC1 in various cancerous cell lines (Nawarak *et al.*, 2009, Keinan *et al.*, 2013). Similar up-regulation of Tom40 as a mechanism for triggering apoptosis could be envisioned, given that Tom40 and VDAC1 share common structural features. On a related note, upregulation of Tom40 observed

in nine human ovarian cancer cell lines has been correlated to cause an inhibitory effect on the proliferation, invasion and migration capabilities of cancerous cells, suggesting a tumour suppressive effect of Tom40 (Kim *et al.*, 2014).

As yet, there is little information pointing to a functional overlap of the TOM and apoptotic machineries, and arguments for and against can be found. For instance, Tom40 and Tom22 have been implicated as receptors for pro-apoptotic proteins of the Bcl-2 family, like Bax/tBid, to facilitate insertion into the outer membrane (Ahting *et al.*, 2005, Bellot *et al.*, 2006). Antibodies against Tom40 and Tom22 inhibit Bax/tBid integration into isolated rat liver mitochondria (Cartron *et al.*, 2008) and immuno-precipitation experiments appear to show direct interaction of Bax/tBid with Tom40 and Tom22 (Bellot *et al.*, 2006). Loss-of-function mutants of *Drosophila* Tom22 and Tom70 suppress an aberrant wing phenotype induced by heterologous expression of full-length murine Bax in flies, tentatively indicating a role in cell death (Colin *et al.*, 2009). Moreover, functional expression of murine Bax in *Drosophila* suggests that the apoptotic mechanisms between flies and humans are at least partially conserved, although this is still being debated (Mollereau, 2009). The reason for the suppression effect noted above is not yet known. It could be due to disruption of the process for mitochondrial localization of Bax, given that Tom22 is a putative receptor for Bax import (Bellot *et al.*, 2006) or, alternatively, the phenotype may be caused by depleting the number of functional TOM complexes available for potential association with Bax and/or other pro-apoptotic proteins during apoptotic events. TOM is not essential for apoptosis, however, as other studies have demonstrated TOM-independent apoptotic mechanisms. For instance, the absence of TOM subunits in mammalian mitochondria (*i.e.*, via individual shRNA knockdown of Tom40, Tom22 and Tom70) does not affect either translocation of Bax or formation of Bak/Bax complexes (Ross *et al.*, 2009), while in yeast, mutant strains of Tom40 and deletions of Tom22 or other components does not significantly impair Bax-induced release of cytochrome C (Sanjuan Szklarz *et al.*, 2007). Overall, while there is evidence for crosstalk between the protein import and apoptosis machinery, the level of overlap between the two processes has not yet been ascertained.

Of the fly eyes used for purification of TOM complex, those in which Tom40 was expressed as a single copy, did not exhibit an apparent eye phenotype, although one cannot rule out that the level of cell death was higher than normal. We do not yet know if proportionally more VDAC associates with Tom40 in the flies with a severe eye phenotype linked to increased Tom40 expression. This would point to a more direct link between TOM and apoptosis than

has been supposed and is a point to be addressed in the short term. It would also be interesting to understand whether this cell death phenomenon we observe is restricted to the eye tissues of *Drosophila* or is applicable to other tissue types such as muscle, brain etc. This could be tested by targeting expression to specific tissue types and studying the phenotypes displayed by flies. Further, the glossy eye phenotype associated with double-copy Tom40 expression can be used in a genetic screen to identify interaction partners that are capable of enhancing or suppressing the phenotype. In particular, it will be very interesting to explore potential links between Bcl-2 pro-apoptotic family members, VDAC/ANT and Tom40 during apoptosis and obtain insights into the mode of action.

Chapter 5

General discussion

5.1 Introduction

The aim of this chapter is to place the findings of the project in the context of the mitochondrial import field. The stoichiometry and estimated mass of TOM complexes are considered in the light of cryo-EM data, followed by a discussion of VDAC-TOM association in the mitochondrial outer membrane. A model that may explain some of the more unexpected findings is presented. The chapter concludes with an overview of the significance and future directions of the project.

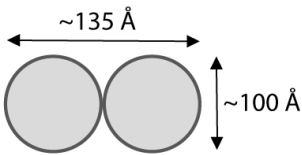
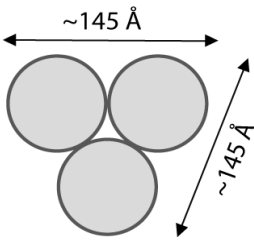
5.1.1 Architecture and stoichiometry of TOM complexes

The precise stoichiometry, molecular mass and quaternary organisation of the three-pore TOM import complex is uncertain. However, previous structural studies have lent important insights, for example, establishing that the three-pore complex contains the Tom20 subunit in addition to the core TOM subunits (Model *et al.*, 2002) and that, in contrast, Tom70 does not appear to be an essential requirement (Model *et al.*, 2008). Unexpectedly, comparison of two recent cryo-EM structures revealed that superposition of the *Neurospora* two-pore TOM onto the *Saccharomyces* three-pore complex map is not straightforward (Bausewein *et al.*, 2017). Merely adding a third core heteromeric unit (*i.e.* Tom40, Tom22, Tom5, Tom6, Tom7), or even a Tom40 β -barrel alone, to the two-pore structure does not explain regions of cohesive density in the three-pore maps, implying some rearrangement of quaternary structure in transitioning between two- and three-pore complexes.

The molecular mass of the purified three-pore TOM complex has been estimated to be in the broad range of 400-550 kDa, based on blue-native PAGE analysis (Model *et al.*, 2002, Model *et al.*, 2008). This estimate, more than three times the mass of the two-pore core TOM complex, must be viewed with caution; the molecular mass of the two-pore TOM core complex was similarly estimated at approximately 400 kDa based on blue-native PAGE and gel filtration chromatography analyses (Ahting *et al.*, 1999), but the exact mass of this complex, as later determined by laser-induced liquid bead ion desorption (LILBID) native mass spectroscopy, turned out to be significantly smaller, at 148 kDa (Mager *et al.*, 2010, Bausewein *et al.*, 2017). Association of lipid, detergent or Coomassie blue molecules, commonly observed for membrane proteins (Crichton *et al.*, 2013) could partly explain the discrepancy, but it is likely that a better explanation lies in the flattened shape and hydrodynamic radii of both protein complexes retarding migration through the polyacrylamide matrix (Wittig *et al.*, 2006). The longest dimensions of the two-pore and three-pore complexes, determined from cryo-EM models, are very close at 135 Å and 145 Å, respectively (Table. 1), consistent with their similar migration through the gel. On this basis, it seems possible that the true mass of the three-pore complex will also prove less than expected. A smaller than predicted molecular mass for the three-pore complex also makes sense from the perspective of structural organisation. In the core TOM structure both pores in the complex are β -barrels, each corresponding to a single Tom40 subunit. The cryo-EM model of the yeast three-pore complex (Model *et al.*, 2008) is approximately 50 % larger and has imprecise three-fold symmetry. The subunit stoichiometry of the three-pore complex is unknown, but an approximate calculation of its mass can be made

by assuming the addition of one heteromeric unit of the core complex (mass 74 kDa) and one copy of Tom20 per Tom40 (60 kDa total). Using the mass of the core two-pore complex as a starting point, the total mass of the three-pore complex would be less than 300 kDa.

Table 1. Comparison of dimensions, molecular mass and stoichiometry of TOM complexes

	Core complex	Tom20 - Core complex
		
	(Bausewein et al., 2017)	(Model et al., 2008)
Molecular mass estimation		
by BN-PAGE	~400 kDa	~400 - 550 kDa
by Native Mass Spectrometry	148 kDa	Not determined
Subunit stoichiometry	Two molecules each of Tom40, Tom22, Tom5, Tom6 and Tom7	Not determined

5.1.2 Tom40 does not exclusively associate with translocase subunits

An interesting finding was the co-elution of VDAC and ANT with Tom40. While these are the most abundant of mitochondrial membrane proteins, they remain attached to Tom40 after affinity purification with stringent salt and urea wash steps (see Chapter 2, section 2.4.5.3). The protein bands are absent in a control pull down on wild type flies, clarifying that their presence is not artefactual due to non-specific binding to the affinity resin.

The association of Tom40 with VDAC and ANT is thus robust, but may be direct, indirect or, conceivably, VDAC and ANT may be present only in the form of arrested import

intermediates. Assuming the VDAC/ANT/TOM association exists within a quaternary assembly, it remains to determine whether VDAC preferentially associates with two- or three-pore TOM complexes. It could incorporate as a ‘third pore’, but its strong presence in LMNG extractions, where we observed only two-pore complexes by negative stain EM, consistent with the absence of Tom20, does not endorse this. Alternatively, it may indicate that binding of Tom20 and VDAC is mutually exclusive, perhaps due to a common binding interface. If it exists, a three-pore TOM complex containing VDAC may not be sufficiently robust to survive on the cryo-EM grid. Extractions in digitonin show a pattern of protein bands that vary somewhat in relative intensity between extractions. We presently interpret this as a mix of populations of Tom20-core TOM (three-pore), core TOM (two-pore), and TOM-VDAC complexes (that may also contain ANT). These are by no means the only possibilities and VDAC association might also be mediated via another TOM subunit or a specific lipid. The interpretation takes into account western blot analyses of the digitonin and LMNG-solubilised membranes on blue-native PAGE indicating Tom40 is present in at least three different complexes, 146 kDa, 450/480 kDa and 720 kDa (Fig. 10, Chapter 2). Finding which of the three complexes contains VDAC is now a priority.

5.1.3 Context for a three-pore TOM complex

It is not intuitively obvious why a third pore would be required for general import, but structural evidence supports its presence. It has been widely assumed that the third pore in the TOM holo-complex is another Tom40 molecule, although no direct evidence specifically supports this over other options.

Other major pore-forming proteins in the metazoan mitochondrial outer membrane that might be candidates for a third pore are VDAC and Sam50, the central β -barrel component of the SAM complex. It has been suggested that Sam50 might account for the third pore (Bausewein *et al.*, 2017), consistent with identification of a TOM-SAM super-complex in yeast (Qiu *et al.*, 2013). In the study, co-enrichment of TOM components with SAM was recognized using the quantitative approach of stable isotope labelling of amino acids in cell culture (SILAC)-based mass spectrometry. However, inspection of the SILAC data reveals that Por1, the yeast homologue of VDAC1, is also significantly enriched to levels comparable to the TOM subunits, suggesting it also as a candidate. Indeed, a supramolecular assembly of TOM and VDAC was discovered in rat brain mitochondria, and later corroborated in yeast (Muller *et al.*, 2016); Por1 was found in a 440 kDa complex containing Tom40, Tom22 with immuno-

precipitation experiments confirming the interaction. Other possible candidates are the mitochondrial distribution and morphology protein Mdm10, (Meisinger *et al.*, 2004, Flinner *et al.*, 2013) and newly identified outer membrane channels in yeast, Mim1 and Ayr1 (Krüger *et al.*, 2017), although homologues have not yet been identified in the genomes of higher eukaryotes.

5.1.4 A model for VDAC interaction with TOM

Based on the preceding discussion, a hypothetical model that represents a possible explanation for our findings is presented in Figure 1. In this proposal, the core TOM complex (two-pore) acts as a scaffold that, in response to cellular signals/requirements, is recruited either i) to the holo-TOM complex or ii) to an apoptotic complex, by associating with either Tom20 (+ third pore) or VDAC (+ANT) respectively. Inclusion of a third pore is likely to involve some remodelling of the interfaces within the core complex, as suggested by Bausewein *et al.* (2017).

A model for formation of a three-pore complex containing Tom20 (or) VDAC

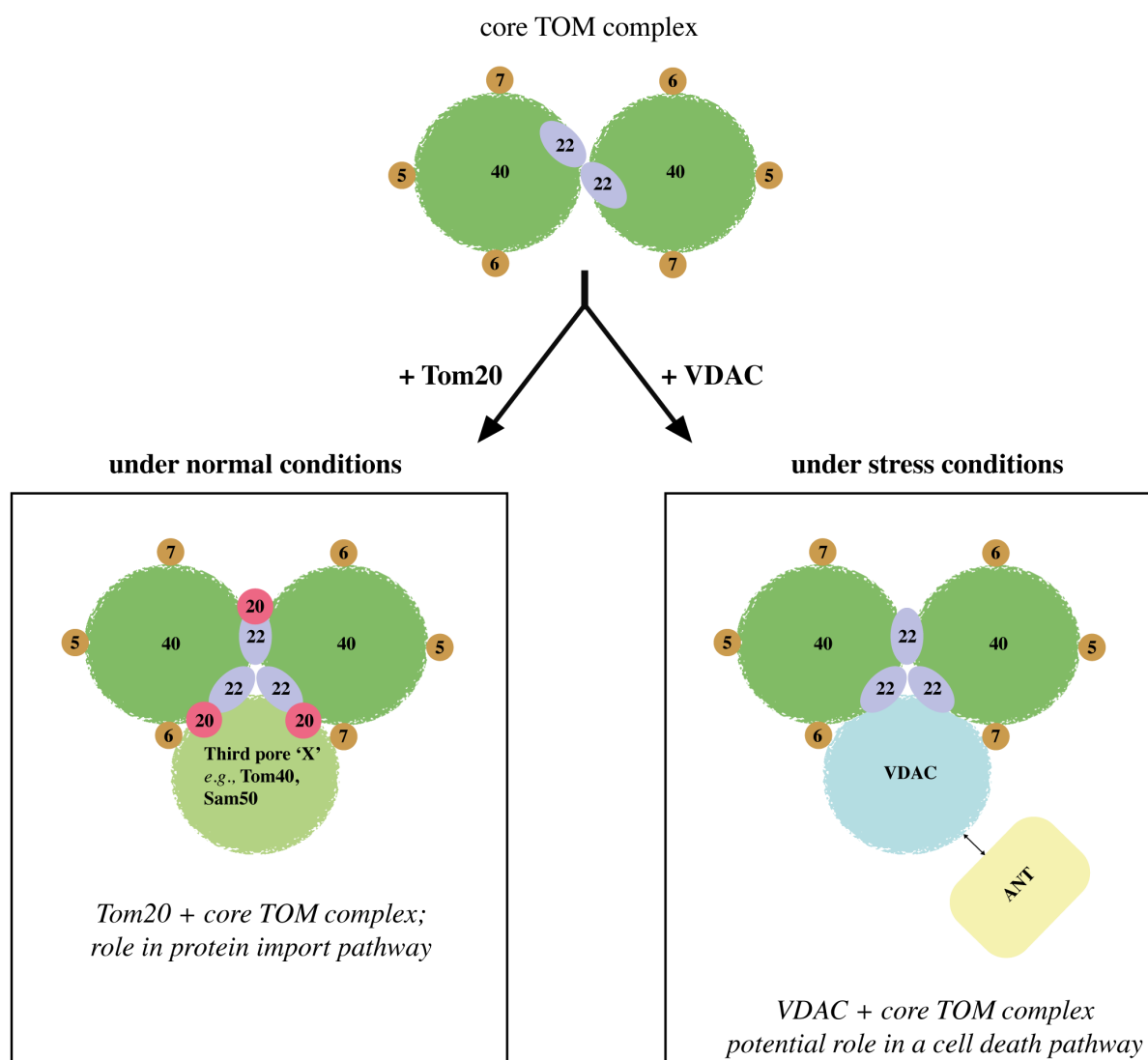


Figure 1. A hypothetical model to explain VDAC association with Tom40/TOM. Under normal cellular conditions (left panel), TOM exists as a two- and three-pore species, with the three-pore structure forming exclusively in the presence of Tom20 (left panel) (Model et al., 2002). These depicted complexes might exist in equilibrium with one another in the outer membrane (Model et al., 2001, Rapaport et al., 2001, Shiota et al., 2015). Upon a stress stimulus (this might be the overexpression of Tom40, in our case), the association with VDAC may be promoted at the expense of association with Tom20 (right panel). VDAC-TOM complexes may exist alongside the standard TOM complexes and may recruit ANT in the inner membrane. Oligomerization of TOM-VDAC complexes might subsequently mediate mitochondrial outer membrane permeabilization (MOMP), inducing cellular apoptosis.

5.2 Concluding remarks and future directions

The general import pore of TOM is the gateway for protein entry into mitochondria, for nuclear-encoded mitochondrial proteins as well as for pathogenic peptides and proteins implicated in human diseases. In the work presented in this thesis, *Drosophila* has served as a novel platform for structure-function analysis of the mitochondrial translocase, which include functional *in vivo* expression of Tom40 and preparative scale purification of TOM for biochemical and structural analysis. Phenotypic read-outs can be utilised to interrogate the role of TOM in an organism that has components highly homologous to human TOM, with implications for understanding more about the impact of mitochondria on disease. This is illustrated by our novel discovery of a cell death eye phenotype linked to elevated Tom40 expression, which we were able to investigate using fly genetics and other tools. Further, this system may prove invaluable in illuminating the cross-talk between TOM and other proteins in mitochondrial membranes. Importantly, it may help to identify novel interacting components in the context of a living metazoan organism. It is possible that Tom40 plays a regulatory role in mitochondrial and cellular function by maintaining a balance between mitochondrial growth and cell death. Apart from its known function of import of mitochondrial proteins, Tom40/TOM complex might possess additional roles, that have so far remained largely unexplored. The interesting result that VDAC and ANT pull-down with Tom40, both implicated in the cell death process, might be an indicator for other such roles.

The next step in this project is structure determination of a three-pore TOM assembly, with and without a precursor molecule engaged, offering unprecedented possibilities for probing the assembly of translocase complexes, mechanisms of precursor import into mitochondria, and the functional overlap of translocases and other mitochondrial machinery.

Chapter 6

Materials and Methods

6.1 Materials and Reagents

Unless otherwise stated, all chemicals were purchased from Sigma-Aldrich (MO, USA). Metal sieves used for sorting of fly heads were purchased from Impact Test Equipment Ltd. (Scotland, UK). Dounce tissue grinders (1 ml and 40 ml) were from WHEATON Industries Inc., (NJ, USA). ANTI-FLAG® M2 Affinity Gel was from Sigma-Aldrich (MO, USA). 3.5 mm diameter glass beads were from BioSpec Products (OK, USA). Pierce™ Anti-HA Agarose beads, Silver Staining kit and components of the Native PAGE system including 4-16 % Native PAGE gels were from ThermoFischer Scientific (MA, USA). 100 kDa microcentrifuge filter units, Immobilon Western Chemiluminescent HRP Substrate and 0.2 µm PVDF membrane were from Merck Millipore (MA, USA). Holey carbon EM grids were from Quantifoil Micro Tools GmbH (Großlobichau, Germany). FLAG peptide (DYKDDDDK) was from GenScript (NJ, USA). 10 ml plastic purification columns, Precision Plus Protein™ Dual Color Standards, glass plates and acrylamide for preparation of hand poured gels, western transfer thick blot paper were from Bio-Rad Laboratories (CA, USA). DNase I and protease inhibitor cocktail tablets were from Roche, Merck Millipore (MA, USA). Digitonin detergent was from Biosynth AG (Staad, Switzerland) and all other detergents that were used in the study were from Anatrace (OH, USA).

6.2 General fly handling procedures

6.2.1 Fly food

Strains are reared on molasses-based *Drosophila* medium made using the following protocol and the reagents listed in Table 1. Briefly, 1.4 kg of molasses is mixed in 3 L of water and 900 g of yeast was mixed with 3 L of water before pouring into a 30 L metal pot and placing on a gas burner. The mixture is brought to 100°C with occasional stirring. 630 g of semolina is mixed with 3 L of water and added to the pot. Upon the mixture obtaining a homogeneous consistency, the gas was turned off and the mixture cooled to 80°C prior to the addition of the Acid mix and Tegosept. The mixture is then dispensed into trays of polypropylene *Drosophila* culture vials using the "drosofiller" automated fly food dispenser (Flystuff, CA).

Table 1. List of ingredients in *Drosophila* culture medium

Name	Amount
Molasses	1400 g
Agar	60 g
Glucose	160 g
Fresh yeast	900 g
Semolina	1260 g
Acid mix	138 mL (546 mL H ₂ O + 412 mL Propionic acid + 42 mL Phosphoric acid)
Tegosept	262 mL (1000 mL 95 % ethanol+100 g hydrobenzoic acid methyl ester)

6.2.2 Fly rearing and maintenance

Flies are reared in vials plugged with a cotton ball containing solidified food (Fig. 4, Chapter 2). Fly stocks are maintained at room temperature (21°C) and turned into fresh vials every 3-4 weeks to avoid mite contamination.

6.2.3 Setting up of genotype crosses/genetic mating schemes

Male and unmated female (virgin) flies from two different genotypes were crossed. To select flies for gender, virginity and phenotypic markers, freshly eclosed flies were tipped from their vial onto a porous pad dispensing CO₂. CO₂ acts as an anaesthetic and flies can be inspected on this pad under a dissection microscope.

6.3 Experimental procedures

6.3.1 Establishment of *Drosophila* fly strains

6.3.1.1 Cloning and generation of new transgenic fly strains

pUASTattb vector was a kind gift from Dr. Michael Murray (The University of Melbourne). DNA constructs of *Drosophila* Tom40 (isoform 2) and Tom22 (schematic of constructs presented in Fig. 5) were designed and purchased as genomic blocks (Integrated DNA Technologies, Singapore). Constructs were ligated into restrictively digested pUASTattb vector between ECoRI and XhoI sites. 20 µg of each sequence-verified plasmid was utilised for generation of transgenic fly lines. BestGene (Chino Hills, USA) carried out microinjection of plasmids into *Drosophila* embryos for site-specific chromosome recombination using the Phi31 integrase system (Bischof et al., 2007). Transformant flies were selected and were shipped to Australian quarantine and importation facility before delivery.

6.3.1.2 Other fly strains

Other fly lines used in the project were obtained from various *Drosophila* stock centres as tabulated in Table 2.

Table 2. List of fly strains used in the study

Genotype	Stock Number	Chromosome	Source
UAS-Tom40-FLAG.HA	DP0631	3	Bangalore Fly Resource Centre, India
UAS-Tom22-FLAG.HA	DP1045	3	Bangalore Fly Resource Centre, India
UAS-Tom20-3xHA	F003545	3	FlyORF, Switzerland
w1118	BL39831	1	Bloomington Stock Centre, US
Tubulin-GAL4/Tm6B	BL5138	3	Bloomington Stock Centre, US
<i>GMR</i> -GAL4	BL9416	2	Bloomington Stock Centre, US
eYFP-mito	BL7194	3	Gary Hime, AUS
P[lacW]Tom40 ^{G0216} /FM7c	BL11859	1	Bloomington Stock Centre, US
Tom40 TRiP (RNAi)	BL26005	3	Bloomington Stock Centre, US

6.3.2 Immunostaining and confocal microscopy

6.3.2.1 Tissue dissection and fixation

Wandering third instar larvae were collected and placed in a glass cavity block, containing Phosphate Buffered Saline (PBS) (Table 3), on ice. Unless otherwise stated, larval heads were dissected in PBS and then fixed in 4 % para-formaldehyde (PFA, Table 3) in PBS for 20 min, followed by three quick rinses and three 20 min washes in PBS with 0.1 % Triton-X (PBT) (Table 3). Fixation, washes and rinses were done on a tabletop nutator (BD Adams) at room temperature (RT).

6.3.2.2 Antibody staining

Larval heads were blocked in 5 mg/ml Goat Serum in PBT (Table 3) for at least 1 hour at room temperature, followed by primary antibody incubation with appropriate antibodies (1:100 dilution) overnight at 4°C. Larval heads were then subjected to three 20 min washes in PBT and incubated with the appropriate fluorescently-tagged secondary antibody (1:1000 dilution) for at least 1 hour at RT. Subsequently, tissues were incubated in DAPI solution (Table 3) for 10 min and washed in PBS three times 10 min each. Finally, tissues were stored in 80 %

glycerol at 4°C prior to dissection. Antibodies were diluted in Blocking Solution (Table 3) and are listed in Table 4.

6.3.2.3 Mounting of larval eye discs

Eye imaginal discs were dissected away from the other larval tissues under an Olympus SZ microscope and mounted in 80 % glycerol on a glass microscope slide. Eye discs were then placed under a glass coverslip and sealed with clear nail polish for imaging.

6.3.2.4 Microscopy imaging

A Zeiss LSM 800 running Zen Blue software was used to visualize and analyze the eye imaginal discs. Serial Z-series were captured in 1 µm sections at 40x magnification. Fluorophores were imaged using band-pass filters to remove cross-detection between channels and pseudo-coloured for image preparation.

6.3.2.5 Image analysis

Confocal images were saved in .czi format and processed using Image J 1.48v, and Adobe Photoshop CS5 Version 12.0.4.I. For caspase pixel intensity quantification, Imaris software was utilised. For quantification of caspase staining, images were imported into Imaris software and caspase signal was set to basal level. The posterior region of the eye discs was selected and a 3D volume-based measurement of caspase and DAPI signals was carried out. Proportional caspase staining (to DAPI) was calculated and a graph was plotted in Prism 7.

6.3.3 Imaging of adult *Drosophila* eyes

Flies were anesthetized under CO₂ under an Olympus SZ microscope Dissecting Microscope, with a KL 1500 LCD light source (Carl Zeiss, Germany) and imaged at the highest possible magnification.

Table 3. List of immunohistochemistry reagents

Name	Preparation	Supplier
1X Phosphate Buffered Saline (PBS)	One Sachet (Sodium Phosphate 10 mM, NaCl 150 mM) in 500 mL distilled water	CLP Direct
Phosphate Buffered Saline with 0.1 % Triton-X 100 (PBT)	500 µl of Triton X-100 in 50ml of PBS	Triton-X Sigma
Blocking Solution		
Bovine Serum Albumin (BSA)	5 mg/ml BSA/Goat Serum in PBT	Roche
DAPI	1' 4' 6-Diamidino-2-Phenylindole diluted 1:1000 in distilled water	Sigma
80 % Glycerol	80 % Glycerol in PBT	Sigma
4 % paraformaldehyde	1:4 dilution of 16 % PFA in PBS	Electron Microscopy Sciences

Table 4. List of antibodies

Antibody name	Type	Supplier	Catalogue number
Anti-HA	Rat monoclonal	Roche	11867423001
Anti-FLAG	Mouse monoclonal	Aviva Systems Biology	OAEA00002
Human VDAC	Mouse monoclonal	Abcam	14734
Human ANT1	Mouse monoclonal	Mitosciences	110322
<i>Drosophila</i> caspase-1	Rabbit polyclonal	Cell Signalling Technologies	9578
Anti-rat HRP	Rabbit polyclonal	ThermoFisher Scientific	61-9520
Anti-mouse HRP	Rabbit polyclonal	Sigma-Aldrich	A9044
Anti-rat rhodamine	Goat polyclonal	Invitrogen	31680
Anti-rat 647	Chicken polyclonal	Invitrogen	21472

6.3.4 Protein expression, purification and detection

Buffers used in the following procedures are listed in Table 5.

6.3.4.1 Protein expression trials

UAS-GAL4 based protein expression was carried out by setting up genetic crosses between male flies harbouring UAS-transgenes and virgin female flies with promoter-GAL4 driver sequence. Tubulin-GAL4 (ubiquitous expression) and *GMR*-GAL4 (eye-specific expression) driver strains were used for experiments. For generation of experimental flies, approximately 5 - 8 virgin females and 2 - 4 males were added to fresh vials for mating. All crossings were carried out at 25°C unless otherwise stated. Parents were cleared from the vial before eclosion of progeny flies. 24 hrs after eclosion, ten flies were collected from each vial and tissue homogenates were prepared in Lysis Buffer (Table 5) using a plastic Eppendorf pestle. Depending on the type of expression, either whole fly lysates or fly head lysates were analysed by SDS-PAGE and western blotting. Heads were decapitated from bodies under CO₂ anaesthesia using a razor blade.

6.3.4.2 Isolation of mitochondria

Mitochondria were isolated from adult *Drosophila* (whole flies or heads) with existing protocols (Schwarze *et al.*, 1998, Miwa *et al.*, 2003) with some modifications. Fifty flies were gently crushed, in 300 µl of chilled Mitochondrial Isolation Buffer (Table 5) supplemented with protease inhibitor cocktail, using a plastic homogeniser. Lysates were filtered using a 100 µm filter unit to remove debris and made up to 1000 µl with the same buffer. The sample was centrifuged at 10,000 x g for 10 min at 4°C to sediment intact mitochondria. The supernatant was discarded without disturbing the pellet and the mitochondrial pellet was resuspended in a small volume (30 µl) of 20 mM Tris-HCl pH 8.0, 50 mM NaCl, 5 % glycerol and 0.1 mM EDTA and snap-frozen in liquid nitrogen and stored at -80°C until further use.

6.3.4.3 Large-scale harvesting of fly heads

Approximately 10 ml of frozen flies were placed in a 50 ml Falcon tube with 5 ml of glass beads pre-cooled with liquid nitrogen. The mixture was briefly vortexed on a high setting followed by vigorous manual agitation. The mixture of flies and glass beads was then transferred to the top of a pre-cooled stack of stainless-steel sieves with decreasing pore diameters of 710, 500, 355 and 250 µm top to bottom, respectively. The stack was shaken vigorously to separate the fractionated body parts based on size. Fly heads collected in the 500

μm sieve compartment were transferred to Eppendorf tubes using a pre-cooled funnel. 10 ml of flies provide approximately 0.5 ml of fly heads. A total volume of 50 ml or 100 ml flies per session were processed, based on requirements for downstream experiments. Harvested fly heads were used immediately for membrane preparation or stored at -80°C for further use.

6.3.4.4 Isolation of membranes and detergent solubilisation

For analytical purposes, membranes were prepared from approximately 100 whole flies or heads. Flies were placed in an Eppendorf and homogenised using a plastic pestle in Lysis Buffer supplemented with DNase I and protease inhibitor cocktail. Crude lysates were filtered using a 100 μm filter unit to remove debris and subjected to ultracentrifugation at 100,000 x g for 1 hour at 4°C . Supernatant was removed and the entire pellet comprising of mitochondrial and other cellular membranes was collected. Membranes were resuspended in Solubilisation Buffer (Table 5) containing 1 % (w/v) detergent of choice and incubated at 4°C for 30 min. Samples were centrifuged at 20,000 x g for 30 min at 4°C and supernatant containing solubilised membranes was collected and immediately used for further analysis.

For large scale isolations, fly heads collected in eppendorf tubes, corresponding to 10 ml of flies were pressed firmly using a plastic pestle for crude homogenisation with 500 μl of Lysis Buffer. Homogenates from multiple tubes were pooled together and added to a glass dounce homogeniser. Three strokes were performed to maximize tissue disruption and lysates were then filtered using a 100 μm cap filter to remove debris. Membranes were pelleted by ultracentrifugation at 100,000 x g for 1 hr at 4°C . Typically, 50 ml of fly heads provide approximately 0.5 g of membranes. Membranes were snap-frozen in liquid nitrogen and stored at -80°C until further use.

Membranes were thawed out rapidly in Lysis Buffer and re-homogenised using a Dounce homogeniser with 10 ml of buffer per 0.1 g of membranes. For membrane solubilisation, lysates were supplemented with 1 % final concentration of detergent (digitonin or LMNG) and incubated under mixing for 45 min at 4°C . A centrifugation at 20,000 x g was performed to clear out insolubilized material. Supernatant was filtered using a 0.45 μm syringe filter unit.

6.3.4.5 Purification of TOM complex by immuno-affinity methods

Filtered supernatant was applied to a gravity drip column packed with FLAG antibody conjugated beads pre-equilibrated with Lysis Buffer containing 0.1 % digitonin or 0.005 % LMNG. In case of digitonin, detergent concentration of lysate was brought down to 0.2 %

with a 1:5 dilution with lysis buffer before application. Flowthrough was collected and re-applied once again to maximize binding. Column was washed with 5 column volumes (CV) of lysis buffer containing 0.1 % digitonin or 0.005 % LMNG (Wash Buffer 1), followed by two washing steps of 5 CV of 1M urea containing buffer (Wash Buffer 2) and 5CV of 500 mM NaCl containing buffer (Wash Buffer 3), which were performed to remove non-specific binding contaminants. The sample was reequilibrated by washing with 10 CV of Wash Buffer 1 prior to elution.

For elution under non-denaturing conditions, one CV of Wash Buffer supplemented with FLAG peptide at 0.5 mg/ml (Elution Buffer) was added. The column was incubated at room temperature for one hour. The eluate was collected, and elution was repeated once. Eluates were pooled together, concentrated using a 100 kDa centrifugal filter and snap frozen using liquid nitrogen and stored at -80°C until further use.

6.3.5 Protein detection methods

6.3.5.1 SDS-Polyacrylamide Gel Electrophoresis (SDS-PAGE)

SDS-PAGE was carried out under denaturing conditions, as described (Laemmli, 1970). Tris-Glycine hand-poured gels were prepared as follows: To make 15 % gels, a resolving gel composed of 15 % (w/v) polyacrylamide, 375 mM Tris-HCl pH 8.8, 0.1 % (w/v) SDS, 0.05 % (w/v) APS and 0.05 % (w/v) TEMED comprised the lower 80 %. The upper 20 % stacking gel layer was prepared with 5 % (w/v) Polyacrylamide, 375 mM Tris-HCl pH 6.8, 0.1 % (w/v) SDS, 0.05 % (w/v) APS and 0.05 % (w/v) TEMED.

Sample Loading buffer was added to samples before prior to loading. Dual colour Precision Plus Prestained Protein Standard (5 µl) was loaded concurrently to identify band sizes. Gels were run in a mini-gel apparatus (Bio-Rad), using Tris-Glycine Running Buffer at a constant voltage of up to 200 mV for 45 minutes.

Proteins were stained using a Silver Stain kit (ThermoFischer Scientific) according to manufacturer's instructions.

6.3.5.2 Blue Native PAGE (BN-PAGE)

BN-PAGE was performed using the Native PAGE Bis-Tris Gel System (Invitrogen). Protein samples containing detergents were combined with Native PAGE Sample Buffer. Immediately prior to loading, 5 % G-250 Sample Additive was added to the samples and gently mixed until combined. NativeMark unstained protein standards were loaded alongside. Precast 4-16 % Bis-

Tris Native gels were run with Native PAGE Running Buffer (1X) and Dark Blue Cathode Buffer (1X) for 2 hours at 150 V in a NOVEX tank at 4°C. In the case of a downstream western blotting application, after an initial 40 min, the run was paused and the Dark Blue Cathode Buffer was removed after the dye front migrated to one-third of the gel. It was replaced with a Light Blue Cathode Buffer before the run was resumed.

6.3.5.3 Western blotting and immunodetection

Proteins bands from SDS-PAGE and BN-PAGE were transferred to methanol-activated PVDF membranes (Millipore) using the semidry transfer method (Towbin et al., 1979; Kyhse-Anderson, 1984). Gels and thick blot filter papers (Bio-Rad) were soaked in Western Transfer Buffer for 5 min and electroblotting was performed with the voltage limited to 20 V for either 1 hr or 2 hrs and 30 min for SDS-PAGE and BN-PAGE gels, respectively.

After blotting, PVDF membranes were incubated in Western Blocking Solution for 1 hr at RT on a rolling platform. In the case of BN-PAGE gels, blotted membrane was de-stained with methanol before the blocking step. Immunodetection was performed with an anti-HA monoclonal antibody (1:1000) in blocking solution and incubated at RT for 1 hr. The membrane was washed three times (10 min each) with Western Wash Buffer and goat anti-rat secondary antibody conjugated to horseradish peroxidase (1:5000) was added and incubated for 30 min at RT. The membrane was washed again as above and treated with 5 ml of Immobilon Western Chemiluminescent HRP Substrate (Merck) for 5 min and excess substrate was removed. Chemiluminescent protein bands were detected using a ChemiDoc system (Bio-Rad).

6.3.5.4 In-gel tryptic digestion and mass spectrometry

Identification of proteins by mass spectrometry was carried out at Monash proteomics facility. Briefly, protein bands were excised from a silver stained SDS-PAGE gel and proteolysed by trypsin to generate a peptide digest. The peptide fragments were analysed using nano-liquid chromatography coupled with electrospray ionization mass spectrometry (nano-LC-ESI MS/MS). Mass spectra were recorded on a QExactive Plus 1 machine (Thermo Scientific). Data were analysed using Mascot software V2.4 (Matrix Science) and searched against protein sequence databases namely, Uniprot and Swissprot.

Table 5. Miscellaneous buffers and solutions

Name	Components
Lysis Buffer	20 mM Tris-HCl pH 7.4, 150 mM NaCl
Solubilisation Buffer	Lysis Buffer + 1 % (w/v) detergent
Wash Buffer 2	Wash Buffer 1 + 1M urea
Wash Buffer 3	Wash Buffer 1 + 500 mM NaCl
Elution Buffer	Wash Buffer 1 + 0.5 mg/ml FLAG peptide
Mitochondria Isolation Buffer	250 mM sucrose, 10 mM Tris pH 8.0 and 0.15 mM MgCl ₂
Mitochondria Resuspension Buffer	20 mM Tris-HCl pH 8.0, 50 mM NaCl, 5 % glycerol and 0.1 mM EDTA
4X Sample Loading buffer	250 mM Tris-HCl pH 6.8, 8 % (w/v) SDS, 50 % glycerol, 5 % (v/v) β-mercaptoethanol and 0.2 μg bromo-phenol blue
Tris-Glycine Running Buffer	25 mM Tris-HCl pH 8.3, 250 mM glycine, 0.1 % SDS
Phosphate Buffered Saline (PBS)	16 mM disodium hydrogen phosphate, 4 mM sodium dihydrogen phosphate, 120 mM sodium chloride
Western Transfer Buffer	25 mM Tris-HCl pH 8.3, 192 mM glycine, 10 % (v/v) methanol, 0.05 % (w/v) SDS
Western Blocking Solution	5 % (w/v) skim milk powder, 0.05 % TWEEN-20, made up with PBS
Western Wash Buffer	PBS + 0.05 % TWEEN-20

6.3.6 Electron microscopy (EM) and image processing

6.3.6.1 Negative stain EM imaging

A sample comprising 3 μ l of purified protein was added on top of a glow-discharged holey carbon coated copper grid with a 5 nm carbon layer (Quantifoil, Germany) and incubated for 30 secs to promote sample adsorption. Excess sample was blotted from edge of the grid with filter paper, followed by two quick washes where grids (sample side down) were placed over the top of a droplet of MilliQ water, blotting the excess in between washes. Subsequent staining with a 1 % aqueous solution of uranyl acetate was performed in a similar manner by placing the grid over the liquid droplet. The grids were air dried and imaged at magnifications of x 27,500 or x 78,000 using a Tecnai F30 transmission electron microscope at the Bio21 Advanced Microscopy Facility (The University of Melbourne).

6.3.6.2 Particle selection and 2D classification of particles

Micrographs were converted from .tif to .mrc using EMAN2 and particles were manually picked and extracted from the micrographs and 2D classification was performed using RELION3.1.

6.3.7 Cryo-EM methods

These were carried out on purified TOM samples provided to Prof. Werner Kühlbrandt (Frankfurt, Germany).

6.3.7.1 Preparation of graphene oxide covered holey carbon grids

C-Flat 1/1 grids were glow discharged with 30 mA for 60 seconds. A 1:10 dilution of a 2 mg/ml graphene oxide solution was prepared and 3 μ l of the solution was applied on grid and incubated for 25 seconds. The grid was blotted, washed with water and dried for storage.

6.3.7.2 Cryo-EM specimen preparation

3 μ l of protein solution was applied on holey carbon grid (glow discharged), attached to tweezers. Solution was blotted in Vitrobot chamber for 9 seconds maintained at 100 % humidity and 10 °C. and rapidly frozen in liquid ethane. Afterwards transferred to liquid nitrogen for storage and further use.

6.3.7.3 Data acquisition

Movies were acquired with a JEOL JEM-3200 FSC with 0.2 seconds per frame within 9 seconds, equivalent to 45 frames. Beam-induced motion correction was done with MotionCor2

using a dose filter of 1.5 electrons per frame. Contrast Transfer Function (CTF) values were estimated with Gctf-v1.06.

6.3.7.4 Microscopy information

Electron microscope	JEOL JEM-3200 FSC with Energy filter
Voltage	300 kV
Direct Detector	K2 Summit
Magnification	30.000 x
Pixel size	1.12 Å/px
Electron dose	~60 electrons/Å ²
Grid type	C-Flat 1/1

6.3.7.5 Image processing

Particles were auto-picked and extracted with Relion2.1 with a box size of 200x200 pixels. Particle images were aligned and classified in 2D with Relion2.1.

Appendix

A. Amino acid sequences of Tom40 and Tom22 of *Drosophila*

> *Drosophila melanogaster* |Q9U4L6|Tom40 homolog 1 (Tom40-1)
 MGNVLAASSGAPGSGASNLGLGLOEPAPLPSNSGSLTESSSSAEGLDLAAAKDAALENP
 GTVEELHKKCKDIQAITFEGAKIMLNKGLSNHFQVSHTINMSNVVPSGYRFGATYVGTKE
 FSPTAEAFPVLLGDIDPAGNLNANVIHQFSARLRCKFASQIQESKVVASQLTTDYRGSYDT
 LSLTVANPSIFTNSGVVVGQYLQSVTPALALGSELAYQFGPNVPGRQIAIMSVVGRYTAG
 SSVWSGTLGQSGLHVCYYQKASDQLQIGAEVETSLRMQESVATLAYQIDLPAKANLVFRGG
 IDSNWQIFGVLEKRLAPLPFTLALSGRMNHVKNNFRLGCGLMIG

> |A1Z6L1| *Drosophila melanogaster* Tom40 homolog 2 (Tom40-2)
 MGNVMASSTADAESSRGRGHLASGLRLPEAPQYSGGVPPQMVEALKAEAKKPELTNPGLTE
 ELHSRCRDIQANTFEGAKIMVNKGLSNHFQVTHHTINMNSAGPSGYRFGATYVGTQYGP
 EAFPVLLGEIDPMGNLNANVIHQLTSLRCKFASQFQDSKLVGTQLTGDYRGRDYTLTLT
 MGNPFFTSSGVFVCQYLQSVTKRLALGSEFAYHYGNVPGRQVAVLSAVGRYAFGDTVW
 SCTLGPAGFHLSYYQKASDQLQIGVEVETNIRQQESTATVAYQIDLPAKADLVFRGSLDSN
 WLISGVLEKRLQPLPFSLAISGRMNHQKNSFRLGCGLMIG

>|Q9VZL1| *Drosophila melanogaster* Tom22 (Maggie)
 MDSPEIEFIEKDSGMSLGGSKDETPERRAVAATSNDPQRENYDDEPDETASERFWGLT
 EMFPEPVRNAVAVSSATVKSVKGFYSFSCNASWIFFTSAVILFAPVIFETERAQMEELH
 KSQQKQVLLGPGSAMGPGPSPSLPLIR

References

- Abe, Y., T. Shodai, T. Muto, K. Mihara, H. Torii, S. Nishikawa, T. Endo and D. Kohda (2000). "Structural basis of presequence recognition by the mitochondrial protein import receptor Tom20." *Cell* 100(5): 551-560.
- Ahting, U., M. Thieffry, H. Engelhardt, R. Hegerl, W. Neupert and S. Nussberger (2001). "Tom40, the pore-forming component of the protein-conducting TOM channel in the outer membrane of mitochondria." *Journal of Cell Biology* 153(6): 1151-1160.
- Ahting, U., C. Thun, R. Hegerl, D. Typke, F. E. Nargang, W. Neupert and S. Nussberger (1999). "The TOM core complex: the general protein import pore of the outer membrane of mitochondria." *J Cell Biol* 147(5): 959-968.
- Ahting, U., T. Waizenegger, W. Neupert and D. Rapaport (2005). "Signal-anchored proteins follow a unique insertion pathway into the outer membrane of mitochondria." *J Biol Chem* 280(1): 48-53.
- Albrecht, R., P. Rehling, A. Chacinska, J. Brix, S. A. Cadamuro, R. Volkmer, B. Guiard, N. Pfanner and K. Zeth (2006). "The Tim21 binding domain connects the preprotein translocases of both mitochondrial membranes." *EMBO Reports* 7(12): 1233-1238.
- Alconada, A., M. Kubrich, M. Moczko, A. Honlinger and N. Pfanner (1995). "The mitochondrial receptor complex: the small subunit Mom8b/Isp6 supports association of receptors with the general insertion pore and transfer of preproteins." *Mol Cell Biol* 15(11): 6196-6205.
- Allegretti, M., N. Klusch, D. J. Mills, J. Vonck, W. Kuhlbrandt and K. M. Davies (2015). "Horizontal membrane-intrinsic alpha-helices in the stator a-subunit of an F-type ATP synthase." *Nature* 521(7551): 237-240.
- Antignani, A. and R. J. Youle (2006). "How do Bax and Bak lead to permeabilization of the outer mitochondrial membrane?" *Curr Opin Cell Biol* 18(6): 685-689.
- Ashburner, M., K. G. Golic and R. S. Hawley (2005). *Drosophila: A Laboratory Handbook*, Cold Spring Harbor Laboratory Press.
- Bai, X. C., C. Yan, G. Yang, P. Lu, D. Ma, L. Sun, R. Zhou, S. H. W. Scheres and Y. Shi (2015). "An atomic structure of human gamma-secretase." *Nature* 525(7568): 212-217.
- Baker, K. P., A. Schaniel, D. Vestweber and G. Schatz (1990). "A yeast mitochondrial outer membrane protein essential for protein import and cell viability." *Nature* 348(6302): 605-609.
- Baker, M. J., C. T. Webb, D. A. Stroud, C. S. Palmer, A. E. Frazier, B. Guiard, A. Chacinska, J. M. Gulbis and M. T. Ryan (2009). "Structural and Functional Requirements for Activity of the Tim9–Tim10 Complex in Mitochondrial Protein Import." *Molecular Biology of the Cell* 20(3): 769-779.

- Bammes, B. E., R. H. Rochat, J. Jakana, D.-H. Chen and W. Chiu (2012). "Direct electron detection yields cryo-EM reconstructions at resolutions beyond $\frac{3}{4}$ Nyquist frequency." *Journal of Structural Biology* 177(3): 589-601.
- Banerjee, J. and S. Ghosh (2004). "Bax increases the pore size of rat brain mitochondrial voltage-dependent anion channel in the presence of tBid." *Biochem Biophys Res Commun* 323(1): 310-314.
- Bausewein, T., D. J. Mills, J. D. Langer, B. Nitschke, S. Nussberger and W. Kuhlbrandt (2017). "Cryo-EM Structure of the TOM Core Complex from *Neurospora crassa*." *Cell* 170(4): 693-700 e697.
- Bay, D. C., M. Hafez, M. J. Young and D. A. Court (2012). "Phylogenetic and coevolutionary analysis of the β -barrel protein family comprised of mitochondrial porin (VDAC) and Tom40." *Biochimica et Biophysica Acta (BBA) - Biomembranes* 1818(6): 1502-1519.
- Bayrhuber, M., T. Meins, M. Habeck, S. Becker, K. Giller, S. Villinger, C. Vonrhein, C. Griesinger, M. Zweckstetter and K. Zeth (2008). "Structure of the human voltage-dependent anion channel." *Proceedings of the National Academy of Sciences* 105(40): 15370.
- Bellot, G., P. F. Cartron, E. Er, L. Oliver, P. Juin, L. C. Armstrong, P. Bornstein, K. Mihara, S. Manon and F. M. Vallette (2006). "TOM22, a core component of the mitochondria outer membrane protein translocation pore, is a mitochondrial receptor for the proapoptotic protein Bax." *Cell Death And Differentiation* 14: 785.
- Bender, A., P. Desplats, B. Spencer, E. Rockenstein, A. Adame, M. Elstner, C. Laub, S. Mueller, A. O. Koob, M. Mante, E. Pham, T. Klopstock and E. Masliah (2013). "TOM40 mediates mitochondrial dysfunction induced by alpha-synuclein accumulation in Parkinson's disease." *PLoS One* 8(4): e62277.
- Bhangoo, M. K., S. Tzankov, A. C. Y. Fan, K. Dejgaard, D. Y. Thomas and J. C. Young (2007). "Multiple 40-kDa Heat-Shock Protein Chaperones Function in Tom70-dependent Mitochondrial Import." *Molecular Biology of the Cell* 18(9): 3414-3428.
- Bhola, P. D. and A. Letai (2016). "Mitochondria-Judges and Executioners of Cell Death Sentences." *Mol Cell* 61(5): 695-704.
- Biasutto, L., M. Azzolini, I. Szabò and M. Zoratti (2016). "The mitochondrial permeability transition pore in AD 2016: An update." *Biochimica et Biophysica Acta (BBA) - Molecular Cell Research* 1863(10): 2515-2530.
- Bischof, J., R. K. Maeda, M. Hediger, F. Karch and K. Basler (2007). "An optimized transgenesis system for *Drosophila* using germ-line-specific phiC31 integrases." *Proc Natl Acad Sci U S A* 104(9): 3312-3317.
- Blaza, J. N., K. R. Vinothkumar and J. Hirst (2018). "Structure of the Deactive State of Mammalian Respiratory Complex I." *Structure* 26(2): 312-319.e313.

- Bolliger, L., T. Junne, G. Schatz and T. Lithgow (1995). "Acidic receptor domains on both sides of the outer membrane mediate translocation of precursor proteins into yeast mitochondria." *The EMBO Journal* 14(24): 6318-6326.
- Brand, A. H. and N. Perrimon (1993). "Targeted Gene-Expression as a Means of Altering Cell Fates and Generating Dominant Phenotypes." *Development* 118(2): 401-415.
- Brenner, C., K. Subramaniam, C. Pertuiset and S. Pervaiz (2010). "Adenine nucleotide translocase family: four isoforms for apoptosis modulation in cancer." *Oncogene* 30: 883.
- Brix, J., K. Dietmeier and N. Pfanner (1997). "Differential recognition of preproteins by the purified cytosolic domains of the mitochondrial import receptors Tom20, Tom22, and Tom70." *Journal of Biological Chemistry* 272(33): 20730-20735.
- Brix, J., S. Rudiger, B. Bukau, J. Schneider-Mergener and N. Pfanner (1999). "Distribution of binding sequences for the mitochondrial import receptors Tom20, Tom22, and Tom70 in a presequence-carrying preprotein and a non-cleavable preprotein." *Journal of Biological Chemistry* 274(23): 16522-16530.
- Caldwell, J. T., G. C. Melkani, T. Huxford and S. I. Bernstein (2012). "Transgenic expression and purification of myosin isoforms using the *Drosophila melanogaster* indirect flight muscle system." *Methods* 56(1): 25-32.
- Cali, T., D. Ottolini and M. Brini (2012). "Mitochondrial Ca(2+) and neurodegeneration." *Cell Calcium* 52(1): 73-85.
- Callegari, S., F. Richter, K. Chojnacka, D. C. Jans, I. Lorenzi, D. Pacheu-Grau, S. Jakobs, C. Lenz, H. Urlaub, J. Dudek, A. Chacinska and P. Rehling (2016). "TIM29 is a subunit of the human carrier translocase required for protein transport." *FEBS Lett* 590(23): 4147-4158.
- Calvo, S. E., K. R. Clauser and V. K. Mootha (2016). "MitoCarta2.0: an updated inventory of mammalian mitochondrial proteins." *Nucleic Acids Res* 44(D1): D1251-1257.
- Cartron, P.-F., G. Bellot, L. Oliver, X. Grandier-Vazeille, S. Manon and F. M. Vallette (2008). "Bax inserts into the mitochondrial outer membrane by different mechanisms." *FEBS Letters* 582(20): 3045-3051.
- Chacinska, A., B. Guiard, J. M. Müller, A. Schulze-Specking, K. Gabriel, S. Kutik and N. Pfanner (2008). "Mitochondrial Biogenesis, Switching the Sorting Pathway of the Intermembrane Space Receptor Mia40." *The Journal of Biological Chemistry* 283(44): 29723-29729.
- Chacinska, A., C. M. Koehler, D. Milenkovic, T. Lithgow and N. Pfanner (2009). "Importing Mitochondrial Proteins: Machineries and Mechanisms." *Cell* 138(4): 628-644.
- Chacinska, A., S. Pfannschmidt, N. Wiedemann, V. Kozjak, L. K. Sanjuán Szklarz, A. Schulze-Specking, K. N. Truscott, B. Guiard, C. Meisinger and N. Pfanner (2004). "Essential role of Mia40 in import and assembly of mitochondrial intermembrane space proteins." *The EMBO Journal* 23(19): 3735-3746.

- Chan, N. C., V. A. Likic, R. F. Waller, T. D. Mulhern and T. Lithgow (2006). "The C-terminal TPR domain of Tom70 defines a family of mitochondrial protein import receptors found only in animals and fungi." *Journal of Molecular Biology* 358(4): 1010-1022.
- Choi, S., X. Quan, S. Bang, H. Yoo, J. Kim, J. Park, K. S. Park and J. Chung (2017). "Mitochondrial calcium uniporter in *Drosophila* transfers calcium between the endoplasmic reticulum and mitochondria in oxidative stress-induced cell death." *J Biol Chem* 292(35): 14473-14485.
- Colin, J., J. Garibal, B. Mignotte and I. Guenal (2009). "The mitochondrial TOM complex modulates bax-induced apoptosis in *Drosophila*." *Biochem Biophys Res Commun* 379(4): 939-943.
- Colombini, M. (2012). "VDAC structure, selectivity, and dynamics." *Biochimica et Biophysica Acta (BBA) - Biomembranes* 1818(6): 1457-1465.
- Crichton, P. G., M. Harding, J. J. Ruprecht, Y. Lee and E. R. Kunji (2013). "Lipid, detergent, and Coomassie Blue G-250 affect the migration of small membrane proteins in blue native gels: mitochondrial carriers migrate as monomers not dimers." *J Biol Chem* 288(30): 22163-22173.
- Crivat, G. and J. W. Taraska (2012). "Imaging proteins inside cells with fluorescent tags." *Trends in biotechnology* 30(1): 8-16.
- Csordas, G., A. P. Thomas and G. Hajnoczky (1999). "Quasi-synaptic calcium signal transmission between endoplasmic reticulum and mitochondria." *Embo j* 18(1): 96-108.
- Curado, S., E. A. Ober, S. Walsh, P. Cortes-Hernandez, H. Verkade, C. M. Koehler and D. Y. Stainier (2010). "The mitochondrial import gene *tomm22* is specifically required for hepatocyte survival and provides a liver regeneration model." *Dis Model Mech* 3(7-8): 486-495.
- Curran, S. P., D. Leuenberger, W. Oppliger and C. M. Koehler (2002). "The Tim9p-Tim10p complex binds to the transmembrane domains of the ADP/ATP carrier." *Embo j* 21(5): 942-953.
- D'andrea, L. D. and L. Regan (2003). "TPR proteins: the versatile helix." *Trends in Biochemical Sciences* 28(12): 655-662.
- da Fonseca, P. C. A. and E. P. Morris (2015). "Cryo-EM reveals the conformation of a substrate analogue in the human 20S proteasome core." *Nature Communications* 6: 7573.
- Daithankar, V. N., S. A. Schaefer, M. Dong, B. J. Bahnson and C. Thorpe (2010). "Structure of the human sulfhydryl oxidase augments liver regeneration and characterization of a human mutation causing an autosomal recessive myopathy." *Biochemistry* 49(31): 6737-6745.
- Davies, K. M., M. Strauss, B. Daum, J. H. Kief, H. D. Osiewacz, A. Rycovska, V. Zickermann and W. Kühlbrandt (2011). "Macromolecular organization of ATP synthase and complex I in whole mitochondria." *Proceedings of the National Academy of Sciences* 108(34): 14121.

- de Brito, O. M. and L. Scorrano (2010). "An intimate liaison: spatial organization of the endoplasmic reticulum-mitochondria relationship." *Embo j* 29(16): 2715-2723.
- Dekker, P. J., M. T. Ryan, J. Brix, H. Muller, A. Honlinger and N. Pfanner (1998). "Preprotein translocase of the outer mitochondrial membrane: molecular dissection and assembly of the general import pore complex." *Mol Cell Biol* 18(11): 6515-6524.
- Di Fonzo, A., D. Ronchi, T. Lodi, E. Fassone, M. Tigano, C. Lamperti, S. Corti, A. Bordoni, F. Fortunato, M. Nizzardo, L. Napoli, C. Donadoni, S. Salani, F. Saladino, M. Moggio, N. Bresolin, I. Ferrero and G. P. Comi (2009). "The Mitochondrial Disulfide Relay System Protein GFER Is Mutated in Autosomal-Recessive Myopathy with Cataract and Combined Respiratory-Chain Deficiency." *The American Journal of Human Genetics* 84(5): 594-604.
- Di Maio, R., P. J. Barrett, E. K. Hoffman, C. W. Barrett, A. Zharikov, A. Borah, X. Hu, J. McCoy, C. T. Chu, E. A. Burton, T. G. Hastings and J. T. Greenamyre (2016). " α -Synuclein binds to TOM20 and inhibits mitochondrial protein import in Parkinson's disease." *Science Translational Medicine* 8(342): 342ra378.
- Diekert, K., G. Kispal, B. Guiard and R. Lill (1999). "An internal targeting signal directing proteins into the mitochondrial intermembrane space." *Proceedings of the National Academy of Sciences* 96(21): 11752.
- Dolezal, P., V. Likic, J. Tachezy and T. Lithgow (2006). "Evolution of the molecular machines for protein import into mitochondria." *Science* 313(5785): 314-318.
- Dubochet, J., M. Adrian, J. J. Chang, J. C. Homo, J. Lepault, A. W. McDowell and P. Schultz (1988). "Cryo-electron microscopy of vitrified specimens." *Q Rev Biophys* 21(2): 129-228.
- Duffy, J. B. (2002). "GAL4 system in *Drosophila*: a fly geneticist's Swiss army knife." *Genesis* 34(1-2): 1-15.
- Eakin, R. M. (1972). *Structure of Invertebrate Photoreceptors. Photochemistry of Vision.* H. J. A. Dartnall. Berlin, Heidelberg, Springer Berlin Heidelberg: 625-684.
- Eroglu, C., P. Cronet, V. Panneels, P. Beaufils and I. Sinning (2002). "Functional reconstitution of purified metabotropic glutamate receptor expressed in the fly eye." *EMBO Rep* 3(5): 491-496.
- Fan, A. C., G. Kozlov, A. Hoegl, R. C. Marcellus, M. J. Wong, K. Gehring and J. C. Young (2011). "Interaction between the human mitochondrial import receptors Tom20 and Tom70 in vitro suggests a chaperone displacement mechanism." *J Biol Chem* 286(37): 32208-32219.
- Fischer, N., P. Neumann, A. L. Konevega, L. V. Bock, R. Ficner, M. V. Rodnina and H. Stark (2015). "Structure of the *E. coli* ribosome-EF-Tu complex at <3 Å resolution by Cs-corrected cryo-EM." *Nature* 520(7548): 567-570.
- Flinner, N., L. Ellenrieder, S. B. Stiller, T. Becker, E. Schleiff and O. Mirus (2013). "Mdm10 is an ancient eukaryotic porin co-occurring with the ERMES complex." *Biochimica et Biophysica Acta (BBA) - Molecular Cell Research* 1833(12): 3314-3325.

- Flotenmeyer, M., H. Weiss, C. Tribet, J. L. Popot and K. Leonard (2007). "The use of amphipathic polymers for cryo electron microscopy of NADH:ubiquinone oxidoreductase (complex I)." *J Microsc* 227(Pt 3): 229-235.
- Frauenfeld, J., R. Loving, J. P. Armache, A. F. Sonnen, F. Guettou, P. Moberg, L. Zhu, C. Jegerschold, A. Flayhan, J. A. Briggs, H. Garoff, C. Low, Y. Cheng and P. Nordlund (2016). "A saposin-lipoprotein nanoparticle system for membrane proteins." *Nat Methods* 13(4): 345-351.
- Freeman, M. (1996). "Reiterative use of the EGF receptor triggers differentiation of all cell types in the *Drosophila* eye." *Cell* 87(4): 651-660.
- Fujiki, M. and K. Verner (1993). "Coupling of cytosolic protein synthesis and mitochondrial protein import in yeast. Evidence for cotranslational import in vivo." *J Biol Chem* 268(3): 1914-1920.
- Fukasawa, Y., T. Oda, K. Tomii and K. Imai (2017). "Origin and Evolutionary Alteration of the Mitochondrial Import System in Eukaryotic Lineages." *Mol Biol Evol* 34(7): 1574-1586.
- Garcia, M., X. Darzacq, T. Delaveau, L. Jourden, R. H. Singer and C. Jacq (2007). "Mitochondria-associated Yeast mRNAs and the Biogenesis of Molecular Complexes." *Molecular Biology of the Cell* 18(2): 362-368.
- Gessmann, D., N. Flinner, J. Pfannstiel, A. Schlosinger, E. Schleiff, S. Nussberger and O. Mirus (2011). "Structural elements of the mitochondrial preprotein-conducting channel Tom40 dissolved by bioinformatics and mass spectrometry." *Biochim Biophys Acta* 1807(12): 1647-1657.
- Ghosh, T., N. Pandey, A. Maitra, S. K. Brahmachari and B. Pillai (2007). "A Role for Voltage-Dependent Anion Channel Vdac1 in Polyglutamine-Mediated Neuronal Cell Death." *PLoS ONE* 2(11): e1170.
- Godbole, A., J. Varghese, A. Sarin and M. K. Mathew (2003). "VDAC is a conserved element of death pathways in plant and animal systems." *Biochim Biophys Acta* 1642(1-2): 87-96.
- Goh, L. K., W. S. Lim, S. Teo, A. Vijayaraghavan, M. Chan, L. Tay, T. P. Ng, C. H. Tan, T. S. Lee and M. S. Chong (2015). "TOMM40 alterations in Alzheimer's disease over a 2-year follow-up period." *J Alzheimers Dis* 44(1): 57-61.
- Gold, V. A., P. Chroscicki, P. Bragoszewski and A. Chacinska (2017). "Visualization of cytosolic ribosomes on the surface of mitochondria by electron cryo-tomography." *EMBO Rep* 18(10): 1786-1800.
- Gottschalk, W. K., M. W. Lutz, Y. T. He, A. M. Saunders, D. K. Burns, A. D. Roses and O. Chiba-Falek (2014). "The Broad Impact of TOM40 on Neurodegenerative Diseases in Aging." *J Parkinsons Dis Alzheimers Dis* 1(1).
- Graveley, B. R., A. N. Brooks, J. W. Carlson, M. O. Duff, J. M. Landolin, L. Yang, C. G. Artieri, M. J. van Baren, N. Boley, B. W. Booth, J. B. Brown, L. Cherbas, C. A. Davis, A. Dobin, R. Li, W. Lin, J. H. Malone, N. R. Mattiuzzo, D. Miller, D. Sturgill, B. B. Tuch, C.

- Zaleski, D. Zhang, M. Blanchette, S. Dudoit, B. Eads, R. E. Green, A. Hammonds, L. Jiang, P. Kapranov, L. Langton, N. Perrimon, J. E. Sandler, K. H. Wan, A. Willingham, Y. Zhang, Y. Zou, J. Andrews, P. J. Bickel, S. E. Brenner, M. R. Brent, P. Cherbas, T. R. Gingeras, R. A. Hoskins, T. C. Kaufman, B. Oliver and S. E. Celniker (2010). "The developmental transcriptome of *Drosophila melanogaster*." *Nature* 471: 473.
- Gray, M. W. (2015). "Mosaic nature of the mitochondrial proteome: Implications for the origin and evolution of mitochondria." *Proc Natl Acad Sci U S A* 112(33): 10133-10138.
- Gray, M. W., G. Burger and B. F. Lang (2001). "The origin and early evolution of mitochondria." *Genome Biology* 2(6): reviews1018.1011.
- Green, D. R. and J. C. Reed (1998). "Mitochondria and apoptosis." *Science* 281(5381): 1309-1312.
- Guruharsha, K. G., R. A. Obar, J. Mintseris, K. Aishwarya, R. T. Krishnan, K. VijayRaghavan and S. Artavanis-Tsakonas (2012). "Drosophila Protein interaction Map (DPiM): A paradigm for metazoan protein complex interactions." *Fly* 6(4): 246-253.
- Haga, K., A. C. Kruse, H. Asada, T. Yurugi-Kobayashi, M. Shiroishi, C. Zhang, W. I. Weis, T. Okada, B. K. Kobilka, T. Haga and T. Kobayashi (2012). "Structure of the human M2 muscarinic acetylcholine receptor bound to an antagonist." *Nature* 482(7386): 547-551.
- Hales, K. G., C. A. Korey, A. M. Larracuenta and D. M. Roberts (2015). "Genetics on the Fly: A Primer on the *Drosophila* Model System." *Genetics* 201(3): 815-842.
- Hammon, J., D. V. Palanivelu, J. Chen, C. Patel and D. L. Minor (2009). "A green fluorescent protein screen for identification of well-expressed membrane proteins from a cohort of extremophilic organisms." *Protein Science : A Publication of the Protein Society* 18(1): 121-133.
- Hansson Petersen, C. A., N. Alikhani, H. Behbahani, B. Wiehager, P. F. Pavlov, I. Alafuzoff, V. Leinonen, A. Ito, B. Winblad, E. Glaser and M. Ankarcrona (2008). "The amyloid β -peptide is imported into mitochondria via the TOM import machinery and localized to mitochondrial cristae." *Proceedings of the National Academy of Sciences* 105(35): 13145.
- Harbauer, A. B., M. Opalinska, C. Gerbeth, J. S. Herman, S. Rao, B. Schonfisch, B. Guiard, O. Schmidt, N. Pfanner and C. Meisinger (2014). "Cell cycle-dependent regulation of mitochondrial preprotein translocase." *Science* 346(6213): 1109-1113.
- Hauer, F., C. Gerle, N. Fischer, A. Oshima, K. Shinzawa-Itoh, S. Shimada, K. Yokoyama, Y. Fujiyoshi and H. Stark (2015). "GraDeR: Membrane Protein Complex Preparation for Single-Particle Cryo-EM." *Structure* 23(9): 1769-1775.
- He, Y., K. Wang and N. Yan (2014). "The recombinant expression systems for structure determination of eukaryotic membrane proteins." *Protein Cell* 5(9): 658-672.
- Henderson, R. (1995). "The potential and limitations of neutrons, electrons and X-rays for atomic resolution microscopy of unstained biological molecules." *Q Rev Biophys* 28(2): 171-193.

- Hill, K., K. Model, M. T. Ryan, K. Dietmeier, F. Martin, R. Wagner and N. Pfanner (1998). "Tom40 forms the hydrophilic channel of the mitochondrial import pore for preproteins [see comment]." *Nature* 395(6701): 516-521.
- Hiller, S., J. Abramson, C. Mannella, G. Wagner and K. Zeth (2010). "The 3D structures of VDAC represent a native conformation." *Trends in biochemical sciences* 35(9): 514-521.
- Hiller, S., R. G. Garces, T. J. Malia, V. Y. Orekhov, M. Colombini and G. Wagner (2008). "Solution structure of the integral human membrane protein VDAC-1 in detergent micelles." *Science* 321(5893): 1206-1210.
- Hofmann, S., U. Rothbauer, N. Muhlenbein, K. Baiker, K. Hell and M. F. Bauer (2005). "Functional and mutational characterization of human MIA40 acting during import into the mitochondrial intermembrane space." *J Mol Biol* 353(3): 517-528.
- Hoppins, S. C. and F. E. Nargang (2004). "The Tim8-Tim13 complex of *Neurospora crassa* functions in the assembly of proteins into both mitochondrial membranes." *J Biol Chem* 279(13): 12396-12405.
- Humphries, A. D., I. C. Streimann, D. Stojanovski, A. J. Johnston, M. Yano, N. J. Hoogenraad and M. T. Ryan (2005). "Dissection of the mitochondrial import and assembly pathway for human Tom40." *J Biol Chem* 280(12): 11535-11543.
- Huynh, K. W., J. Jiang, N. Abuladze, K. Tsirulnikov, L. Kao, X. Shao, D. Newman, R. Azimov, A. Pushkin, Z. H. Zhou and I. Kurtz (2018). "CryoEM structure of the human SLC4A4 sodium-coupled acid-base transporter NBCe1." *Nature Communications* 9(1): 900.
- Hwa, J. J., A. J. Zhu, M. A. Hiller, C. Y. Kon, M. T. Fuller and A. Santel (2004). "Germ-line specific variants of components of the mitochondrial outer membrane import machinery in *Drosophila*." *FEBS Letters* 572(1): 141-146.
- Iwata, S. (2003). *Methods and results in crystallization of membrane proteins*, Internat. Univ. Line.
- Johnston, A. J., J. Hoogenraad, D. A. Dougan, K. N. Truscott, M. Yano, M. Mori, N. J. Hoogenraad and M. T. Ryan (2002). "Insertion and assembly of human tom7 into the preprotein translocase complex of the outer mitochondrial membrane." *J Biol Chem* 277(44): 42197-42204.
- Kabius, B., P. Hartel, M. Haider, H. Muller, S. Uhlemann, U. Loebau, J. Zach and H. Rose (2009). "First application of Cc-corrected imaging for high-resolution and energy-filtered TEM." *J Electron Microsc (Tokyo)* 58(3): 147-155.
- Kang, Y., M. J. Baker, M. Liem, J. Louber, M. McKenzie, I. Atukorala, C. S. Ang, S. Keerthikumar, S. Mathivanan and D. Stojanovski (2016). "Tim29 is a novel subunit of the human TIM22 translocase and is involved in complex assembly and stability." *Elife* 5.
- Kang, Y., D. A. Stroud, M. J. Baker, D. P. De Souza, A. E. Frazier, M. Liem, D. Tull, S. Mathivanan, M. J. McConville, D. R. Thorburn, M. T. Ryan and D. Stojanovski (2017).

"Sengers Syndrome-Associated Mitochondrial Acylglycerol Kinase Is a Subunit of the Human TIM22 Protein Import Complex." *Mol Cell* 67(3): 457-470.e455.

Karlberg, O., B. Canbäck, G. Kurland Charles and G. E. Andersson Siv (2000). "The dual origin of the yeast mitochondrial proteome." *Yeast* 17(3): 170-187.

Karnkowska, A., V. Vacek, Z. Zubáčová, S. C. Treitli, R. Petrželková, L. Eme, L. Novák, V. Žárský, L. D. Barlow, E. K. Herman, P. Soukal, M. Hroudová, P. Doležal, C. W. Stairs, A. J. Roger, M. Eliáš, J. B. Dacks, Č. Vlček and V. Hampl (2016). "A Eukaryote without a Mitochondrial Organelle." *Current Biology* 26(10): 1274-1284.

Kato, H., Q. Lu, D. Rapaport and V. Kozjak-Pavlovic (2013). "Tom70 Is Essential for PINK1 Import into Mitochondria." *PLoS ONE* 8(3): e58435.

Kato, H. and K. Mihara (2008). "Identification of Tom5 and Tom6 in the preprotein translocase complex of human mitochondrial outer membrane." *Biochemical and Biophysical Research Communications* 369(3): 958-963.

Keinan, N., H. Pahima, D. Ben-Hail and V. Shoshan-Barmatz (2013). "The role of calcium in VDAC1 oligomerization and mitochondria-mediated apoptosis." *Biochim Biophys Acta* 1833(7): 1745-1754.

Kerscher, O., J. Holder, M. Srinivasan, R. S. Leung and R. E. Jensen (1997). "The Tim54p-Tim22p complex mediates insertion of proteins into the mitochondrial inner membrane." *J Cell Biol* 139(7): 1663-1675.

Kerscher, O., N. B. Sepuri and R. E. Jensen (2000). "Tim18p is a new component of the Tim54p-Tim22p translocon in the mitochondrial inner membrane." *Mol Biol Cell* 11(1): 103-116.

Khoshouei, M., M. Radjainia, W. Baumeister and R. Danev (2017). "Cryo-EM structure of haemoglobin at 3.2 Å determined with the Volta phase plate." *Nat Commun* 8: 16099.

Kiebler, M., P. Keil, H. Schneider, I. J. van der Klei, N. Pfanner and W. Neupert (1993). "The mitochondrial receptor complex: a central role of MOM22 in mediating preprotein transfer from receptors to the general insertion pore." *Cell* 74(3): 483-492.

Kiebler, M., R. Pfaller, T. Sollner, G. Griffiths, H. Horstmann, N. Pfanner and W. Neupert (1990). "Identification of a mitochondrial receptor complex required for recognition and membrane insertion of precursor proteins." *Nature* 348(6302): 610-616.

Kim, S., H. Cho, W. Yang, H. Kwon, H. y. Shin, E. Lee, E.-S. Kang and J.-h. Kim (2014). "Abstract 2456: Overexpression of TOM40 (translocase in the outer mitochondrial membrane 40) inhibits the cell proliferation, invasion and migration abilities in ovarian cancer cell lines." *Cancer Research* 74(19 Supplement): 2456.

Kinoshita, J. Y., K. Mihara and T. Oka (2007). "Identification and characterization of a new tom40 isoform, a central component of mitochondrial outer membrane translocase." *J Biochem* 141(6): 897-906.

- Koehler, C. M., D. Leuenberger, S. Merchant, A. Renold, T. Junne and G. Schatz (1999). "Human deafness dystonia syndrome is a mitochondrial disease." *Proceedings of the National Academy of Sciences* 96(5): 2141.
- Kramer, J. M. and B. E. Staveley (2003). "GAL4 causes developmental defects and apoptosis when expressed in the developing eye of *Drosophila melanogaster*." *Genet Mol Res* 2(1): 43-47.
- Krüger, V., T. Becker, L. Becker, M. Montilla-Martinez, L. Ellenrieder, F. N. Vögtle, H. E. Meyer, M. T. Ryan, N. Wiedemann, B. Warscheid, N. Pfanner, R. Wagner and C. Meisinger (2017). "Identification of new channels by systematic analysis of the mitochondrial outer membrane." *The Journal of Cell Biology*.
- Kühlbrandt, W. (2014). "The Resolution Revolution." *Science* 343(6178): 1443-1444.
- Kunkele, K. P., S. Heins, M. Dembowski, F. E. Nargang, R. Benz, M. Thieffry, J. Walz, R. Lill, S. Nussberger and W. Neupert (1998a). "The preprotein translocation channel of the outer membrane of mitochondria." *Cell* 93(6): 1009-1019.
- Kunkele, K. P., P. Juin, C. Pompa, F. E. Nargang, J. P. Henry, W. Neupert, R. Lill and M. Thieffry (1998b). "The isolated complex of the translocase of the outer membrane of mitochondria. Characterization of the cation-selective and voltage-gated preprotein-conducting pore." *J Biol Chem* 273(47): 31032-31039.
- Kuszak, A. J., D. Jacobs, P. A. Gurnev, T. Shiota, J. M. Louis, T. Lithgow, S. M. Bezrukov, T. K. Rostovtseva and S. K. Buchanan (2015). "Evidence of Distinct Channel Conformations and Substrate Binding Affinities for the Mitochondrial Outer Membrane Protein Translocase Pore Tom40." *J Biol Chem* 290(43): 26204-26217.
- Kuzmenko, A., S. Tankov, B. P. English, I. Tarassov, T. Tenson, P. Kamenski, J. Elf and V. Hauryliuk (2011). "Single molecule tracking fluorescence microscopy in mitochondria reveals highly dynamic but confined movement of Tom40." *Scientific Reports* 1: 195.
- Lackey, S. W., R. D. Taylor, N. E. Go, A. Wong, E. L. Sherman and F. E. Nargang (2014). "Evidence supporting the 19 beta-strand model for Tom40 from cysteine scanning and protease site accessibility studies." *J Biol Chem* 289(31): 21640-21650.
- LaJeunesse, D. R., S. M. Buckner, J. Lake, C. Na, A. Pirt and K. Fromson (2004). "Three new *Drosophila* markers of intracellular membranes." *Biotechniques* 36(5): 784-788, 790.
- Lang, B. F., M. W. Gray and G. Burger (1999). "Mitochondrial Genome Evolution and the Origin of Eukaryotes." *Annual Review of Genetics* 33(1): 351-397.
- Laughlin, S. B., R. R. de Ruyter van Steveninck and J. C. Anderson (1998). "The metabolic cost of neural information." *Nature Neuroscience* 1: 36.
- Lebiedzinska, M., G. Szabadkai, A. W. Jones, J. Duszynski and M. R. Wieckowski (2009). "Interactions between the endoplasmic reticulum, mitochondria, plasma membrane and other subcellular organelles." *Int J Biochem Cell Biol* 41(10): 1805-1816.

- Lee, S. C., T. J. Knowles, V. L. Postis, M. Jamshad, R. A. Parslow, Y. P. Lin, A. Goldman, P. Sridhar, M. Overduin, S. P. Muench and T. R. Dafforn (2016). "A method for detergent-free isolation of membrane proteins in their local lipid environment." *Nat Protoc* 11(7): 1149-1162.
- Lemasters, J. J. and E. Holmuhamedov (2006). "Voltage-dependent anion channel (VDAC) as mitochondrial governor--thinking outside the box." *Biochim Biophys Acta* 1762(2): 181-190.
- Lesnik, C., A. Golani-Armon and Y. Arava (2015). "Localized translation near the mitochondrial outer membrane: An update." *RNA Biology* 12(8): 801-809.
- Li, J. X., X. G. Qian, J. B. Hu and B. D. Sha (2009). "Molecular Chaperone Hsp70/Hsp90 Prepares the Mitochondrial Outer Membrane Translocon Receptor Tom71 for Preprotein Loading." *Journal of Biological Chemistry* 284(35): 23852-23859.
- Liao, M., E. Cao, D. Julius and Y. Cheng (2013). "Structure of the TRPV1 ion channel determined by electron cryo-microscopy." *Nature* 504(7478): 107-112.
- Likić, V. A., A. Perry, J. Hulett, M. Derby, A. Traven, R. F. Waller, P. J. Keeling, C. M. Koehler, S. P. Curran, P. R. Gooley and T. Lithgow (2005). "Patterns that Define the Four Domains Conserved in Known and Novel Isoforms of the Protein Import Receptor Tom20." *Journal of Molecular Biology* 347(1): 81-93.
- Lindsley, D. L. and G. G. Zimm (1992). *SPECIAL CHROMOSOMES. The Genome of Drosophila Melanogaster*. San Diego, Academic Press: 1071-1095.
- Lippincott-Schwartz, J. (2011). "Emerging In Vivo Analyses of Cell Function Using Fluorescence Imaging." *Annual review of biochemistry* 80: 327-332.
- Lithgow, T., T. Junne, K. Suda, S. Gratzer and G. Schatz (1994). "The mitochondrial outer membrane protein Mas22p is essential for protein import and viability of yeast." *Proc Natl Acad Sci U S A* 91(25): 11973-11977.
- Lithgow, T. and A. Schneider (2010). "Evolution of macromolecular import pathways in mitochondria, hydrogenosomes and mitosomes." *Philos Trans R Soc Lond B Biol Sci* 365(1541): 799-817.
- Lu, P., X. C. Bai, D. Ma, T. Xie, C. Yan, L. Sun, G. Yang, Y. Zhao, R. Zhou, S. H. W. Scheres and Y. Shi (2014). "Three-dimensional structure of human gamma-secretase." *Nature* 512(7513): 166-170.
- Macasev, D., J. Whelan, E. Newbigin, M. C. Silva-Filho, T. D. Mulhern and T. Lithgow (2004). "Tom22', an 8-kDa trans-site receptor in plants and protozoans, is a conserved feature of the TOM complex that appeared early in the evolution of eukaryotes." *Molecular Biology and Evolution* 21(8): 1557-1564.
- Mager, F., D. Gessmann, S. Nussberger and K. Zeth (2011). "Functional refolding and characterization of two Tom40 isoforms from human mitochondria." *J Membr Biol* 242(1): 11-21.

- Mager, F., L. Sokolova, J. Lintzel, B. Brutschy and S. Nussberger (2010). "LILBID-mass spectrometry of the mitochondrial preprotein translocase TOM." *J Phys Condens Matter* 22(45): 454132.
- Marcotte, E. M., I. Xenarios, A. M. van Der Blik and D. Eisenberg (2000). "Localizing proteins in the cell from their phylogenetic profiles." *Proc Natl Acad Sci U S A* 97(22): 12115-12120.
- Massotte, D. (2003). "G protein-coupled receptor overexpression with the baculovirus-insect cell system: a tool for structural and functional studies." *Biochim Biophys Acta* 1610(1): 77-89.
- Meisinger, C., M. Rissler, A. Chacinska, L. K. Szklarz, D. Milenkovic, V. Kozjak, B. Schonfisch, C. Lohaus, H. E. Meyer, M. P. Yaffe, B. Guiard, N. Wiedemann and N. Pfanner (2004). "The mitochondrial morphology protein Mdm10 functions in assembly of the preprotein translocase of the outer membrane." *Dev Cell* 7(1): 61-71.
- Meisinger, C., M. T. Ryan, K. Hill, K. Model, J. H. Lim, A. Sickmann, H. Müller, H. E. Meyer, R. Wagner and N. Pfanner (2001). "Protein Import Channel of the Outer Mitochondrial Membrane: a Highly Stable Tom40-Tom22 Core Structure Differentially Interacts with Preproteins, Small Tom Proteins, and Import Receptors." *Molecular and Cellular Biology* 21(7): 2337-2348.
- Melin, J., M. Kilisch, P. Neumann, O. Lytovchenko, R. Gomkale, A. Schendzielorz, B. Schmidt, T. Liepold, R. Ficner, O. Jahn, P. Rehling and C. Schulz (2015). "A presequence-binding groove in Tom70 supports import of Mdl1 into mitochondria." *Biochim Biophys Acta* 1853(8): 1850-1859.
- Mi, W., Y. Li, S. H. Yoon, R. K. Ernst, T. Walz and M. Liao (2017). "Structural basis of MsbA-mediated lipopolysaccharide transport." *Nature* 549: 233.
- Milazzo, A.-C., A. Cheng, A. Moeller, D. Lyumkis, E. Jacovetty, J. Polukas, M. H. Ellisman, N.-H. Xuong, B. Carragher and C. S. Potter (2011). "Initial evaluation of a Direct Detection Device detector for single particle cryo-electron microscopy." *Journal of structural biology* 176(3): 404-408.
- Mise, A., Y. Yoshino, K. Yamazaki, Y. Ozaki, T. Sao, T. Yoshida, T. Mori, Y. Mori, S. Ochi, J. I. Iga and S. I. Ueno (2017). "TOMM40 and APOE Gene Expression and Cognitive Decline in Japanese Alzheimer's Disease Subjects." *J Alzheimers Dis* 60(3): 1107-1117.
- Miwa, S., J. St-Pierre, L. Partridge and M. D. Brand (2003). "Superoxide and hydrogen peroxide production by *Drosophila* mitochondria." *Free Radic Biol Med* 35(8): 938-948.
- Miyazawa, A., Y. Fujiyoshi, M. Stowell and N. Unwin (1999). "Nicotinic acetylcholine receptor at 4.6 Å resolution: transverse tunnels in the channel wall." *J Mol Biol* 288(4): 765-786.
- Model, K., C. Meisinger and W. Kuhlbrandt (2008). "Cryo-Electron Microscopy Structure of a Yeast Mitochondrial Preprotein Translocase." *Journal of Molecular Biology* 383(5): 1049-1057.

- Model, K., C. Meisinger, T. Prinz, N. Wiedemann, K. N. Truscott, N. Pfanner and M. T. Ryan (2001). "Multistep assembly of the protein import channel of the mitochondrial outer membrane." *Nature Structural Biology* 8(4): 361-370.
- Model, K., T. Prinz, T. Ruiz, M. Radermacher, T. Krimmer, W. Kuhlbrandt, N. Pfanner and C. Meisinger (2002). "Protein translocase of the outer mitochondrial membrane: role of import receptors in the structural organization of the TOM complex." *J Mol Biol* 316(3): 657-666.
- Molday, L. L. and R. S. Molday (2014). "1D4 – A Versatile Epitope Tag for the Purification and Characterization of Expressed Membrane and Soluble Proteins." *Methods in molecular biology* (Clifton, N.J.) 1177: 1-15.
- Mollereau, B. (2009). "Cell death: what can we learn from flies? Editorial for the special review issue on *Drosophila* apoptosis." *Apoptosis* 14(8): 929-934.
- Muhlenbein, N., S. Hofmann, U. Rothbauer and M. F. Bauer (2004). "Organization and function of the small Tim complexes acting along the import pathway of metabolite carriers into mammalian mitochondria." *J Biol Chem* 279(14): 13540-13546.
- Muller, C. S., W. Bildl, A. Haupt, L. Ellenrieder, T. Becker, C. Hunte, B. Fakler and U. Schulte (2016). "Cryo-slicing Blue Native-Mass Spectrometry (csBN-MS), a Novel Technology for High Resolution Complexome Profiling." *Mol Cell Proteomics* 15(2): 669-681.
- Murakami, H., D. Pain and G. Blobel (1988). "70-kD heat shock-related protein is one of at least two distinct cytosolic factors stimulating protein import into mitochondria." *J Cell Biol* 107(6 Pt 1): 2051-2057.
- Nagayama, K. and R. Danev (2009). "Phase-plate electron microscopy: a novel imaging tool to reveal close-to-life nano-structures." *Biophysical Reviews* 1(1): 37-42.
- Nargang, F. E., D. Rapaport, R. G. Ritzel, W. Neupert and R. Lill (1998). "Role of the Negative Charges in the Cytosolic Domain of TOM22 in the Import of Precursor Proteins into Mitochondria." *Molecular and Cellular Biology* 18(6): 3173-3181.
- Nawarak, J., R. Huang-Liu, S. H. Kao, H. H. Liao, S. Sinchaikul, S. T. Chen and S. L. Cheng (2009). "Proteomics analysis of A375 human malignant melanoma cells in response to arbutin treatment." *Biochim Biophys Acta* 1794(2): 159-167.
- Neupert, W. (1997). "Protein import into mitochondria." *Annual Review of Biochemistry* 66: 863-917.
- Oluwole, A. O., B. Danielczak, A. Meister, J. O. Babalola, C. Vargas and S. Keller (2017). "Solubilization of Membrane Proteins into Functional Lipid-Bilayer Nanodiscs Using a Diisobutylene/Maleic Acid Copolymer." *Angewandte Chemie (International Ed. in English)* 56(7): 1919-1924.
- Orrenius, S., V. Gogvadze and B. Zhivotovsky (2007). "Mitochondrial Oxidative Stress: Implications for Cell Death." *Annual Review of Pharmacology and Toxicology* 47(1): 143-183.

- Palmieri, F. (2004). "The mitochondrial transporter family (SLC25): physiological and pathological implications." *Pflugers Archiv-European Journal of Physiology* 447(5): 689-709.
- Pandey, U. B. and C. D. Nichols (2011). "Human Disease Models in *Drosophila melanogaster* and the Role of the Fly in Therapeutic Drug Discovery." *Pharmacological Reviews* 63(2): 411-436.
- Panneels, V., I. Kock, J. Krijnse-Locker, M. Rezaoui and I. Sinning (2011). "*Drosophila* photoreceptor cells exploited for the production of eukaryotic membrane proteins: receptors, transporters and channels." *PLoS One* 6(4): e18478.
- Pantelic, R. S., J. C. Meyer, U. Kaiser, W. Baumeister and J. M. Plitzko (2010). "Graphene oxide: a substrate for optimizing preparations of frozen-hydrated samples." *J Struct Biol* 170(1): 152-156.
- Petaja-Repo, U. E., M. Hogue, A. Laperriere, P. Walker and M. Bouvier (2000). "Export from the endoplasmic reticulum represents the limiting step in the maturation and cell surface expression of the human delta opioid receptor." *J Biol Chem* 275(18): 13727-13736.
- Peter, A., P. Schottler, M. Werner, N. Beinert, G. Dowe, P. Burkert, F. Mourkioti, L. Dentzer, Y. He, P. Deak, P. V. Benos, M. K. Gatt, L. Murphy, D. Harris, B. Barrell, C. Ferraz, S. Vidal, C. Brun, J. Demaille, E. Cadieu, S. Dreano, S. Gloux, V. Lelaure, S. Mottier, F. Galibert, D. Borkova, B. Minana, F. C. Kafatos, S. Bolshakov, I. Siden-Kiamos, G. Papagiannakis, L. Spanos, C. Louis, E. Madueno, B. de Pablos, J. Modolell, A. Bucheton, D. Callister, L. Campbell, N. S. Henderson, P. J. McMillan, C. Salles, E. Tait, P. Valenti, R. D. Saunders, A. Billaud, L. Pachter, R. Klapper, W. Janning, D. M. Glover, M. Ashburner, H. J. Bellen, H. Jackle and U. Schafer (2002). "Mapping and identification of essential gene functions on the X chromosome of *Drosophila*." *EMBO Rep* 3(1): 34-38.
- Petronilli, V., D. Penzo, L. Scorrano, P. Bernardi and F. Di Lisa (2001). "The mitochondrial permeability transition, release of cytochrome c and cell death. Correlation with the duration of pore openings in situ." *J Biol Chem* 276(15): 12030-12034.
- Pfaller, R., H. F. Steger, J. Rassow, N. Pfanner and W. Neupert (1988). "Import Pathways of Precursor Proteins into Mitochondria - Multiple Receptor-Sites Are Followed by a Common Membrane Insertion Site." *Journal of Cell Biology* 107(6): 2483-2490.
- Pfanner, N., M. G. Douglas, T. Endo, N. J. Hoogenraad, R. E. Jensen, M. Meijer, W. Neupert, G. Schatz, U. K. Schmitz and G. C. Shore (1996). "Uniform nomenclature for the protein transport machinery of the mitochondrial membranes." *Trends in Biochemical Sciences* 21(2): 51-52.
- Pfanner, N. and A. Geissler (2001). "Versatility of the mitochondrial protein import machinery." *Nature Reviews Molecular Cell Biology* 2: 339.
- Prussing, K., A. Voigt and J. B. Schulz (2013). "*Drosophila melanogaster* as a model organism for Alzheimer's disease." *Molecular Neurodegeneration* 8.
- Punjani, A., J. L. Rubinstein, D. J. Fleet and M. A. Brubaker (2017). "cryoSPARC: algorithms for rapid unsupervised cryo-EM structure determination." *Nat Methods* 14(3): 290-296.

- Qiu, J., L. S. Wenz, R. M. Zerbes, S. Oeljeklaus, M. Bohnert, D. A. Stroud, C. Wirth, L. Ellenrieder, N. Thornton, S. Kutik, S. Wiese, A. Schulze-Specking, N. Zufall, A. Chacinska, B. Guiard, C. Hunte, B. Warscheid, M. van der Laan, N. Pfanner, N. Wiedemann and T. Becker (2013). "Coupling of Mitochondrial Import and Export Translocases by Receptor-Mediated Supercomplex Formation." *Cell* 154(3): 596-608.
- Quinn, L., M. Coombe, K. Mills, T. Daish, P. Colussi, S. Kumar and H. Richardson (2003). "Buffy, a Drosophila Bcl-2 protein, has anti-apoptotic and cell cycle inhibitory functions." *Embo j* 22(14): 3568-3579.
- Rao, S., C. Gerbeth, A. Harbauer, D. Mikropoulou, C. Meisinger and O. Schmidt (2011). "Signaling at the gate: phosphorylation of the mitochondrial protein import machinery." *Cell Cycle* 10(13): 2083-2090.
- Rapaport, D., K.-P. Künkele, M. Dembowski, U. Ahting, F. E. Nargang, W. Neupert and R. Lill (1998a). "Dynamics of the TOM Complex of Mitochondria during Binding and Translocation of Preproteins." *Molecular and Cellular Biology* 18(9): 5256-5262.
- Rapaport, D., A. Mayer, W. Neupert and R. Lill (1998b). "cis and trans sites of the TOM complex of mitochondria in unfolding and initial translocation of preproteins." *J Biol Chem* 273(15): 8806-8813.
- Rapaport, D., R. D. Taylor, M. Käser, T. Langer, W. Neupert and F. E. Nargang (2001). "Structural Requirements of Tom40 for Assembly into Preexisting TOM Complexes of Mitochondria." *Molecular Biology of the Cell* 12(5): 1189-1198.
- Rasmussen, S. G., H. J. Choi, D. M. Rosenbaum, T. S. Kobilka, F. S. Thian, P. C. Edwards, M. Burghammer, V. R. Ratnala, R. Sanishvili, R. F. Fischetti, G. F. Schertler, W. I. Weis and B. K. Kobilka (2007). "Crystal structure of the human beta2 adrenergic G-protein-coupled receptor." *Nature* 450(7168): 383-387.
- Rawson, S., S. Davies, J. D. Lippiat and S. P. Muench (2016). "The changing landscape of membrane protein structural biology through developments in electron microscopy." *Mol Membr Biol* 33(1-2): 12-22.
- Rehling, P., K. Model, K. Brandner, P. Kovermann, A. Sickmann, H. E. Meyer, W. Kuhlbrandt, R. Wagner, K. N. Truscott and N. Pfanner (2003). "Protein insertion into the mitochondrial inner membrane by a twin-pore translocase." *Science* 299(5613): 1747-1751.
- Reid, G. A. and G. Schatz (1982). "Import of proteins into mitochondria. Extramitochondrial pools and post-translational import of mitochondrial protein precursors in vivo." *J Biol Chem* 257(21): 13062-13067.
- Reiter, L. T., L. Potocki, S. Chien, M. Gribskov and E. Bier (2001). "A systematic analysis of human disease-associated gene sequences in Drosophila melanogaster." *Genome Res* 11(6): 1114-1125.
- Ritchie, T. K., Y. V. Grinkova, T. H. Bayburt, I. G. Denisov, J. K. Zolnerciks, W. M. Atkins and S. G. Sligar (2009). "Reconstitution of Membrane Proteins in Phospholipid Bilayer Nanodiscs." *Methods in enzymology* 464: 211-231.

- Rizzuto, R., D. De Stefani, A. Raffaello and C. Mammucari (2012). "Mitochondria as sensors and regulators of calcium signalling." *Nature Reviews Molecular Cell Biology* 13: 566.
- Rodal, A. A., S. J. Del Signore and A. C. Martin (2015). "Drosophila comes of age as a model system for understanding the function of cytoskeletal proteins in cells, tissues, and organisms." *Cytoskeleton (Hoboken, N.J.)* 72(5): 207-224.
- Rodríguez, A. d. V., D. Didiano and C. Desplan (2011). "Power tools for gene expression and clonal analysis in Drosophila." *Nature methods* 9(1): 47-55.
- Roise, D. and G. Schatz (1988). "Mitochondrial presequences." *J Biol Chem* 263(10): 4509-4511.
- Roos, W. P. and B. Kaina (2006). "DNA damage-induced cell death by apoptosis." *Trends in Molecular Medicine* 12(9): 440-450.
- Ross, K., T. Rudel and V. Kozjak-Pavlovic (2009). "TOM-independent complex formation of Bax and Bak in mammalian mitochondria during TNF α -induced apoptosis." *Cell Death And Differentiation* 16: 697.
- Russo, C. J. and L. A. Passmore (2014). "Ultrastable gold substrates for electron cryomicroscopy." *Science (New York, N.Y.)* 346(6215): 1377-1380.
- Ryan, M. T., H. Muller and N. Pfanner (1999). "Functional staging of ADP ATP carrier translocation across the outer mitochondrial membrane." *Journal of Biological Chemistry* 274(29): 20619-20627.
- Saeki, K., H. Suzuki, M. Tsuneoka, M. Maeda, R. Iwamoto, H. Hasuwa, S. Shida, T. Takahashi, M. Sakaguchi, T. Endo, Y. Miura, E. Mekada and K. Mihara (2000). "Identification of mammalian TOM22 as a subunit of the preprotein translocase of the mitochondrial outer membrane." *Journal of Biological Chemistry* 275(41): 31996-32002.
- Sahdev, S., S. K. Khattar and K. S. Saini (2008). "Production of active eukaryotic proteins through bacterial expression systems: a review of the existing biotechnology strategies." *Mol Cell Biochem* 307(1-2): 249-264.
- Saitoh, T., M. Igura, T. Obita, T. Ose, R. Kojima, K. Maenaka, T. Endo and D. Kohda (2007). "Tom20 recognizes mitochondrial presequences through dynamic equilibrium among multiple bound states." *Embo Journal* 26(22): 4777-4787.
- Sanjuan Szklarz, L. K., V. Kozjak-Pavlovic, F. N. Vogtle, A. Chacinska, D. Milenkovic, S. Vogel, M. Durr, B. Westermann, B. Guiard, J. C. Martinou, C. Borner, N. Pfanner and C. Meisinger (2007). "Preprotein transport machineries of yeast mitochondrial outer membrane are not required for Bax-induced release of intermembrane space proteins." *J Mol Biol* 368(1): 44-54.
- Sankala, H., C. Vaughan, J. Wang, S. Deb and P. R. Graves (2011). "Upregulation of the mitochondrial transport protein, Tim50, by mutant p53 contributes to cell growth and chemoresistance." *Archives of Biochemistry and Biophysics* 512(1): 52-60.

- Scheres, S. H. (2016). "Processing of Structurally Heterogeneous Cryo-EM Data in RELION." *Methods Enzymol* 579: 125-157.
- Scheres, S. H. W. (2012). "RELION: Implementation of a Bayesian approach to cryo-EM structure determination." *Journal of Structural Biology* 180(3): 519-530.
- Schmidt, O., A. B. Harbauer, S. Rao, B. Eyrich, R. P. Zahedi, D. Stojanovski, B. Schonfisch, B. Guiard, A. Sickmann, N. Pfanner and C. Meisinger (2011). "Regulation of mitochondrial protein import by cytosolic kinases." *Cell* 144(2): 227-239.
- Schwarze, S. R., R. Weindruch and J. M. Aiken (1998). "Oxidative stress and aging reduce COX I RNA and cytochrome oxidase activity in *Drosophila*." *Free Radical Biology and Medicine* 25(6): 740-747.
- Scott, I. and R. J. Youle (2010). "Mitochondrial fission and fusion." *Essays Biochem* 47: 85-98.
- Sherman, E. L., N. E. Go and F. E. Nargang (2005). "Functions of the small proteins in the TOM complex of *Neurospora crassa*." *Molecular Biology of the Cell* 16(9): 4172-4182.
- Shimizu, S., M. Narita, Y. Tsujimoto and Y. Tsujimoto (1999). "Bcl-2 family proteins regulate the release of apoptogenic cytochrome c by the mitochondrial channel VDAC." *Nature* 399: 483.
- Shiota, T., K. Imai, J. Qiu, V. L. Hewitt, K. Tan, H. H. Shen, N. Sakiyama, Y. Fukasawa, S. Hayat, M. Kamiya, A. Elofsson, K. Tomii, P. Horton, N. Wiedemann, N. Pfanner, T. Lithgow and T. Endo (2015). "Molecular architecture of the active mitochondrial protein gate." *Science* 349(6255): 1544-1548.
- Shoshan-Barmatz, V., D. Mizrachi and N. Keinan (2013). "Oligomerization of the mitochondrial protein VDAC1: from structure to function and cancer therapy." *Progress in molecular biology and translational science* 117: 303-334.
- Sinha, D., S. Srivastava, L. Krishna and P. D'Silva (2014). "Unraveling the intricate organization of mammalian mitochondrial presequence translocases: existence of multiple translocases for maintenance of mitochondrial function." *Mol Cell Biol* 34(10): 1757-1775.
- Sirrenberg, C., M. F. Bauer, B. Guiard, W. Neupert and M. Brunner (1996). "Import of carrier proteins into the mitochondrial inner membrane mediated by Tim22." *Nature* 384: 582.
- Smith, A. C. and A. J. Robinson (2016). "MitoMiner v3.1, an update on the mitochondrial proteomics database." *Nucleic Acids Research* 44(D1): D1258-D1261.
- Sokol, A. M., M. E. Sztolsztener, M. Wasilewski, E. Heinz and A. Chacinska (2014). "Mitochondrial protein translocases for survival and wellbeing." *FEBS Lett* 588(15): 2484-2495.
- Sollner, T., R. Pfaller, G. Griffiths, N. Pfanner and W. Neupert (1990). "A mitochondrial import receptor for the ADP/ATP carrier." *Cell* 62(1): 107-115.

- St Johnston, D. (2002). "The art and design of genetic screens: *Drosophila melanogaster*." *Nat Rev Genet* 3(3): 176-188.
- Stojanovski, D., J. M. Müller, D. Milenkovic, B. Guiard, N. Pfanner and A. Chacinska (2008). "The MIA system for protein import into the mitochondrial intermembrane space." *Biochimica et Biophysica Acta (BBA) - Molecular Cell Research* 1783(4): 610-617.
- Suga, M., F. Akita, K. Hirata, G. Ueno, H. Murakami, Y. Nakajima, T. Shimizu, K. Yamashita, M. Yamamoto, H. Ago and J. R. Shen (2015). "Native structure of photosystem II at 1.95 Å resolution viewed by femtosecond X-ray pulses." *Nature* 517(7532): 99-103.
- Sun, L., L. Zhao, G. Yang, C. Yan, R. Zhou, X. Zhou, T. Xie, Y. Zhao, S. Wu, X. Li and Y. Shi (2015). "Structural basis of human γ -secretase assembly." *Proceedings of the National Academy of Sciences of the United States of America* 112(19): 6003-6008.
- Sunley, K. and M. Butler (2010). "Strategies for the enhancement of recombinant protein production from mammalian cells by growth arrest." *Biotechnol Adv* 28(3): 385-394.
- Suzuki, H., Y. Okazawa, T. Komiya, K. Saeki, E. Mekada, S. Kitada, A. Ito and K. Mihara (2000). "Characterization of rat TOM40, a central component of the preprotein translocase of the mitochondrial outer membrane." *J Biol Chem* 275(48): 37930-37936.
- Szklarczyk, R. and M. A. Huynen (2010). "Mosaic origin of the mitochondrial proteome." *Proteomics* 10(22): 4012-4024.
- Tait, S. W. G. and D. R. Green (2010). "Mitochondria and cell death: outer membrane permeabilization and beyond." *Nature Reviews Molecular Cell Biology* 11: 621.
- Tan, Y. Z., P. R. Baldwin, J. H. Davis, J. R. Williamson, C. S. Potter, B. Carragher and D. Lyumkis (2017). "Addressing preferred specimen orientation in single-particle cryo-EM through tilting." *Nat Methods* 14(8): 793-796.
- Thomas, L., E. Blachly-Dyson, M. Colombini and M. Forte (1993). "Mapping of residues forming the voltage sensor of the voltage-dependent anion-selective channel." *Proceedings of the National Academy of Sciences* 90(12): 5446.
- Tinbergen, J. and D. G. Stavenga (1987). "Spectral sensitivity of light induced respiratory activity of photoreceptor mitochondria in the intact fly." *Journal of Comparative Physiology A* 160(2): 195-203.
- Tranebjaerg, L., B. C. Hamel, F. J. Gabreels, W. O. Renier and M. Van Ghelue (2000). "A de novo missense mutation in a critical domain of the X-linked DDP gene causes the typical deafness-dystonia-optic atrophy syndrome." *Eur J Hum Genet* 8(6): 464-467.
- Tribet, C., R. Audebert and J.-L. Popot (1996). "Amphipols: Polymers that keep membrane proteins soluble in aqueous solutions." *Proceedings of the National Academy of Sciences of the United States of America* 93(26): 15047-15050.

- Trindade, D., C. Pereira, S. R. Chaves, S. Manon, M. Corte-Real and M. J. Sousa (2016). "VDAC regulates AAC-mediated apoptosis and cytochrome c release in yeast." *Microb Cell* 3(10): 500-510.
- Truscott, K. N., N. Wiedemann, P. Rehling, H. Muller, C. Meisinger, N. Pfanner and B. Guiard (2002). "Mitochondrial import of the ADP/ATP carrier: the essential TIM complex of the intermembrane space is required for precursor release from the TOM complex." *Mol Cell Biol* 22(22): 7780-7789.
- Twomey, E. C., M. V. Yelshanskaya, R. A. Grassucci, J. Frank and A. I. Sobolevsky (2017). "Channel opening and gating mechanism in AMPA-subtype glutamate receptors." *Nature* 549(7670): 60-65.
- Ujwal, R., D. Cascio, J. P. Colletier, S. Faham, J. Zhang, L. Toro, P. Ping and J. Abramson (2008). "The crystal structure of mouse VDAC1 at 2.3 Å resolution reveals mechanistic insights into metabolite gating." *Proc Natl Acad Sci U S A* 105(46): 17742-17747.
- Uren, R. T., M. O'Hely, S. Iyer, R. Bartolo, M. X. Shi, J. M. Brouwer, A. E. Alsop, G. Dewson and R. M. Kluck (2017). "Disordered clusters of Bak dimers rupture mitochondria during apoptosis." *eLife* 6: e19944.
- van Wilpe, S., M. T. Ryan, K. Hill, A. C. Maarse, C. Meisinger, J. Brix, P. J. T. Dekker, M. Moczko, R. Wagner, M. Meijer, B. Guiard, A. Honlinger and N. Pfanner (2000). "Tom22 is a multifunctional organizer of the mitochondrial preprotein translocase (vol 401, pg 485, 1999)." *Nature* 408(6812): 616-+.
- Vance, J. E. (1990). "Phospholipid synthesis in a membrane fraction associated with mitochondria." *J Biol Chem* 265(13): 7248-7256.
- Vander Heiden, M. G., X. X. Li, E. Gottlieb, R. B. Hill, C. B. Thompson and M. Colombini (2001). "Bcl-xL promotes the open configuration of the voltage-dependent anion channel and metabolite passage through the outer mitochondrial membrane." *J Biol Chem* 276(22): 19414-19419.
- Vaskova, M., A. M. Bentley, S. Marshall, P. Reid, C. S. Thummel and A. J. Andres (2000). "Genetic analysis of the *Drosophila* 63F early puff. Characterization of mutations in E63-1 and maggie, a putative Tom22." *Genetics* 156(1): 229-244.
- Veesler, D., M. G. Campbell, A. Cheng, C.-y. Fu, Z. Murez, J. E. Johnson, C. S. Potter and B. Carragher (2013). "Maximizing the potential of electron cryomicroscopy data collected using direct detectors." *Journal of structural biology* 184(2): 10.1016/j.jsb.2013.1009.1003.
- Vestweber, D., J. Brunner, A. Baker and G. Schatz (1989). "A 42K outer-membrane protein is a component of the yeast mitochondrial protein import site." *Nature* 341(6239): 205-209.
- Vinothkumar, K. R., J. Zhu and J. Hirst (2014). "Architecture of mammalian respiratory complex I." *Nature* 515(7525): 80-84.
- von Heijne, G., J. Steppuhn and R. G. Herrmann (1989). "Domain structure of mitochondrial and chloroplast targeting peptides." *Eur J Biochem* 180(3): 535-545.

- Voorhees, Rebecca M., Israel S. Fernández, Sjors H. Scheres and Ramanujan S. Hegde (2014). "Structure of the Mammalian Ribosome-Sec61 Complex to 3.4 Å Resolution." *Cell* 157(7): 1632-1643.
- Vukotic, M., H. Nolte, T. König, S. Saita, M. Ananjew, M. Krüger, T. Tatsuta and T. Langer (2017). "Acylglycerol Kinase Mutated in Sengers Syndrome Is a Subunit of the TIM22 Protein Translocase in Mitochondria." *Mol Cell* 67(3): 471-483.e477.
- Wadhwa, R., S. Takano, K. Kaur, C. Deocaris Custer, M. Pereira-Smith Olivia, R. Reddel Roger and C. Kaul Sunil (2006). "Upregulation of mortalin/mthsp70/Grp75 contributes to human carcinogenesis." *International Journal of Cancer* 118(12): 2973-2980.
- Waegemann, K., D. Popov-Čeleketić, W. Neupert, A. Azem and D. Mokranjac (2015). "Cooperation of TOM and TIM23 Complexes during Translocation of Proteins into Mitochondria." *Journal of Molecular Biology* 427(5): 1075-1084.
- Wang, C. and R. J. Youle (2009). "The role of mitochondria in apoptosis*." *Annu Rev Genet* 43: 95-118.
- Wang, L. (2016). "Mitochondrial purine and pyrimidine metabolism and beyond." *Nucleosides Nucleotides Nucleic Acids* 35(10-12): 578-594.
- Wang, X. (2001). "The expanding role of mitochondria in apoptosis." *Genes Dev* 15(22): 2922-2933.
- Webb, C. T., M. A. Gorman, M. Lazarou, M. T. Ryan and J. M. Gulbis (2006). "Crystal structure of the mitochondrial chaperone TIM9 center dot 10 reveals a six-bladed alpha-propeller." *Molecular Cell* 21(1): 123-133.
- Weinberg, S. E., L. A. Sena and N. S. Chandel (2015). "Mitochondria in the regulation of innate and adaptive immunity." *Immunity* 42(3): 406-417.
- Weisthal, S., N. Keinan, D. Ben-Hail, T. Arif and V. Shoshan-Barmatz (2014). "Ca²⁺-mediated regulation of VDAC1 expression levels is associated with cell death induction." *Biochimica et Biophysica Acta (BBA) - Molecular Cell Research* 1843(10): 2270-2281.
- Westphal, D., G. Dewson, M. Menard, P. Frederick, S. Iyer, R. Bartolo, L. Gibson, P. E. Czabotar, B. J. Smith, J. M. Adams and R. M. Kluck (2014). "Apoptotic pore formation is associated with in-plane insertion of Bak or Bax central helices into the mitochondrial outer membrane." *Proceedings of the National Academy of Sciences* 111(39): E4076.
- Wiedemann, N., V. Kozjak, A. Chacinska, B. Schönfisch, S. Rospert, M. T. Ryan, N. Pfanner and C. Meisinger (2003). "Machinery for protein sorting and assembly in the mitochondrial outer membrane." *Nature* 424: 565.
- Wiedemann, N. and N. Pfanner (2017). "Mitochondrial Machineries for Protein Import and Assembly." *Annu Rev Biochem* 86: 685-714.

- Wiedemann, N., N. Pfanner and M. T. Ryan (2001). "The three modules of ADP/ATP carrier cooperate in receptor recruitment and translocation into mitochondria." *Embo Journal* 20(5): 951-960.
- Wienhues, U., K. Becker, M. Schleyer, B. Guiard, M. Tropschug, A. L. Horwich, N. Pfanner and W. Neupert (1991). "Protein folding causes an arrest of preprotein translocation into mitochondria in vivo." *The Journal of Cell Biology* 115(6): 1601.
- Wittig, I., H. P. Braun and H. Schagger (2006). "Blue native PAGE." *Nat Protoc* 1(1): 418-428.
- Wu, S., A. Avila-Sakar, J. Kim, D. S. Booth, C. H. Greenberg, A. Rossi, M. Liao, X. Li, A. Alian, S. L. Griner, N. Juge, Y. Yu, C. M. Mergel, J. Chaparro-Riggers, P. Strop, R. Tampe, R. H. Edwards, R. M. Stroud, C. S. Craik and Y. Cheng (2012). "Fabs enable single particle cryoEM studies of small proteins." *Structure* 20(4): 582-592.
- Wu, Y. K. and B. D. Sha (2006). "Crystal structure of yeast mitochondrial outer membrane translocon member Tom70p." *Nature Structural & Molecular Biology* 13(7): 589-593.
- Xu, X., M. Qiao, Y. Zhang, Y. Jiang, P. Wei, J. Yao, B. Gu, Y. Wang, J. Lu, Z. Wang, Z. Tang, Y. Sun, W. Wu and Q. Shi (2010). "Quantitative proteomics study of breast cancer cell lines isolated from a single patient: Discovery of TIMM17A as a marker for breast cancer." *PROTEOMICS* 10(7): 1374-1390.
- Yan, Z., X. Bai, C. Yan, J. Wu, Z. Li, T. Xie, W. Peng, C. Yin, X. Li, S. H. W. Scheres, Y. Shi and N. Yan (2015). "Structure of the rabbit ryanodine receptor RyR1 at near-atomic resolution." *Nature* 517(7532): 50-55.
- Yang, D., Y. Oyaizu, H. Oyaizu, G. J. Olsen and C. R. Woese (1985). "Mitochondrial origins." *Proceedings of the National Academy of Sciences* 82(13): 4443.
- Yano, M., N. Hoogenraad, K. Terada and M. Mori (2000). "Identification and Functional Analysis of Human Tom22 for Protein Import into Mitochondria." *Molecular and Cellular Biology* 20(19): 7205-7213.
- Ye, Y. and M. E. Fortini (1999). "Apoptotic Activities of Wild-Type and Alzheimer's Disease-Related Mutant Presenilins in *Drosophila melanogaster*." *The Journal of Cell Biology* 146(6): 1351-1364.
- Yoshizumi, T., T. Ichinohe, O. Sasaki, H. Otera, S. Kawabata, K. Mihara and T. Koshiba (2014). "Influenza A virus protein PB1-F2 translocates into mitochondria via Tom40 channels and impairs innate immunity." *Nat Commun* 5: 4713.
- Young, J. C., J. M. Barral and F. U. Hartl (2003a). "More than folding: localized functions of cytosolic chaperones." *Trends in Biochemical Sciences* 28(10): 541-547.
- Young, J. C., N. J. Hoogenraad and F. U. Hartl (2003b). "Molecular chaperones Hsp90 and Hsp70 deliver preproteins to the mitochondrial import receptor Tom70." *Cell* 112(1): 41-50.

Zaid, H., S. Abu-Hamad, A. Israelson, I. Nathan and V. Shoshan-Barmatz (2005). "The voltage-dependent anion channel-1 modulates apoptotic cell death." *Cell Death Differ* 12(7): 751-760.

Zalk, R., O. B. Clarke, A. des Georges, R. A. Grassucci, S. Reiken, F. Mancina, W. A. Hendrickson, J. Frank and A. R. Marks (2014). "Structure of a mammalian ryanodine receptor." *Nature* 517: 44.

Zeitlow, K., L. Charlabous, I. Ng, S. Gagrani, M. Mihovilovic, S. Luo, D. L. Rock, A. Saunders, A. D. Roses and W. K. Gottschalk (2017). "The biological foundation of the genetic association of TOMM40 with late-onset Alzheimer's disease." *Biochim Biophys Acta* 1863(11): 2973-2986.

Zeth, K. (2010). "Structure and evolution of mitochondrial outer membrane proteins of beta-barrel topology." *Biochim Biophys Acta* 1797(6-7): 1292-1299.

Zouni, A., H.-T. Witt, J. Kern, P. Fromme, N. Krauss, W. Saenger and P. Orth (2001). "Crystal structure of photosystem II from *Synechococcus elongatus* at 3.8 Å resolution." *Nature* 409: 739.



Minerva Access is the Institutional Repository of The University of Melbourne

Author/s:

Periasamy, Agalya

Title:

Investigation of the mitochondrial translocase of the outer membrane (TOM) of *Drosophila melanogaster*

Date:

2018

Persistent Link:

<http://hdl.handle.net/11343/214490>

File Description:

Investigation of the Mitochondrial Translocase of the Outer Membrane (TOM) of *Drosophila melanogaster*

Terms and Conditions:

Terms and Conditions: Copyright in works deposited in Minerva Access is retained by the copyright owner. The work may not be altered without permission from the copyright owner. Readers may only download, print and save electronic copies of whole works for their own personal non-commercial use. Any use that exceeds these limits requires permission from the copyright owner. Attribution is essential when quoting or paraphrasing from these works.